Development of Samarium Doped Ceria (SDC) and SDC-based Composite Electrolytes for Applications in Intermediate Temperature Solid Oxide Fuel Cells (SOFCs)

By

MUSTAFA ANWAR

Reg. #: NUST201260710MCES64112F

Session 2012-14

Supervised by

Dr. Zuhair S. Khan

A Thesis Submitted to the Centre for Energy Systems in partial fulfillment of the requirements for the degree of

MASTERS of SCIENCE

in

ENERGY SYSTEMS ENGINEERING

Center for Energy Systems (CES)

National University of Sciences and Technology (NUST)

H-12, Islamabad 44000, Pakistan

September 2014

Certificate

This is to certify that work in this thesis has been carried out by **Mr. Mustafa Anwar** and completed under my supervision in Advanced Energy Materials and Fuel Cells Lab, Centre for Energy Systems, National University of Sciences and Technology, H-12, Islamabad, Pakistan.

Supervisor:
                                            _____
Dr. Zuhair S. Khan
Centre for Energy Systems
NUST, Islamabad

GEC member # 1:
                                            _____
Dr. Mrs. Naveed K. Janjua
Department of Chemistry
QAU, Islamabad

GEC member # 2:
                                            _____
Dr. M Bilal Khan
Centre for Energy Systems
NUST, Islamabad

GEC member # 3:
                                            _____
Dr. Syed Tauqir A. Sherzai
Department of Chemistry
CIIT, Abbottabad

HoD-CES:
                                            _____
Dr. Zuhair S. Khan
Centre for Energy Systems
NUST, Islamabad

Principal / Dean:
                                      _____
Dr. M Bilal Khan
Centre for Energy Systems
NUST, Islamabad

I dedicated this thesis to my beloved Parents, Siblings & Teachers

Abstract

Solid oxide fuel cells (SOFCs) are the most efficient devices for clean energy that directly convert the chemical energy of fuels into electrical power. Traditional SOFCs employ yttria-stabilized zirconia (YSZ) as an electrolyte but YSZ exhibited sufficient ionic conductivities at high temperatures (800-1000°C). Due to this high temperature, the commercial utilization of the conventional SOFCs is limited because of the resistive causes, e.g. expensive materials, thermal stress and long start-up and shut-down time etc. In the last decade, the research of SOFCs had concentrated on decreasing the operating temperature through the evolution of novel materials, notably the electrolyte materials having sufficient ionic conductivity. Doped ceria based electrolytes has higher oxygen ion conductivity than YSZ, especially at lower temperatures.

In the first part of the dissertation, samarium doped ceria (SDC), and samarium doped ceria-based composite electrolyte with addition of lithium & sodium carbonates, $(LiNa)_2CO_3$-SDC were prepared by co-precipitation route. Cubic fluorite structures have been observed in both electrolytes and crystallite sizes of SDC and $(LiNa)_2CO_3$-SDC were found to be 14 nm and 55 nm, respectively. SEM images showed that SDC nanoparticles appeared to be spherical in shape while $(LiNa)_2CO_3$-SDC composite nanoparticles are irregular in shape and consisted of agglomerated nanocrystallites. The conductivities of SDC and $(LiNa)_2CO_3$-SDC at 650 °C are 5.502×10^{-5} S/cm and 1.90×10^{-3} S/cm, respectively. Furthermore, the conductivity of $(LiNa)_2CO_3$-SDC is also calculated at 700 °C and found to be 2.94×10^{-3} S/cm.

In the second part of the thesis, the effects of pH of medium on the microstructure of SDC have been studied and SDC-based composite with addition of potassium carbonate (SDC-K_2CO_3) has also developed to study the effect of calcination temperature on the microstructure of SDC-K_2CO_3. XRD and SEM studies showed that the crystallite size and particle size of SDC increases with the increase in pH. The SEM images of all the samples of SDC synthesized at different pH values showed the irregular shaped and dispersed particles. SDC-K_2CO_3 was calcined at 600 °C, 700 °C and 800 °C for 4 h and XRD results showed that crystallite size increases while lattice strain decreases with the increase in calcination temperature and no

peaks were detected for K_2CO_3 because it is present in the electrolyte as amorphous phase. The conductivity of SDC-K_2CO_3 at 700 °C is found to be 3.2×10^{-3} S/cm.

In the last part of the thesis, co-doped SDC with the addition of yttrium has been developed in order to find the effect of yttrium co-doping on the conductivity of SDC. The conductivity of YSDC at 650 °C is found to be 2.0×10^{-4} S/cm which is higher than the SDC electrolyte. At the end, chemical compatibility test of YSDC with lithiated nickel oxide cathode was performed at 800 °C for 3 h in order to check the compatibility of these two materials and it was found from XRD data that neither new reaction occurs nor new phases are formed between the YSDC electrolyte and lithiated nickel oxide cathode. So we may say that these two materials can be used as an electrolyte and a cathode in intermediate temperature SOFCs. The result in this dissertation may benefit the development of ITSOFCs and expand the related research to a new horizon.

Keywords: SOFC, Electrolyte, SDC, Carbonate, Co-doping

Table of Contents

List of Figures

List of Tables

List of Journals/Conference Papers

Journal Article (Under review):

1. <u>Mustafa Anwar</u>, M. N. Akbar, M. A. Rana, K. Mustafa, S. Shakir, Zuhair S. Khan, Development of Samarium Doped Ceria (SDC) and SDC-based Composite Electrolytes for Applications in Intermediate Temperature Solid Oxide Fuel Cells (SOFCs), Journal of Electroceramics, Springer (Attached to Annexure-C).

Review Article:

1. <u>Mustafa Anwar</u>, Zuhair S. Khan, A review on synthesis routes for samarium doped ceria (SDC) and SDC-carbonate composite electrolyte materials for Intermediate Temperature Solid Oxide Fuel Cells (SOFCs). (Attached to Annexure-B).

Conference Papers from this work:

1. <u>Mustafa Anwar</u>, M. N. Akbar, Naveed K. Janjua, M. A. Rana, Kamal Mustafa, S. Shakir, Z. S. Khan, Development of Samarium-doped ceria based electrolytes for use in Intermediate Temperature Solid Oxide Fuel Cells (IT-SOFCs), Conference on Frontiers of Nanoscience & Nanotechnology, June 03-05, 2014, PINSTECH Islamabad, Pakistan (Attached to Annexure-A).

Conference Papers from other work not included:

1. M. Akmal Rana, <u>Mustafa Anwar</u>, M. N. Akbar, Kamal Mustafa, S. Shakir, Zuhair S. Khan, Investigations on doped ceria electrolytes and their structural and electrical properties for applications in low temperature solid oxide fuel cells, Conference on Frontiers of Nanoscience & Nanotechnology, June 03-05, 2014, PINSTECH Islamabad, Pakistan.

2. M. N. Akbar, <u>Mustafa Anwar</u>, M. A. Rana, S. Shakir, Kamal Mustafa, Naveed K. Janjua, Zuhair S. Khan, Synthesis of NiO-SDC by co-precipitation for anode applications in low temperature solid oxide fuel cells, Conference on Frontiers of Nanoscience & Nanotechnology, June 03-05, 2014, PINSTECH Islamabad, Pakistan.

3. Kamal Mustafa, M. A. Rana, <u>Mustafa Anwar</u>, M. N. Akbar, S. Shakir, Zuhair S. Khan, Synthesis of cobalt doped lithiated NiO cathode material and investigation on corrosion performance of $LiAlO_2$ matrices for MCFCs

applications, Conference on Frontiers of Nanoscience & Nanotechnology, June 03-05, 2014, PINSTECH Islamabad, Pakistan.

4. Sehar Shakir, Abdur Rehman, M. A. Rana, M. N. Akbar, <u>Mustafa Anwar</u>, Kamal Mustafa, Zuhair S. Khan, Sol-gel fabrication of TiO_2 Nanoparticles and investigations on Cu doping effects for application in dye sensitized solar cells, Conference on Frontiers of Nanoscience & Nanotechnology, June 03-05, 2014, PINSTECH Islamabad, Pakistan.

List of Abbreviations

PEMFC	Proton Exchange Membrane Fuel Cell
PAFC	Phosphoric Acid Fuel Cell
MCFC	Molten Carbonate Fuel Cell
AFC	Alkaline Fuel Cell
SOFC	Solid Oxide Fuel Cell
ITSOFC	Intermediate Temperature Solid Oxide Fuel Cell
LTSOFC	Low Temperature Solid Oxide Fuel Cell
YSZ	Yttria Stabilized Zirconia
EMF	Electromotive Force
GDC	Gadolinium Doped Ceria
SDC	Samarium Doped Ceria
LSM	Lanthanum Strontium Manganite
OCV	Open Circuit Voltage
XRD	X-Ray Diffraction
SEM	Scanning Electron Microscope
DC	Direct Current
YSDC	Yttrium Samarium Doped Ceria

Chapter 1
Introduction

Energy drives the global economy and is considered a basic input for the climate and sustainable advancement. Development has always been correlated with the growth of demand of energy. Sustainable development craves a sustainable supply of clean and affordable energy sources that do not cause adverse social impacts. Supplies of such energy sources as fossil fuels and uranium are limited. Up to now, the fossil fuels are being used in order to meet the energy requirements and because of the fast depletion of fossil fuels it is evident that the use of conventional power plants cannot fulfill the ever-growing demand for energy. In addition to this, the burning of natural gas, coal and furnace oil is the main cause of adverse air pollution in the form of emission of greenhouse gases e.g., carbon dioxide etc., especially in industrial and commercial areas. In order to get rid of the critical challenges of energy security and environmental deterioration we must implement the efficient and environmentally benign energy systems to harvest electricity [1,2]. In this context, advanced energy conversion technologies have attracted viable attention during the past few decades. There is a great interest in electrochemical energy storage such as advanced batteries, fuel cells and supercapacitors. Among them, fuel cell is notably attractive as fuel cell is considered to be the most efficient and less polluting electricity generating device [3].

1.1 Fuel Cell

Fuel cell is an electrochemical device that directly converts the chemical energy of fuels such as methane, methanol, hydrogen, ethanol and other hydrocarbons to electrical energy [1]. The origin of fuel cells goes back to the middle of the 18th century when Welsh chemical-physicist Sir William Grove described the principle of fuel cells in 1839 [4]. He executed the first fuel cell (which he termed the gas voltaic battery) with which he demonstrated that an electric current is generated by the electrochemical reaction between oxygen and hydrogen. His fuel cell had three main components; electrolyte, anode and cathode. It was operated at room temperature. In this fuel cell, the electrolyte used was dilute sulphuric acid while hydrogen and oxygen were used as an anode and cathode respectively. The term fuel cell was first introduced by the British chemist Ludwig Mond (1839 – 1909) and Charles Langer

when they employed coal as fuel and obtaining a current density of 20 Am^{-2} at 0.73 V. Subsequently in 1950s, Polymer Electrolyte Membrane Fuel Cell was designed by Willard Thomas Grubb and Leonard Niedrach and was used in Gemini space programme by NASA; later, an Alkaline Fuel Cell having capacity of 12 kW has been used in space shuttle [1]. After further R & D efforts at the end of 20th century, fuel cells have fascinated the researchers because of their ability for use in transportation, stationary and distributed power stations [4]. Since 2007, they are commercialized and are mostly used in electric vehicles. Now-a-day, fuel cells can be used in various power systems as follows [1]:

➤ 1 W–10 kW: mobile phones, personal computers and personal electric equipment;

➤ 1–100 kW: public transportation and power vehicles;

➤ 1–10 MW: power plants for energy generation and distribution

Currently, five different types of fuel cells, namely, polymer electrolyte membrane or proton exchange membrane fuel cell (PEMFC), the phosphoric acid fuel cell (PAFC), the molten carbonate fuel cell (MCFC), the alkaline fuel cell (AFC), and the solid oxide fuel cell (SOFC) have been primarily developed. These fuel cells are distinguished from one another by the electrolyte used, which in turn describes the working temperature [5]. Fig. 1.1 shows the basic principle of five main kinds of fuel cells while the characteristics of these different types of fuel cells are summarized in Table 1.1.

It is clear from the Table 1.1 that SOFCs offer high energy conversion efficiency (up to 60%) and because of this they can be used in electric power generation systems. Other advantages of SOFCs include fuel flexibility because internal reforming of the fuel can be done inside the cell due to its high operating temperature and ease in the system design. Furthermore, the exhaust heat can be used as a heat source for various processes such as steam generation etc. [7]. Some of the unique and particular advantages of SOFC technology are [5]:

➤ The cell components are fabricated by non-strategic, non-noble and cheap materials in comparison with other fuel cells.

➤ Flexibility in stack size which may ranges from the construction of W to MW systems.

➤ Systems for "near zero" greenhouse gas emissions.
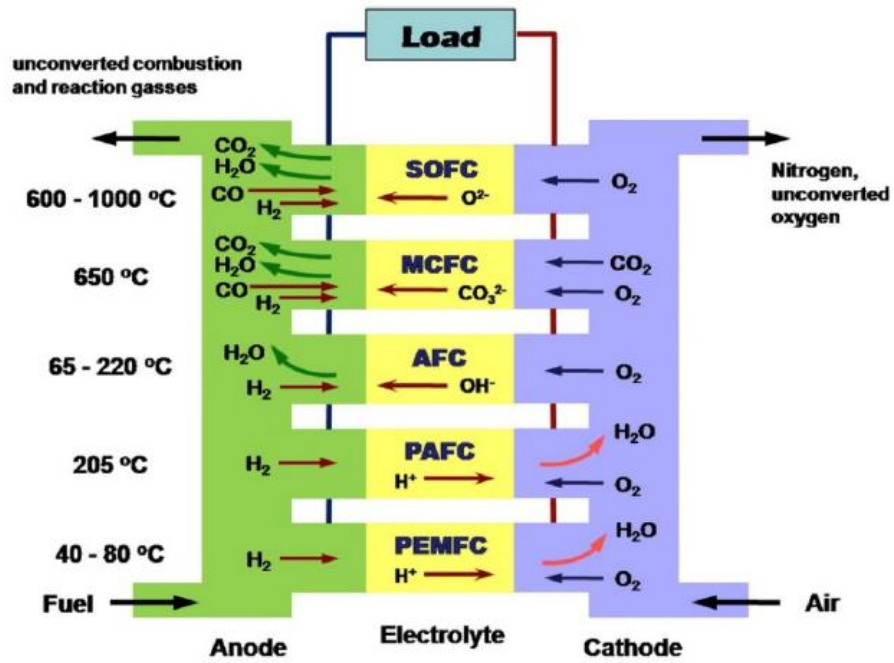
Fig. 1.1 Scheme of basic principle of different kinds of fuel cells [6]

Table 1.1 Properties of basic types of fuel cells [1,4,5]

Properties	PEMFC	AFC	PAFC	MCFC	SOFC
Working temperature (°C)	40 – 80	65 – 100	150 - 200	650	600 – 1000
Electrolyte	Hydrated polymeric ion exchange membrane	Mobilized or immobilized KOH in asbestos matrix	Immobilized liquid H_3PO_4 in SiC	Immobilized liquid molten carbonate in $LiAlO_2$ matrix	Ceramics
Electrodes	Carbon	Platinum	Carbon	Nickel and NiO	Ceramic based
Catalyst	Platinum	Platinum	Platinum	Electrode material	Electrode material
Interconnect	Carmon or metal	Metal	Graphite	Stainless steel or nickel	Nickel, ceramic or steel
Charge Carrier	H^+	OH^-	H^+	CO_3^{2-}	O^{2-}
Fuel Compatibility	H_2, methanol	H_2	H_2	H_2, CH_4	H_2, CH_4, CO
Efficiency	30 – 40%	50%	40%	45 – 50%	60%

1.2 Solid Oxide Fuel Cell

Solid oxide fuel cell (SOFC) is a type of fuel cell in which a solid oxide material is used as an electrolyte, which traditionally acts as an oxygen ions conductor [8]. SOFC is also known as ceramic fuel cell (CFC) because of the use of ceramic materials in the fabrication of SOFC. Fig. 1.2 shows the working principle of SOFC with an oxide ion conductor. The oxide ions are produced at the cathode because of the reduction of oxidizing agent (oxygen) under the influence of an external load which is applied to the cell. These oxide ions transfer through the solid ceramic electrolyte to the anode (fuel electrode), where the oxidation of fuel occurs and as a result electricity, heat and water are produced as the basic reaction products. If CO or CH_4 is used as fuel then CO_2 is also produced. Alternatively, a proton conducting perovskite solid electrolyte can be used, where protons are produced by the oxidation of hydrogen that subsequently react with oxygen to form water [4]. The half-cell reactions at the electrodes (cathode and anode) can be described expressed by Kroger-Vink Notation as follows:

Reaction at Cathode:

$$O_2 + 4e' + 2V_o^{\bullet\bullet} \rightarrow 2O_o^{\times} \ldots\ldots\ldots\ldots (1.1)$$

Reaction at Anode:

$$H_2 + O_o^{\times} \rightarrow H_2O + V_o^{\bullet\bullet} + 2e' \ldots\ldots\ldots\ldots (1.2)$$

Overall Reaction:

$$2H_2 + O_2 \rightarrow 2H_2O \ldots\ldots\ldots\ldots (1.3)$$
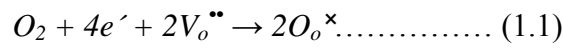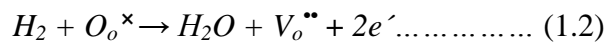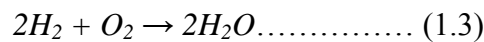
Here, $V_o^{\bullet\bullet}$ is the oxygen vacancy and $O_o^{\times}$ is the oxygen ion in the electrolyte.
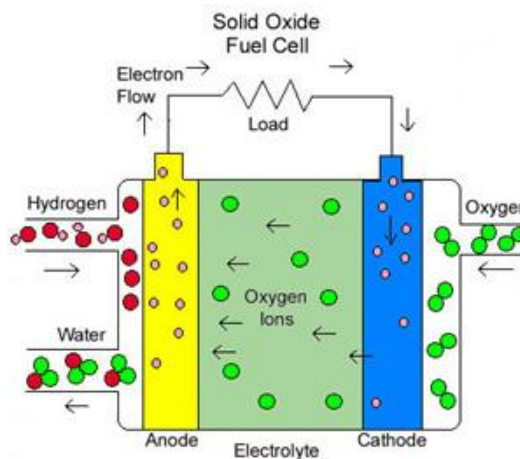
Fig. 1.2 Schematic representation of SOFC principle

Table 1.2 shows the basic nomenclature of Kroger-Vink notation.

Table 1.2 Nomenclature for Kroger-Vink Notation

Defect	Symbol	Effective Charge
Aluminum ion sitting on the aluminum lattice site	$Al^{\times}_{Al}$	Neutral
Nickel ion sitting on a copper lattice site	$Ni^{\times}_{Cu}$	Neutral
Oxygen vacancy	$V_o^{\bullet\bullet}$	+2
Calcium interstitial ion	$Ca_i^{\bullet\bullet}$	+2
Chlorine ion on an interstitial site	Cl_i'	-1
Oxygen ion on an interstitial site	O_i''	-2

The open-circuit voltage, V_o, of the cell can be calculated by two methods:

➢ from the free energy change of the electrochemical reaction, ΔG or

➢ from the partial pressure of the oxygen $P_o(c)$ at the cathode and $P_o(a)$ at the anode

$$V_o = -\frac{\Delta G}{nF} = \frac{RT}{nF}\ln\frac{P_o(c)}{P_o(a)} \ldots\ldots\ldots\ldots (1.4)$$

The above equation is known as Nernst equation, where, R is the universal gas constant; T is the absolute temperature, F is the Faraday's constant and n is the electron equivalent of oxygen (n = 4).

The voltage drop in the cell occurs as current is drained because of polarization. The total polarization of a cell is calculated by the help of following equation:

$$\eta = \eta_a + \eta_c + \eta_r \ldots\ldots\ldots\ldots (1.5)$$

where, η = total polarization, η_a = polarization at anode, η_c = polarization at cathode and η_r = resistance polarization.

The polarization and subsequently voltage drop primarily depends on the electrolyte, anode and cathode materials, the design and the working temperature of the cell.

The first SOFC consisting of oxygen-ion conducting yttria stabilized zirconia (YSZ) was fabricated and electrically tested by Baur and Pries in 1937. This SOFC was operated at 1000°C and in this cell, $ZrO_2 - 15$ weight% Y_2O_3 was used as the electrolyte. Nernst first discovered that YSZ was a solid oxide ion conductor in 1899. Now-a-day, yttria stabilized zirconia with 8 mol% Y_2O_3 is used as the electrolyte material in the most advanced SOFCs. The ionic conductivity of YSZ is approximately 0.1 S/cm at 1000°C [4,5].

1.2.1 Materials for SOFC Components

From a constructional point of view, the SOFC can be described as three layered ceramic bodies, composed by a cathode, a solid electrolyte and an anode, respectively, unless interlayer is necessary for interface improvement between the main layers. Because of the fact that each layer has its own function, there are different requirements for each layer, as described elsewhere. The respective requirements are given in Table 1.3 [7].

1.2.1.1 Electrolyte

The electrolyte is the most principal component for SOFC. The characteristics of an ideal SOFC electrolyte are shown in Table 1.3. The main purpose of an electrolyte is to conduct a specific ion between two electrodes in order to complete the overall electrochemical reaction. SOFCs are based on crystalline oxide ceramic electrolyte materials that conduct ions via defect hopping mechanisms [8,9]. Table 1.4 shows the detailed overview of different electrolytic materials used for SOFCs. Presently cubic fluorite structure materials e.g., zirconia-based and ceria-based oxides, and perovskite lanthanum gallate based materials are extensively employed as electrolytes for SOFCs. Fig. 1.3 shows the ionic conductivity of different solid oxide electrolytes at various temperatures.
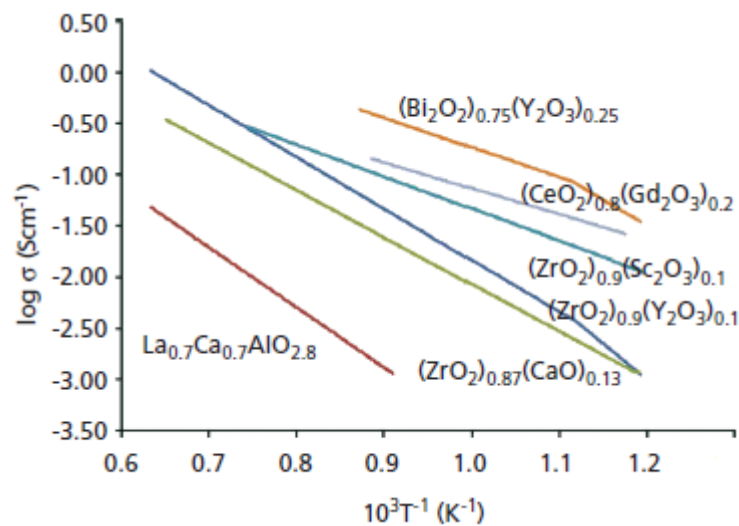
Fig. 1.3 Specific ionic conductivities of some selected solid electrolytes [10]

Table 1.3 Requirements for the Layers

Layer (Component)		
CATHODE	**ELECTROLYTE**	**ANODE**
1. It must have a stable and a sufficient porous microstructure parallel with good adhesion to the remaining ceramic components of SOFC; 2. Cathode must have a high value of electronic conductivity and a sufficient value of ionic (oxygen) conductivity; 3. Possess high catalytic activity to oxygen dissociation and next reduction process; 4. Must be compatible and less reactive with the electrolyte and the interconnection with which cathode comes into contact.	1. Electrochemical: high ionic conductivity; 2. Chemical: structure must be stable at high temperature, completely inert to the other component materials and lack of instability to oxygen and fuel gas at high temperature treatment, lack of phase immiscibility is also necessary; 3. Thermal: It must be thermally phase stable and having low thermal expansion coefficient close to those values of the remaining components of the cell. 4. Fully dense structure; 5. Low cost and environmental friendly	1. It must be highly stable at reduction environment; 2. Anode must be stable at high temperatures; 3. It must be porous; 4. Possess high catalytic activity; 5. High electronic conductivity; 6. High corrosion stability.

An essential element required for the oxygen ion conduction in ceramic electrolytes is the random distribution of vacancies throughout the oxide sublattice. The conventional oxygen ion conductors are the cubic fluorite based oxide materials having a general formula of AO_2, where A is a tetravalent cation. This structure is a face-centered cubic arrangement of cations with oxygen ions occupying all the tetrahedral sites, leading to a large number of octahedral interstitial voids. The structure is a rather open one and rapid ion diffusion can be expected. Oxygen ion conductivity can be enhanced by the addition of lower valence cations because of the production of oxygen vacancies [8–10]. Zirconia (ZrO_2) exhibits three polymorphs. At room temperature, it has a monoclinic structure and above 1170 °C structure will change to tetragonal, and then to the cubic fluorite arrangement when above 2370 °C.

Table 1.4 Comparison of different electrolyte materials in SOFCs

Electrolyte	Advantages	Drawbacks	Conductivity	Reference
1. Yttria – Stabilized Zirconia (YSZ)	➢ Excellent chemical stability and chemical inertness. ➢ Possesses one of the highest fracture toughness values of all the metal oxides. ➢ Shows reasonably good ionic conductivity (at sufficiently high temperature) and little or no electronic conductivity.	➢ At lower temperatures, the ionic conductivity of YSZ is much lower than that of ceria-based electrolytes such as GDC or lanthanum gallate-based electrolytes such as LSGM.	0.14 S cm^{-1} at 1000°C	[8,11]
2. Doped Ceria	➢ Shows higher ionic conductivity than YSZ. This relative conductivity advantage is particularly important at lower temperatures.	➢ Reduction of ceria occurs from Ce^{4+} to Ce^{3+} under the fuel rich conditions at the anode side of the electrolyte. Under these conditions electronic conductivity and lattice expansion is introduced, which causes internal short-circuiting in the cell and associated mechanical stresses.	GDC10 ($Ce_{0.9}Gd_{0.1}O_{1.95}$) has an ionic conductivity of 0.01 S cm^{-1} at 500°C.	[8,12]
3. Bismuth Oxides	➢ Ionic conductivity is among the highest ever measured in oxide ion conductors. ➢ The conductivity is predominantly ionic with O^{2-} being the main charge carrier. ➢ Doped δ-Bi_2O_3 materials show improved stability compared to pure Bi_2O_3.	➢ In reducing environment, these materials are thermodynamically instable. ➢ At moderate temperatures, bismuth oxide shows volatile behavior. ➢ Corrosion activity is high. ➢ Mechanical strength is relatively weak.	1 S cm^{-1} at 750°C, which is far higher than YSZ or even GDC.	[8,10]

Electrolyte	Advantages	Drawbacks	Conductivity	Reference
4. LAMOX Family ($La_2Mo_2O_9$)	➤ Their potential as SOFC electrolyte materials is best suited to oxidizing conditions and intermediate temperatures.	➤ $La_2Mo_2O_9$ is a good ion conductor only in its high-temperature β phase. ➤ Susceptible to reduction. ➤ Their electronic conductivity increases with temperature. ➤ Some $La_2Mo_2O_9$-based materials also exhibit degradation at moderate oxygen pressures.	At 720 °C, conductivity is 0.03 S cm^{-1}	[8,13]
5. Oxygen-Ion-Conducting Perovskite Oxides (Lanthanum Gallate, $LaGaO_3$-based materials such as LSGM, $La_{0.9}Sr_{0.1}Ga_{0.8}Mg_{0.2}O_{3-δ}$)	➤ The conductivity of LSGM is entirely ionic and higher than that of YSZ over a very wide range of oxygen partial pressure and over a wide range of temperatures up to 1000°C. ➤ LSGM does not reduce as easily as GDC. ➤ Its thermal expansion is relatively low and well matched to YSZ.	➤ At much lower temperatures (<700°C), LSGM's ionic conductivity is not as high as GDC. ➤ Gallium is relatively expensive and gallium oxide is a volatile material. ➤ During processing some undesirable secondary phases are formed and significant reactivity with perovskite electrodes under oxidizing conditions as well as with metal anodes in reducing conditions.	Conductivity of LSGM at 800°C is 0.075 S cm^{-1}.	[8,13]
6. Proton-Conducting Perovskites	➤ Higher theoretical e.m.f and electrical efficiency and fuel management is relatively easier than SOFCs based on O^{2-} conducting electrolytes.	➤ Significant chemical instability in CO_2 environments.	As high as 0.1 S cm^{-1} at 500°C.	[8,14]

In this business the role of a dopant ion is very important. By the addition of a dopant ion, the cubic fluorite and tetragonal phases will be achieved at room temperature and the oxygen vacancy concentration will also increase by the addition of dopant ions. In case of zirconia, yttrium is the extensively studied dopant and the fluorite structure of cubic ZrO_2 is shown in Fig. 1.4 [10].
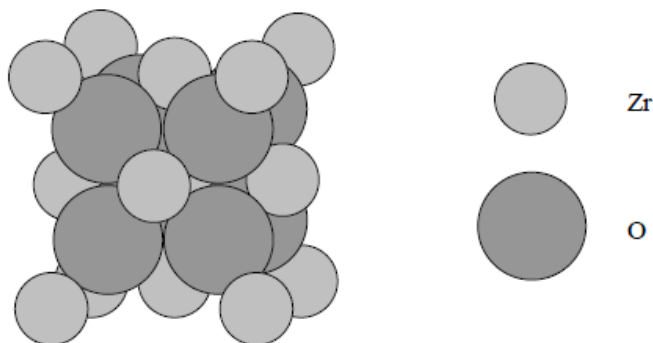
Fig. 1.4 Cubic Fluorite Structure of Zirconia

Doped cerium oxide, also exhibits cubic fluorite structure and is considered to be a promising electrolyte for intermediate and/or low temperature SOFCs. In comparison with YSZ, doped ceria shows high ionic conductivity and lower activation energy below 800 °C. However, at high temperatures (>600 °C) and under reducing conditions, doped ceria based oxides suffer partial reduction from Ce^{4+} to Ce^{3+}, which leads towards the electronic conduction and reduces the performance of the cell. Therefore, the operation of SOFCs with doped ceria based electrolytes is considered most effective in the temperature ranges from 500 – 600 °C [8–11].

Another most important oxygen ion conductors are perovskite based materials. There general formula is ABO_3. Generally, the A-site cation is large, for example rare earth metal, and will be 12-coordinated by anions in the lattice. The B-site cation is typically smaller and having a coordination number of 6. There are two dopant sites in the perovskite oxides upon which to substitute lower valence cations, leading to a much broader range of possible oxygen ion conducting materials. Currently the most extensively studied perovskite conductor that is stable in air and hydrogen is lanthanum gallate. The doping of strontium on A-site of the perovskite and magnesium on the B-site having a composition of $La_{0.9}Sr_{0.1}Ga_{0.8}Mg_{0.2}O_{2.85}$ (LSGM) can be used at temperature of 600 °C. However, LSGM is relatively expensive than cerium oxide based

electrolyte materials and it is also proved that a pure single phase electrolyte of LSGM is difficult to prepare. Some other challenges of thermal, mechanical and chemical compatibility of LSGM need further research and development [8,13].

1.2.1.2 Anode

The role of an anode in SOFC is electro-oxidation of fuel by catalyzing the reaction, and facilitating fuel access and product removal. Therefore, the anode materials should meet several requirements which are given in Table 1.3.

These requirements together with elevated operating temperature limit the choice of the anode materials to nickel (Ni) and the noble metals. Due to the low cost of Ni, currently, the vast majority of SOFCs have a nickel anode. The most commonly used anode materials are cermet composed of nickel and solid electrolyte, such as Ni-YSZ, Ni-GDC, aiming at maintaining porosity of anode by preventing sintering of the Ni particles and giving the anode a TEC comparable to that of the solid electrolyte. However, Ni based anode materials also offer some drawbacks such as at high operating temperatures the direct exposure of hydrocarbon fuels to the conventional nickel based anodes has been problematic due to their high catalytic activity for hydrocarbon cracking reactions, leading to carbon deposition in the anode and thus eventually degrading the cell performance. The need of the hour is to develop alternative anode materials, i.e. replacing nickel by other metals like copper in the cermet anode, since copper dose not catalyze the cracking process [8,15].

1.2.1.3 Cathode

In SOFCs, the function of the cathode is to act as a site for the electrochemical reduction of O_2. To realize this function, the specific requirements for the cathode material are given in Table 1.3.

Various doped oxides have been studied as possible cathode materials for SOFC. Strontium doped lanthanum manganite (LSM), $La_{1-x}Sr_xMnO_3$ is the most widely employed cathode material for YSZ based SOFCs. The conductivity of LSM mainly depends upon the concentration (doping) of strontium. Another perovskite based material used as cathode in SOFC is doped lanthanum cobaltite, $LaCoO_3$. The doping of cations of strontium and iron on lanthanum and cobalt site, respectively significantly increases the conductivity of $LaCoO_3$. These types of perovskite based cathode materials

have a general formula of $La_{1-x}Sr_xCo_{1-y}Fe_yO_{3-\delta}$. Some other proposed new cathode materials for intermediate and/or low temperature solid oxide fuel cells are $(Sm,Sr)CoO_3$, $La_{n+1}Ni_nO_{3n+1}$ and $GdBaCoO_{5+\delta}$. These materials also have shown promising and encouraging performance at lower temperatures [8,15,16].

1.2.2 Current Challenges of SOFC

The operating temperature shows a dominant role in the appreciable performance of SOFC based energy systems. In order to achieve the significant power density, current up-to-date SOFC systems are generally operated at high temperatures (800 – 1000 °C). These high temperature SOFC systems have been successfully developed by organizations like Siemens Westinghouse and Rolls-Royce [6]. However, this high temperature presents some critical challenges in the working of SOFCs such as material degradation problems, technological complications and economic hurdles. With reference to the costs, expensive high temperature alloys and ceramics are used for the fabrication and manufacturing of the cells, which definitely increasing the cost of the SOFC. Material degradation is another challenge and a resistive factor for the broad commercialization of SOFC. The sintering of the nickel particles will be occur at high operating temperature, which eventually deteriorates the porosity and the catalytic activity of the anode. Furthermore, the high operating temperature leads towards long start-up and shutdown timings which greatly limiting the use of SOFCs in portable power and transportation sectors [3,6,12,15]. Therefore, reducing the operating temperature of SOFC to the Intermediate Temperature (IT) regime of 600 – 800 °C, or even low temperature range of less than 600 °C, is a great challenge in the field of SOFC.

1.3 Development of low to intermediate temperature SOFCs

The development of intermediate – temperature solid oxide fuel cell (ITSOFC) or low – temperature solid oxide fuel cell (LTSOFC) is now a global tendency for the commercialization of SOFCs. By the development of LTSOFCs, system cost can be reduce because of broader material choices for interconnects and compressive ceramic seals. Furthermore, the insulation cost and the material degradation mechanism reduce significantly because both radiative heat transfer and sintering rates exponentially drop off at temperatures below 600 °C. Rapid start-up and shut-down will occur at lower

working temperatures. Reduced operating temperatures also offer improved durability, more robust construction through the use of metallic interconnects as well as the advantage of greatly simplified system requirements [6,17]. However, with the decrease in the working temperature, the performance of the cell decreases due to the increase in the internal resistance of a. Therefore, to decrease the internal resistance of SOFC is the key element for the development and deployment of LTSOFCs [6,9,10]. The two main factors to increase the internal resistance of SOFC are following:

- ➢ Resistance of electrolyte, due to low oxygen ion conductivity of electrolyte materials with the decrease in temperature.
- ➢ The polarization resistance of electrodes increases with the decrease of temperature.

In order to reduce the operating temperature of SOFC and to attain a reasonable performance at such temperatures, two main approaches were developed by the researchers and the scientists. First is to reduce the area specific resistance of the fuel cell by decreasing the dimensional thickness of the electrolyte and the second approach is to develop new and novel materials which can give better performance at lower temperatures e.g., the development of novel electrolyte materials which exhibit sufficient ionic conductivity at lower temperatures.

In the past few decades, there has been an enormous increase in the developing of thin film technologies for SOFC to reduce its internal resistance in order to decrease the operation temperature. Thin film processes offer several advantages such as reduction in the ohmic losses, reduction in the sintering temperature, and interfaces can be easily controlled during the synthesis of SOFC electrolyte components. By depositing a thin film of an electrolyte, the electrolyte material can no longer mechanically support the cell. Therefore, in order to support the cell an anode/substrate is commonly employed. However, thin film processes also offer some disadvantages e.g. production period is long, very high cost, film growth is difficult to control. These drawbacks make it difficult to realize the commercialization of LTSOFCs [6].

The second most important practical way to develop ITSOFCs or LTSOFCs is analyzing novel electrolyte materials with enhanced ionic conductivity at reduced temperatures. The oxygen ion conductivity of the traditional electrolyte (YSZ) decreases exponentially

at lower operating temperatures. The ionic conductivity is reduced by approximately three orders of magnitude as the temperature decreases from 800 to 400 °C. Therefore, develop new electrolyte materials with high ionic conductivity in intermediate to low temperature regime is necessary for the development of ITSOFCs and/or LTSOFCs. In this context, doped ceria based materials are the most promising candidates to use as an electrolyte in intermediate and/or low temperature SOFCs [9,11,13,15,17]. The reason behind the use of these materials as an electrolyte along with the objectives of this thesis will be discussed in detail in the second chapter.

1.4 Figurative flow of the thesis

```
                    ┌─────────────────┐
                    │  Introduction   │
                    └─────────────────┘
                             │
                             ▼
            ┌─────────────────────────────────┐
            │  Ceria Based Materials for SOFCs │
            └─────────────────────────────────┘
                             │
                             ▼
    ┌───────────────────────────────────────────────────────┐
    │  Review on Experimentation and Characterization Methods │
    └───────────────────────────────────────────────────────┘
                             │
                             ▼
                  ┌─────────────────────┐
                  │   Experimentation    │
                  └─────────────────────┘
                             │
                             ▼
                ┌─────────────────────────┐
                │  Results and Discussion  │
                └─────────────────────────┘
                             │
                             ▼
          ┌───────────────────────────────────┐
          │  Conclusions & Recommendations     │
          └───────────────────────────────────┘
```
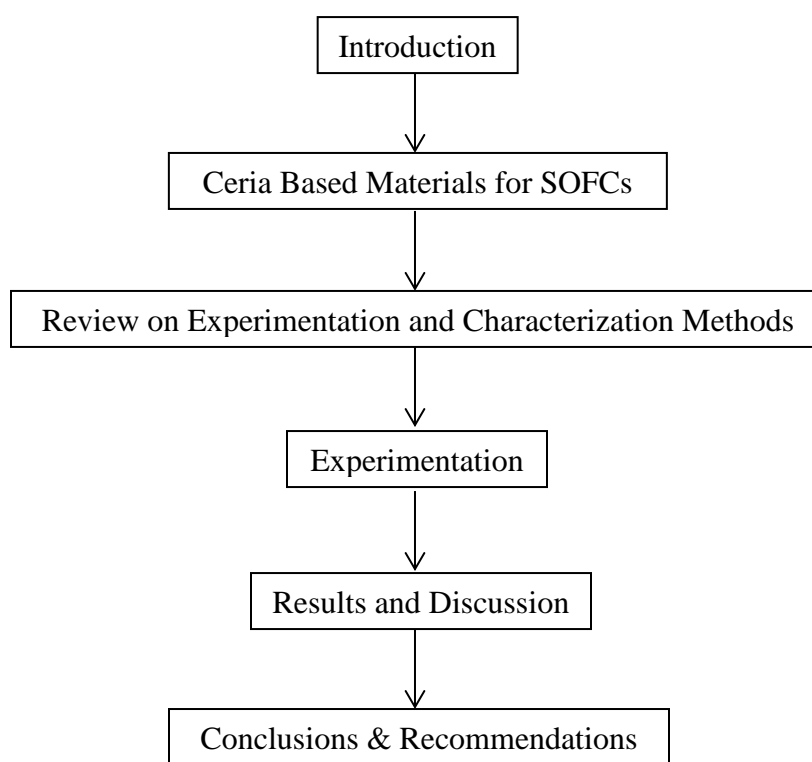
Summary

Fuel cells are electrochemical devices that directly convert the chemical energy of fuels into the electrical energy. Solid oxide fuel cell (SOFC) offers a unique advantage of high efficiency and because of its high operating temperature (800 – 1000 °C) it can be used for both heat and electricity generation. Primarily SOFC consists of three components i.e. anode, electrolyte and cathode. Electrolyte is the heart of a SOFC and traditionally, yttria stabilized zirconia (YSZ) is used as an electrolyte material in SOFC. YSZ offers sufficient ionic conductivity at high temperatures ranges from 800 to 1000 °C. This high operation temperature of SOFC brings some prohibitive factors for its commercialization e.g. material degradation, expensive ceramics and long start-up and shutdown time. Therefore, current challenge in the field of SOFC is to reduce its operating temperature and develop intermediate or low temperature SOFCs. In order to reduce the operating temperature, novel electrolyte materials must be developed that gives sufficient ionic conductivity at relatively low temperatures (500 – 800 °C). Studies shows that the most suitable candidates for intermediate and/or low temperature SOFC are doped ceria based electrolytes. The detail discussion on doped ceria based electrolyte materials will be given in next chapter.

References

[1]   U. Lucia, Overview on fuel cells, Renew. Sustain. Energy Rev. 30 (2014) 164–169.

[2]   I. Dincer, Environmental and sustainability aspects of hydrogen and fuel cell systems, Int. J. Energy Res. 31 (2007) 29–55.

[3]   S. Jiang, Advances and challenges of intermediate temperature solid oxide fuel cells : A concise review, J. Electrochemistry, 18 (2012) 479-495.

[4]   O. Yamamoto, Solid oxide fuel cells: fundamental aspects and prospects, Electrochim. Acta. 45 (2000) 2423–2435.

[5]   P. Singh, N.Q. Minh, Solid oxide fuel cells: Technology status, Int. J. Appl. Ceram. Technol. 1 (2005) 5–15.

[6]   Y. Ma, Ceria-based nanocomposite electrolyte for low-temperature solid oxide fuel cells[Dissertation], Royal Institute of Technology, 2009.

[7]   S. Simeonov, S. Kozhukharov, M. Machkova, N. Saliyski, V. Kozhukharov, Innovative methods and technologies for elaboration of SOFC ceramic materials (Review), Journal of the University of Chemical Technology and Metallurgy, 47, 5 (2012) 485–492.

[8]   R.P. O'Hayre, Fuel Cell Fundamentals, second ed., John Wiley & Sons, INC., 2009.

[9]   M. Lo Faro, D. La Rosa, V. Antonucci, A. Salvatore, Intermediate temperature solid oxide fuel cell electrolytes, Journal of the Indian Institute of Science, 89 (2009) 363-380.

[10]   N. Mahato, K. Balani, A. Gupta, Doped zirconia and ceria-based electrolytes for solid oxide fuel cells : a review, Nanomaterials and Energy, 1 (2011) 27–45.

[11]   A.J. Jacobson, Materials for solid oxide fuel cells †, Chem. Mater. 22 (2010) 660–674.

[12]   B.C. Steele, A Heinzel, Materials for fuel-cell technologies., Nature. 414 (2001) 345–52.

[13]   V. Kharton, F. Marques, A Atkinson, Transport properties of solid oxide electrolyte ceramics: a brief review, Solid State Ionics. 174 (2004) 135–149.

[14] D. Medvedev, A. Murashkina, E. Pikalova, A. Demin, A. Podias, P. Tsiakaras, $BaCeO_3$: Materials development, properties and application, Prog. Mater. Sci. 60 (2014) 72–129.

[15] D. Radhika, A.S. Nesaraj, Materials and components for low temperature solid oxide fuel cells – an overview, Int. J. Renew. Energy Development, 2 (2013) 87–95.

[16] C. Sun, R. Hui, J. Roller, Cathode materials for solid oxide fuel cells : a review, J. Solid State Electrochem, 14 (2009) 1125-1144.

[17] Y. Zhao, C. Xia, L. Jia, Z. Wang, H. Li, J. Yu, et al., Recent progress on solid oxide fuel cell: Lowering temperature and utilizing non-hydrogen fuels, Int. J. Hydrogen Energy. 38 (2013) 16498–16517.

Chapter 2
Ceria Based Materials for SOFCs

The electrolyte material, being the heart of a SOFC unit has been a topic of interest and continuous development. As described in chapter 1 of this thesis, bismuth oxides based materials show highest ionic conductivity and several other oxide materials are also better than doped zirconia and ceria compositions particularly at low temperatures (< 600 °C). Yet, YSZs and ceria-based electrolytes are favored because bismuth oxide based materials are least stable in fuel environments at ~700 °C and possess low-bending strength and toughness. Other oxides have disadvantages, such as high electronic conductivity, increased cost and difficulties in processing. Therefore, YZS and ceria based materials are two most promising options for use as an electrolyte in SOFCs [1]. However, as described in literature, YSZ shows high ionic conductivity only at high temperatures (800 – 1000 °C). The most important advantage associated with ceria based electrolytes is their high ionic conductivity than YSZ particularly at low temperature (<800 °C) [2]. Thus, ceria based electrolyte materials is one of the best option for use in ITSOFCs and/or LTSOFCs.

2.1 Pure Ceria

Cerium oxide or pure ceria (CeO_2) has a cubic fluorite type crystal structure over the complete temperature range from room temperature to the melting point. Cubic fluorite crystal structure of ceria is shown in Fig. 2.1 [3]. The color of pure ceria is pale yellow. The color of ceria also varies with reference to the presence of different lanthanides as dopants e.g. a small doping of almost 0.02% of Pr change the color from pale yellow to brownish yellow. Pure ceria has a density of 7.22 g/cm^3 with the melting point of approximately 2750 K and its specific heat and thermal conductivity is ~0.46 kJ/kg.K and ~0.012 kW/m.K, respectively. Oxygen vacancies are the main ionic defects in pure cerium oxide when the reduction of CeO_2 occurs to CeO_{2-x} [4]. The process of ceria reduction can be written as

$$2O_o + 4Ce_{Ce} \rightarrow O_2 \ (gas) + 2V_o^{\bullet\bullet} + 4Ce_{Ce}^{'} \ \ldots\ldots\ldots\ldots (2.1)$$
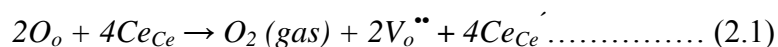
It was found that the pure ceria is an electronic conductor and the ionic transference number for sintered CeO_{2-x} is less than 0.002 when the temperature ranges from 600 °C–

1300 °C [4]. The electronic conductivity of pure ceria is always greater than its ionic conductivity. However, we may say that the pure CeO_2 ceramic is a mixed ionic electronic conductive material and is a poor oxide ion conductor [3]. Magdalena Dudek [5] reported that the bulk electrical conductivity of CeO_2 at 600°C is 6.16×10^{-5} S/cm.
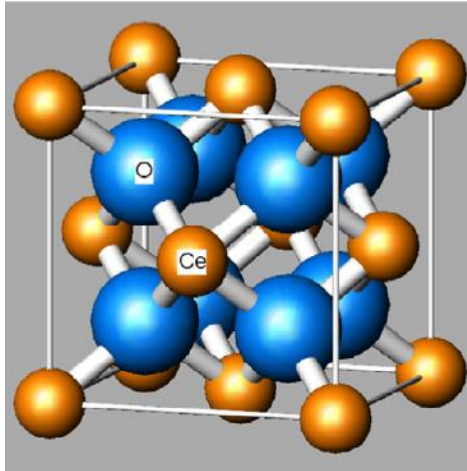
Fig. 2.1 Cubic Fluorite type crystal structure of ceria [3]

The electronic conductivity is caused by polaron hopping and can be described by equation given below [3,4]:

$$\sigma_e T = \sigma_e^0 \exp\left(-\frac{\Delta H_n}{kT}\right) pO_2^{-\frac{1}{4}} \ldots\ldots\ldots\ldots (2.2)$$

where, ΔH_n is the activation energy for the small polaron hopping. It was concluded that a small defect known as polaron is created when the trapping of an electronic carrier becomes occur at a given site as a result of the movement of adjacent atoms or ions [4]. The migration of the entire defect, i.e. the electron (or electron hole) plus distortion is carried out by a thermally activated hopping.

The above equation shows that the electronic conductivity is dependent upon two main factors namely:

- ➢ Temperature
- ➢ Partial pressure of oxygen

It may be concluded that with the increase in temperature and the decrease in the partial pressure of oxygen, the electronic conductivity of pure ceria increases.

The ionic conductivity of pure ceria can be expressed with the help of the following equation:

$$\sigma T = \sigma_0 \exp(-\frac{\Delta E_{act}}{T})\ldots\ldots\ldots\ldots\text{ (2.3)}$$

here, ΔE_{act} is the activation energy involves the enthalpy for movement of O_2 (ΔH_m) and the defect association enthalpy of complexes (ΔH_a).

The ionic conductivity of pure ceria is directly related with the temperature but the problem is that the electronic conductivity also shows the same trend therefore pure ceria cannot be used for applications in solid oxide fuel cell due to its high electronic conductivity.

In order to enhance the ionic conductivity and suppress the electronic conductivity of pure ceria some of the strategies adopted in the literature are given below:

➢ Doping of some trivalent cations of rare earth metals in pure cerium oxide [6].

➢ Addition of carbonates as the secondary phases in the doped ceria based systems [7].

2.2 Doped Ceria

The situation of ionic conductivity is quite different in doped ceria based electrolytes. The ionic conductivity of cerium oxide based electrolyte materials can be enhanced by the introduction of some trivalent dopant ions (Gd^{3+}, Sm^{3+}, Nd^{3+}), due to the increase in the number of oxygen vacancies by charge compensation [8]. The reaction given below show that how the oxygen vacancies are created in doped ceria electrolytes.

$$Gd_2O_3 + CeO_2 \rightarrow 2Gd'_{Ce} + V_o^{\bullet\bullet} + 3O_o\ldots\ldots\ldots\ldots\text{ (2.4)}$$
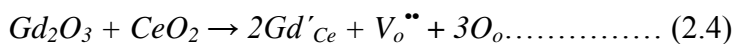
Doped ceria based electrolyte materials are obtained by doping ceria (CeO_2) with a second aliovalent lanthanide metal, yielding a general form denoted by $Ce_{1-\delta}(Ln)_\delta O_{2-1/2\ \delta}$. The addition of substitutional cation (e.g., Gd^{3+}, Sm^{3+}, Y^{3+}), which have lower valency than cerium ion (Ce^{4+}), induces the generation of oxygen vacancies for charge compensation [6].

For example, the substitution of Ce^{4+} with Gd^{3+} causes the negative net charge in the lattice; for every mole of cerium incorporated into the ceria lattice, the charge neutrality condition is kept by forming an oxygen vacancy. Increases the gadolinium concentration increases the number of vacant oxygen sites and thereby leads to significant O^{2-} conductivity. Oxygen is transported by hopping through its vacancy sites (vacancy diffusion mechanism). The amount of oxygen vacancy is determined by the concentration of the dopant ions. However, there is an upper limit to doping because

after a specific upper limit, the concentration of dopant will increase the defects but decrease the conductivity of an electrolyte. This happens because the defects start to interact with each other and eventually the mobility of oxygen vacancies decreases and when mobility decreases, conductivity starts to decrease. The optimal dopant concentration for GDC is approximately 10% [1].

The primary advantage of doped ceria based electrolytes such as gadolinium-doped ceria (GDC) is that it generally shows higher ionic conductivity than YSZ. This relative conductivity advantage is particularly important at low temperatures [1,3]. Fig. 2.2 shows the conductivity of GDC and YSZ at different temperatures and this is evident from the Fig. 2.2 that GDC has low value of activation energy and high value of conductivity at low temperatures as compared to YSZ. The other advantage is the lower cost of doped ceria based electrolyte materials in comparison with LSGM and its derivatives. So, appreciable attention has been concentrated on these materials because they are promising materials in intermediate and/or low temperature SOFCs applications.
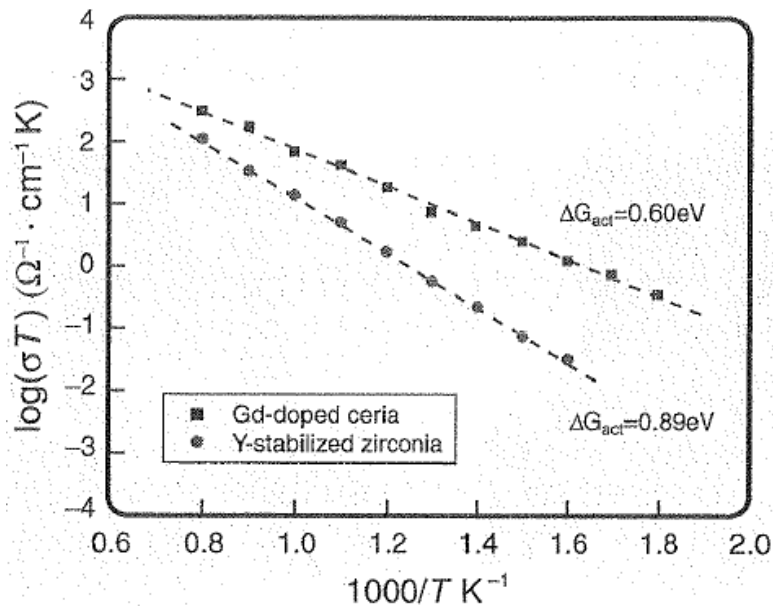
Fig. 2.2 Relationship between conductivity and temperature for GDC and YSZ [6]

Doped ceria based electrolyte materials also offer some disadvantages. The primary disadvantage of doped ceria arises from the fact that under reducing conditions (i.e., at the anode), Ce^{4+} is partially reduced to Ce^{3+}, causing electronic conduction, which can

21

lead to partial internal electronic short circuits, and this problem increases with increasing temperatures. Furthermore, weak mechanical properties generated by the reduction process (ceria chemically expands under reducing conditions) are the question mark on the mechanical stability of SOFC.

A typical and most commonly used electrolyte formulation for SOFC applications is $Ce_{0.9}Gd_{0.1}O_{1.95}$, abbreviated as GDC10. It has an ionic conductivity of 0.01 Scm^{-1} at 500 °C [9]. Fig. 2.3 shows that how the ionic and electronic conductivities of GDC10 vary with temperature. It is evident from Fig. 2.3 that under reducing conditions i.e. at the anode, GDC10 has higher values of electronic conductivity than ionic conductivity when temperature is greater than about 550 °C [6]. Therefore, gadolinium doped ceria (GDC) is not a best option to employ as an electrolyte material in intermediate temperature solid oxide fuel cells (ITSOFCs). In the category of doped ceria based materials, samarium doped ceria (SDC) is another promising candidate to use as an electrolyte in ITSOFCs and/or LTSOFCs. The reason why SDC is used as an electrolyte will also be discussed here in the next section.

Fig. 2.3 Ionic and electronic conductivities of GDC10 at the anode [6]

2.3 Samarium doped ceria

In doped ceria based electrolyte materials, ionic conductivity mainly depends upon the following factors [10]:

➤ type of the dopant ion
➤ concentration of the dopant ion

22

> concentration of oxygen vacancy

> enthalpy for defect association

The ionic conductivity in doped ceria based systems is closely and complicatedly related to the relationships among the above mentioned four factors. Such a relationship is not simple from point to point, but a co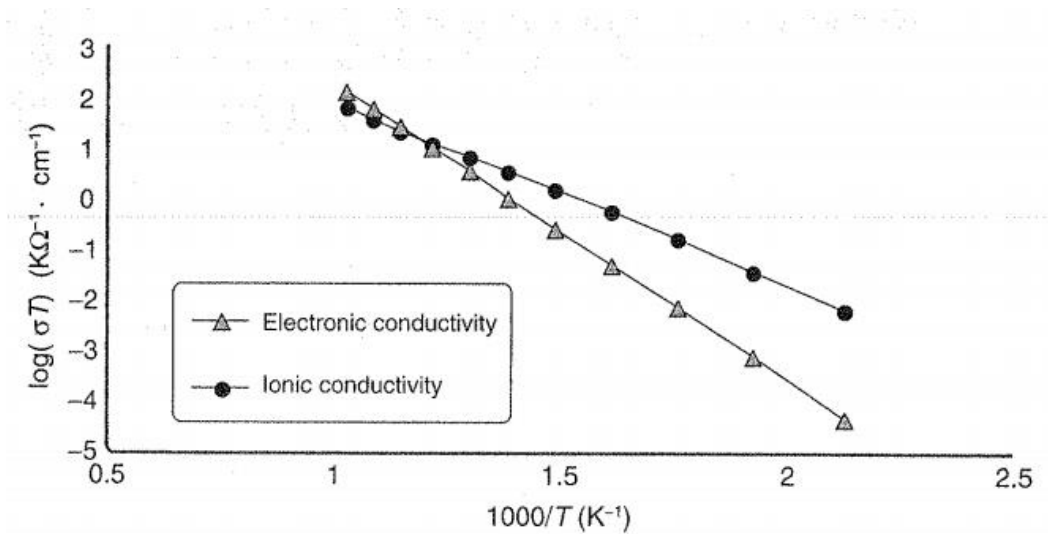mbined result of several factors. Therefore, it is suggested in a few studies that the doped ceria electrolytes will show the highest value of electrical conductivity when the dopant ion has a radius closest to the critical radius. However, along with the radius some other important factors that significantly influence the electrical conductivity are the global lattice parameter change and the localized defect structure and energetics. Among the doped ceria solid electrolyte materials, samarium doped ceria (SDC) was found to have the highest ionic conductivity. The addition (doping) of Sm^{3+} ion among rare-earth metals with an ionic radius of 1.08 Å gives the maximum electrical conductivity [8,10]. This is due to the similar ionic radius of the dopant ion and the host ion [6], which subsequently resulting in the minimum association enthalpy between the dopant ion and oxygen vacancy. The reaction given below in the form of Kroger-Vink notation shows that how the oxygen vacancy is created by the doping of samarium into ceria:

$$Sm_2O_3 + CeO_2 \rightarrow 2Sm'ce + 3O^x_o + V^{\bullet\bullet}_o \ldots\ldots\ldots\ldots (2.5)$$
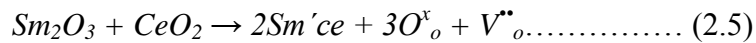
The optimal dopant concentration for SDC is 20 mole% i.e. $Ce_{0.8}Sm_{0.2}O_{1.9}$ [10] after which the ionic conductivity starts to decrease as the dopant concentration increases. This happens because of the increase interaction between the dopant ions and the point defects i.e., oxygen vacancies. The ionic conductivity of $Ce_{0.8}Sm_{0.2}O_{1.9}$ reported at 800 °C is ~0.0223 S/cm with the activation energy of ~0.89 eV. The thermal expansion co-efficient of $Ce_{0.8}Sm_{0.2}O_{1.9}$ is ~17.338 ppm/°C [10]. Samarium doped ceria is relatively inert towards promising electrode materials such as Ni-ceria cermet anodes and LSCF cathodes. Other potential advantage is its comparable thermal expansion coefficient with iron base alloys like stainless steels, which makes SDC a promising candidate for metal-supported SOFCs.

The doping of samarium into the ceria lattice significantly enhances the ionic conductivity but at the mean time some drawbacks/challenges are also associated with

SDC which limits its use as an electrolyte material in SOFCs. Some of the critical drawbacks/challenges are given below [11]:

> Insufficient ionic conductivity as compared to the minimum value required (~ 0.1 S/cm) to use as an electrolyte in SOFCs.

> Partial reduction of cerium ions from Ce^{+4} to Ce^{+3}, which causes n-type conduction and as a result both open circuit voltage (OCV) and efficiency of the fuel cell decreases.

> The electronic conduction also suffers the mechanical properties of the cell because of lattice expansion therefore improper mechanical stability is also a one of the challenges in SDC based SOFCs.

Now the question is how to overcome these challenges? A single line answer of this question is "the addition of some salts like chlorides, carbonates etc. in samarium doped ceria"; but the detailed discussion of this answer will be given in the next paragraph.

2.4 SDC-Carbonate composite electrolyte

Composite electrolytes are mainly physical mixtures comprising of two or more solid phases that acquire different ionic conduction characteristics. Composite electrolyte materials generally exhibit better ionic conductivity, but the effects are not simply additive just like the doping of some rare-earth metals; rather they are synergistic in the sense that the overall conductivity is considerably greater than in both of the fundamental phases. The enhancement in the conductivity, the supposed composite effect, is suggested to be due to high ionic conductivity in the interface region between components. Therefore, the initial data to manufacture composite electrolytes is to achieve more interface region for high ionic conduction pathway. Ceria-carbonate, ceria-halide, ceria-sulfate, ceria-hydroxide and ceria-oxide are generally analyzed and tried as the electrolyte materials for LT-SOFCs. The ceria oxides in composite electrolytes are either Samarium-doped ceria (SDC) or Gadolinium-doped ceria (GDC) or Yttrium-doped ceria (YDC). Among these composite electrolytes, doped ceria-carbonate is the most suitable and potential candidate as compared with other doped ceria-salt composites. Doped ceria-carbonate shows enhanced ionic conductivity, improved stability and low electronic conductivity at reduced operating temperatures [12,13].

The key property and the main advantage of doped ceria-composite electrolyte in SOFC applications over the traditional single-phase electrolytes is the multi-ion effect. It is concluded from the numerous studies and investigations that the ceria-carbonate composite electrolyte is a multi-ion system comprising of both intrinsic and extrinsic natures, intrinsic ions include oxygen ion (O^{2-}) and carbonate ion (CO_3^{2-}) while the extrinsic ion is proton (H^+) when the composite electrolyte is situated in hydrogen environment i.e., hydrogen as a fuel is supplied at the anode side of the solid oxide fuel cell [13].

SDC – carbonate composite electrolytes can be prepared by two processes i.e. multi – step process and single – step process. In the initial step of multi – step process, SDC was prepared in the form of a solid electrolyte usually through wet-chemistry routes and then carbonates are added in the SDC powder generally by solid-state reaction method, while in the single – step process addition of carbonates and preparation of a SDC both are taking place in a single step [14].

Ning Zuo et al. [15] synthesized the samarium doped ceria - carbonate composite electrolyte based on $Ce_{0.8}Sm_{0.2}O_{1.9}$ – 25 wt. % K_2CO_3 by two step process. In the first step, SDC powder was prepared through carbonate co-precipitation process. In the next step, SDC was mixed with 25 wt. % K_2CO_3 and calcined at 680 °C for 30 min to obtain the SDC – carbonate composite electrolyte. A mixture of 45 wt. % electrolyte, 45 wt. % NiO and 10 wt. % starch was used as an anode while the mixture of 40 wt. % electrolyte and 60 wt. % SSC ($Sm_{0.5}Sr_{0.5}CoO_2$) was used as a cathode. In order to construct the anode-supported single cell, a composite electrolyte, an anode and a cathode were uni-axially pressed and the resulted pellets were sintered at 600 °C for 30 min. The single cell was electrically tested in a temperature ranged from 550 °C to 700 °C using hydrogen as a fuel and air as an oxidant. The maximum power density and open circuit voltage achieved were 602 mW/cm^2 and 1.05 V at 700°C, respectively.

Rizwan Raza et al. [11] successfully developed the ceria-carbonate composite electrolyte with one-step chemical co-precipitation process i.e. prepared the SDC and mixed the carbonates in the same process. A suitable amount of Na_2CO_3 solution was gradually added to complete the ceria – carbonate composites within a wet-chemical co-precipitation process. In this way a mixture of carbonate and SDC was obtained in the

same process. The composite electrodes were synthesized by solid state reaction method using lithium, copper and nickel carbonates. The fabrication of the fuel cell was done by hot pressing technique. Anode, electrolyte and cathode were pressed in one step to form a fuel cell assembly. I-V and I-P characteristics of the single fuel cell were determined and it was found that the maximum power density of 1150 mW/cm^2 and an open circuit voltage of 1.018 V were obtained at 500°C. Thus, single-step process is more beneficial for the synthesis of ceria-carbonate composite electrolyte. In the next section, the objectives of this study will be described in order to carry out the experimentation.

2.5 Objectives of the Study

In context of the detailed discussion in the first two chapters of this thesis and after a detailed literature review the objectives of this study are defined and given below:

- Synthesis of samarium doped ceria (SDC) using co-precipitation method in order to develop complete understandings and basics of the synthesis procedure.
- Synthesis of SDC-composite electrolyte by the addition of lithium and sodium carbonate i.e., $(LiNa)_2CO_3$-SDC in order to study the effect of carbonates on the ionic conductivity of the electrolyte.
- To investigate the effect of pH of Medium on the microstructure of SDC electrolyte.
- To analyze the effect of calcination temperature on the microstructure of SDC-K_2CO_3 composite electrolyte.
- To report the effect of co-doping by Yttrium on the ionic conductivity of SDC.
- To perform a chemical compatibility test of co-doped electrolyte (YSDC) with lithiated NiO cathode.

Summary

Ceria based electrolyte materials are the promising candidates for intermediate temperature solid oxide fuel cells (ITSOFCs). The ionic conductivity of pure ceria is very much low and insufficient to use as an electrolyte in SOFCs, furthermore, it is also an electronic conductor thus doping of some trivalent atoms like gadolinium, samarium and yttrium etc. is done in pure ceria to enhance its ionic conductivity. In ceria based electrolytes doped with trivalent atoms, the doping of samarium at the molar concentration of 20 % shows the highest value of ionic conductivity. However, in order to further enhance the ionic conductivity and suppress the electronic conductivity of SDC, a concept of composite electrolyte is developed. In the category of composite electrolytes, ceria-carbonate composite electrolyte materials show the highest value of ionic conductivity and give the best fuel cell performance in hydrogen and oxygen environment. Thus, they are the most suitable candidates to use as an electrolyte in ITSOFCs. At the end of this chapter, the objectives of this study were given in order to carry out the detailed experimentation.

References

[1]   V. Kharton, F. Marques, A Atkinson, Transport properties of solid oxide electrolyte ceramics: a brief review, Solid State Ionics. 174 (2004) 135–149.

[2]   N. Mahato, K. Balani, A. Gupta, Doped zirconia and ceria-based electrolytes for solid oxide fuel cells: a review, Nanomaterials and Energy, 1 (2011) 27–45.

[3]   M. Lo Faro, D. La Rosa, V. Antonucci, A. Salvatore, Intermediate temperature solid oxide fuel cell electrolytes, Journal of the Indian Institute of Science, 89 (2009) 363-380.

[4]   M. Mogensen, N.M. Sammes, G.A. Tompsett, Physical , chemical and electrochemical properties of pure and doped ceria, Solid State Ionics, 129 (2000) 63–94.

[5]   M. Dudek, Ceramic oxide electrolytes based on CeO_2—Preparation, properties and possibility of application to electrochemical devices, J. Eur. Ceram. Soc. 28 (2008) 965–971.

[6]   R.P. O'Hayre, Fuel Cell Fundamentals, second ed., John Wiley & Sons, INC., 2009.

[7]   C. Xia, Y. Li, Y. Tian, Q. Liu, Z. Wang, L. Jia, et al., Intermediate temperature fuel cell with a doped ceria–carbonate composite electrolyte, J. Power Sources. 195 (2010) 3149–3154.

[8]   G. Kim, N. Lee, K. B. Kim, H. Chang, S. J. Song, et al., Various synthesis methods of aliovalent-doped ceria and their electrical properties for intermediate temperature solid oxide electrolytes, Int. J. Hydrogen Energy. 38 (2013) 1571–1587.

[9]   D. Radhika, A.S. Nesaraj, Materials and components for low temperature solid oxide fuel cells–an overview, Int. J. Renew. Energy Development, 2 (2013) 87–95.

[10]   Y. P. Fu, S. B. Wen, C. H. Lu, Preparation and characterization of samaria-doped ceria electrolyte materials for solid oxide fuel cells, J. Am. Ceram. Soc. 91 (2007) 127–131.

[11]   R. Raza, X. Wang, Y. Ma, X. Liu, B. Zhu, Improved ceria–carbonate composite electrolytes, Int. J. Hydrogen Energy. 35 (2010) 2684–2688.

[12]   L. Fan, C. Wang, M. Chen, J. Di, J. Zheng, B. Zhu, Potential low-temperature application and hybrid-ionic conducting property of ceria-carbonate composite electrolytes for solid oxide fuel cells, Int. J. Hydrogen Energy. 36 (2011) 9987–9993.

[13]   X. Wang, Y. Ma, B. Zhu, State of the art ceria-carbonate composites (3C) electrolyte for advanced low temperature ceramic fuel cells (LTCFCs), Int. J. Hydrogen Energy. 37 (2012) 19417–19425.

[14]   M. A. Khan, R. Raza, R. B. Lima, M. A. Chaudhry, E. Ahmed, G. Abbas, Comparative study of the nano-composite electrolytes based on samaria-doped ceria for low temperature solid oxide fuel cells (LT-SOFCs), Int. J. Hydrogen Energy. (2013) 2–9.

[15]   N. Zuo, M. Zhang, Z. Mao, Z. Gao, F. Xie, Fabrication and characterization of composite electrolyte for intermediate-temperature SOFC, J. Eur. Ceram. Soc. 31 (2011) 3103–3107.

Chapter 3
Review on Experimentation and Characterization Methods

In this chapter, a concise review about the different routes for the synthesis of nanoparticles is given along with the characterization tools which are commonly used for the analysis of these synthesized nanoparticles.

3.1   Solid State Reaction Method

The solid state reaction method is commonly implemented for the fabrication of ceramic compounds mainly due to its simplicity. In solid state reaction method, direct reaction of solids occurs to form the final products and principally no decomposition is involved. The reactants must have large surface area in order to maximize the contact between them. Generally, solids do not react with solids at low temperatures even if thermodynamics is favorable so high temperature must be employed to increase the rate of diffusion or decrease the diffusion lengths between the reactants. The rate of nucleation of such type of reactions may be enhanced by providing a structural similarity between the reactants and products [1,2]. The major steps in conventional solid state synthesis are given below:

➢ The selection of the appropriate starting materials e.g., reactive starting materials are better than inert and the reactants must be in the form of fine grain powders to maximize the surface area.

➢ Weigh out the starting materials in proper ratio according to the stoichiometric calculations.

➢ Then thorough mixing of the reactants by using agate mortar and pestle or ball mill. Organic solvent may be used to facilitate the mixing process.

➢ After thorough mixing, heat treatment is done at a suitable temperature to achieve the desired phase. The heating must be done in an inert crucible/container and/or in a specific environment.

➢ At the end, grinding of the product is done to obtain the fine particles.

The major advantages include the solid state reactions are simple to perform; the starting materials for such type of reactions are readily available at low cost and such reactions are clean i.e. they do not involve other chemical elements. However, the main drawbacks of solid state reaction method are homogeneous distribution is difficult to achieve especially for dopants, high calcination temperature, particle size is difficult to control, low surface area and reaction with containers/crucibles etc. [3]. In order to overcome the drawbacks of solid state reaction method, some wet chemistry based routes are developed. In the next section of this chapter, we will discuss the properties and different types these wet chemistry routes.

3.2   Wet Chemistry Routes for the Synthesis of Ceramic Compounds

The major characteristics of wet chemistry routes are the atomic scale homogeneous mixing of raw materials and a particle size, surface morphology along with surface area can be made controllable by the use of such routes. The basic approach is to decrease the diffusion lengths through the intimate mixing of cations. Primary advantages include lower reaction temperatures, elimination of intermediate impurity phases and the products obtained are of high surface area. Major examples of such routes are co-precipitation, sol-gel process and hydrothermal etc. [3]. In the next two sections, a brief review of co-precipitation and sol-gel process is given.

3.2.1   Co-precipitation

Co-precipitation reaction consists of nucleation, growth coarsening and/or agglomeration processes. All these processes occur simultaneously. Co-precipitation method shows the following properties [4]:

➢ The products formed are commonly insoluble species and formed under the conditions of high degree of supersaturation.

➢ The key step during co-precipitation method is nucleation. In this step, the formation of a large number of small particles will occur.

➢ The particle size, surface morphology and the properties of the products during synthesis mainly depend upon the secondary processes e.g., Ostwald ripening and aggregation.

> In order to induce the precipitation, the supersaturation conditions are necessary. These conditions will occur as a result of the following chemical reaction,

$$xA^{y+} (aq) + yB^{x-} (aq) \leftrightarrow A_xB_y (s)\ldots\ldots\ldots\ldots (3.1)$$
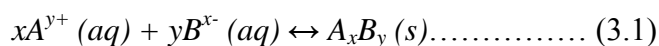
Typical co-precipitation synthetic methods include the formation of metals from aqueous solutions, by reduction from nonaqueous solutions, electrochemical reduction, and decomposition of metalorganic precursors; formation of oxides from aqueous and nonaqueous solutions; formation of metal chalconides by reactions of molecular precursors; microwave/sonication-assisted coprecipitation.

3.2.2 Sol-gel Process

The sol-gel process is a wet chemistry base route in which an integrated network usually known as gel is formed by the combination of sol. Sol is the colloidal particles for the formation of nanoscale particles. Sol may be a chemical solution (sol short for solution). Commonly used precursors for sol-gel process are metal alkoxides and metal chlorides. Sol is formed when the precursors undergo hydrolysis and polycondensation reactions to form a colloid. Sol is basically a system composed of nanoparticles which are completely dispersed in a solvent. The sol evolves then towards the formation of an inorganic continuous network containing a liquid phase (gel).

Formation of a metal oxide involves connecting the metal centers with oxo (M – O – M) or hydroxo (M – OH – M) bridges, therefore generating metal-oxo or metal-hydroxo polymers in solution [5].

Drying is carried out to remove the liquid phase from the integrated network i.e., gel. In order to enhance the mechanical properties and favor further polycondensation reaction a heat treatment (calcination) of the dried sample may be performed.

In addition to these wet chemistry routes some advanced synthetic methods are also exploited and studied in literature. Primarily, such methods include the deposition techniques for the formation of thin films of desired compounds over the substrates.

3.3 Thin Films Deposition Processes

3.3.1 Physical Vapor Deposition

In physical vapor deposition (PVD), film is formed by atoms directly transported from source/target to the substrate. PVD processes take place in a vacuum chamber, and by

one mean or another, create a low-pressure vapor of the material to be deposited. Some of this vapor will condense on the work piece and thereby start to deposit as a thin film. Simply melting a material in vacuum, depending on its vapor pressure, may sometimes produce a useful deposit of material. Sublimation furnaces are engaged to efficiently evaporate selenides, sulfides, and some other oxides [6]. The evaporative materials are sintered and pressed to form pellets that are then subjected to radiant heat source. The most common example of these kind of evaporative materials include graphite and refractory metals, mostly formed by hot pressing of powder to form pellets.

The heating is normally done by external tungsten wire resistance heating elements. The heating of evaporant source by resistive heating element (in conventional evaporation process) include disadvantages like contamination caused by the supportive materials, crucibles, and heaters that hinders the deposition of pure films. It also includes the drawback of evaporating high melting point materials at high rates. Electron beam evaporation overcomes these limitations and therefore it is a better vacuum based evaporative film deposition technique. This technique has the advantage of evaporating a wide range of materials at practical rates. The technique works by placing the evaporative material in water cooled crucible or copper hearth. A small fraction of evaporant sublimes or melts that assured the purity of evaporative material as the crucible is water cooled that hinders its melting and contamination with the source evaporant.

Major types of physical vapor deposition processes are given below [6]:

- Evaporation
  - Thermal evaporation
  - Electron beam evaporation
- Sputtering
  - DC sputtering
  - DC magnetron sputtering
  - Radio frequency sputtering
  - Reactive PVD

3.3.2   Chemical Vapor Deposition

In chemical vapor deposition (CVD), the film is formed by chemical reaction on the surface of a substrate. It does not require vacuum or unusual levels of electric power. CVD has the ability to deposit films or coatings of metals, ceramics and semi-conductors. Major advantages of CVD processes are high growth rate with good reproducibility, it can deposit materials which are hard to deposit e.g., by evaporation, can grow epitaxial films and more conformal coverage. However, CVD processes also offer some disadvantages such as high process temperature, it is a complex process i.e. toxic of corrosive gases and produced films may not be pure e.g., hydrogen incorporation [6,7]. The examples of CVD processes are given below:

➢ Atmospheric chemical vapor deposition (APCVD)

➢ Low pressure chemical vapor deposition (LPCVD)

➢ Plasma enhanced chemical vapor deposition (PECVD)

The factors that distinguished PVD from the CVD are:

➢ In PVD, solid and/or molten sources are used while in CVD gaseous precursors are commonly used.

➢ Source atoms enter into the gas phase by some physical mechanisms, such as, evaporation or collisional impact.

➢ Gaseous species are transported through the reduced pressure environment.

➢ Generally, no chemical reaction occurs in the gas phase and at the surface of the substrate.

After the successful synthesis of nanoparticles and/or thin films the detailed analysis is done by employing different characterization techniques. In the next section, a brief overview of some characterization tools are given which are mostly used in order to analyze the ceramic compounds in this thesis.

3.4   Characterization Techniques

3.4.1   X-ray Diffraction

X-rays are electromagnetic radiation with a wavelength of ~1Å. Their wavelength is shorter than ultraviolet and longer than γ-rays in the electromagnetic spectrum. X-rays are commonly used to study the phase and structural arrangement of atoms and molecules in a broad range of materials because the wavelength of X-rays is comparable

to the size of atoms. X-rays are generated when a high-energy charged electron beam is accelerated through a high voltage field bombards on a solid target, normally copper or molybdenum. As incident electrons collide with atoms in the target, the inner shell electrons in atoms can be ejected through ionization process by the high energy electrons. A free electron in an outer orbital will immediately fill the vacant site and an X-ray photon is emitted due to the energy released in the transition. The relationship between the energy E of X-ray radiation and its wavelength is given by the equation Eq. (3.1) where h is Planck's constant and c is the speed of light in vacuum.

$$E = \frac{hc}{\lambda} \ldots \ldots \ldots \ldots \ldots (3.2)$$

After the collision of X-rays with the crystals, some of them will be deflected away from the direction they originally travel and these deflected X-rays are measured in diffraction experiments. The scattered X-rays carry information about the electron distribution in materials and each crystalline solid has its unique X-ray pattern, therefore it can be used as a 'fingerprint' for identification. Bragg's Law is a simple and straightforward description for crystal diffraction.

The derivation of Bragg's Law is shown in Figure 2.1. The incident beams 1&2 are always in phase and parallel up to the points A&D, where beam 1 strikes the top layer at atom D, while beam 2 continues to the next layer where it is scattered by atom B. Therefore, beam 2 must travel an extra distance (AB + BC) before the two beams continue to travel adjacent and parallel as 1'&2'. This extra distance must equal an integral (n) multiple of the wavelength (λ) for the two beams to be in phase.
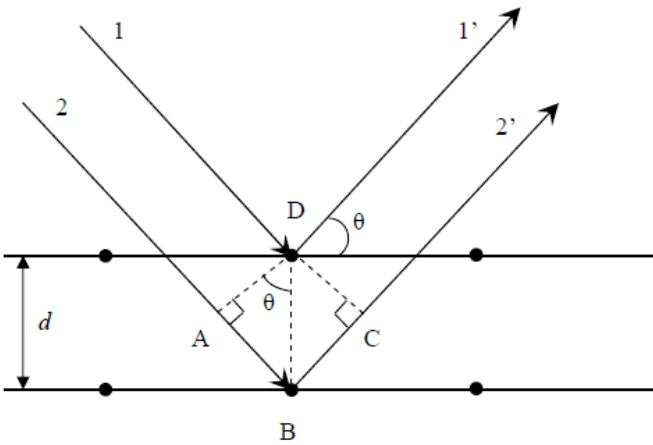

Fig. 3.1 Description of Bragg's Law

35

d is the perpendicular distance between pairs of adjacent planes and θ is the angle of incidence, therefore:

$$AB = BC = d \sin \theta$$

$$2AB = n\lambda$$

$$2d\sin \theta = n\lambda \ldots\ldots\ldots\ldots (3.3)$$

The unit cell parameter of a crystal can be calculated by the distance between adjacent atomic planes d. For cubic crystals ($\alpha = \beta = \gamma = 90°$), the d-spacing for any set of planes is given by,

$$\frac{1}{d_{hkl}^2} = \frac{h^2}{a^2} + \frac{k^2}{b^2} + \frac{l^2}{c^2} \ldots\ldots\ldots\ldots\ldots (3.4)$$

here h, k and l are the miller indices while the unit cell parameters are a, b and c.

The equation will be simplified if the crystal are cubic i.e. $a = b = c$

$$\frac{1}{d_{hkl}^2} = \frac{h^2 + k^2 + l^2}{a^2} \ldots\ldots\ldots\ldots\ldots (3.5)$$

Powder X-ray Diffraction is the most widely used X-ray diffraction technique for materials characterization. Using Debye-Scherrer equation we can calculate the crystallite size of the crystals. Scherrer equation;

$$D_{XRD} = 0.9\,\lambda\,/\,\beta.\cos\theta \ldots\ldots\ldots\ldots (3.6)$$

λ is the wavelength of the X-rays (nm), θ is the diffraction angle, and β is the corrected full width at half maximum (FWHM) intensity. Peaks with significant intensities were used for the calculations.

The density is an important factor for ceramics as it can greatly affect the material property especially the conductivity for electroceramics. The well densified ceramics would have higher conductivity compared to the less densified ones, in which pinholes and cracks could separate and /or block the conduction path. The theoretical density (D) of ceramics can be calculated by the following equation:

$$D = \frac{MZ}{N_{av}V} \ldots\ldots\ldots\ldots (3.7)$$

M is atomic weight (g mol^{-1}), 'V' is the volume of a unit cell (Å^3) which can be calculated by the lattice parameter (a), of the unit cell, N_{Av} is Avogadro's constant and Z is the formula unit and for cubic fluorite based structures like CeO_2 and ZrO_2 the value of Z is 4.

3.4.2   Scanning Electron Microscopy

Electron microscopes are microscopes that use electron beams to illuminate the specimen and take highly magnified images. They can achieve much higher resolution than the light-powered optical microscopy, because the wavelength of electron is about 100,000 times shorter than visible light.

A Scanning Electron Microscope (SEM) takes images by scanning across a rectangular area of the sample with a focused electron beam. Particularly, an electron gun is used for the thermionic emission of the electron beam. This electron gun is fitted with a tungsten filament cathode. Tungsten is used for heating in thermionic electron guns to produce an electron beam because of its highest melting point and lowest vapor pressure among metals. The electron beams are focused by several condenser lenses to a spot with ~4–50 Å diameters and are adjusted and controlled by the deflection coils before finally incident onto the sample. The electrons lose energy when the electron beam interacts with the specimen and the lost energy will be converted into other forms such as heat, emission of secondary electrons and emission of light or X-rays, which can be detected by specialized detectors. Fig. 3.2 shows a schematic diagram of an SEM.
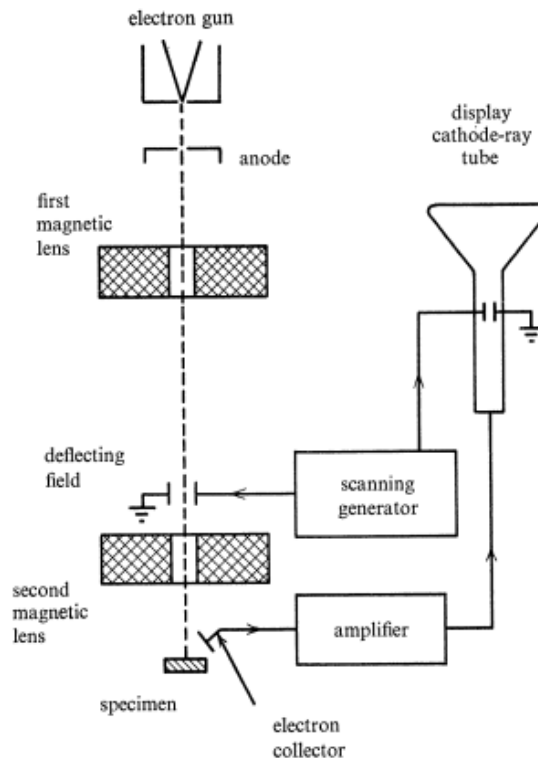

Fig. 3.2 Schematic representation of SEM [8]

The major steps for the sample preparation in order to carry out SEM analysis are:

> ➢ Sectioning
>
> ➢ Mounting
>
> ➢ Grinding
>
> ➢ Polishing
>
> ➢ Etching

3.4.3 Energy Dispersive Spectroscopy

Energy Dispersive Spectroscopy (EDS) or Energy Dispersive X-ray analysis (EDX) is a compositional elemental analysis technique for chemical characterization of the specimen. EDS is always used in conjunction with TEM and/or SEM. The principle of EDS is described as when focused beam of high energy electrons is bombarded onto a solid sample, X-rays are emitted. The detector in make use of these x-rays to obtain localized chemical analysis. Typical resolution is of 150 eV. Quantitative analysis and elemental mapping are also possible through EDS.

When electrons strike the specimen, the electrons contained in specimen are excited creating vacant places in the atomic shells. Electrons in the higher shells fill these vacancies. The energy is released in this process in form of x rays. All elements emit X-rays with characteristic energy values. Each element in periodic table has its specific energy value which makes elemental analysis through EDS possible. Kα X-rays are emitted when an electron from L shell fills the vacancy in K shell of the atom. Letters K, L, M represents the shell from where electrons are emitted and α, β, γ represents the shell where they are substituted. Sample preparation is same as for SEM. In principle, all elements in periodic table from beryllium to uranium (atomic number 4 to 92) can be detected by EDS.

Summary

In this chapter, a brief review of different experimental and characterization methods is given for the synthesis and analysis of ceramic compounds. Conventionally, solid state reaction method is employed because of its simplicity; however, this method also offers some drawbacks like high calcination temperature, inhomogeneity and uncontrollable particle size distribution. Therefore, some wet chemistry routes such as co-precipitation, sol-gel process and hydrothermal etc. are exploited in order to overcome the drawbacks of solid state reaction method. In wet chemistry routes, atomic scale mixing of raw materials is possible and particle size, surface morphology and homogeneity can be made controllable. In addition to wet chemistry routes some thin film deposition processes like physical vapor deposition and chemical vapor deposition are also developed in order to form a thin layer of desired ceramic compound on a substrate. Characterization techniques like X-ray diffraction, scanning electron microscopy and energy dispersive spectroscopy are used for the microstructure analysis of the ceramic compounds.

References

[1]   A. R. West, Solid State Chemistry and its Applications, John Wiley & Sons Ltd. 1984.

[2]   J. D. Corbett, in: A. K. Cheetam and P. Day (Eds.), Solid-State Chemistry - Techniques, Clarendon Press, Oxford, 1987.

[3]   Z. Shao, W. Zhou, Z. Zhu, Advanced synthesis of materials for intermediate-temperature solid oxide fuel cells, Prog. Mater. Sci. 57 (2012) 804–874.

[4]   I.M. Kolthoff, Theory of Coprecipitation - The formation and properties of crystalline precipitates, Academic Press, 1985.

[5]   C.J. Brinker and G.W. Scherer, Sol-gel Science: The Physics and Chemistry of Sol-gel Processing, (1990).

[6]   M. Ohring, Materials Science of Thin Films - Deposition & Structure, second ed., 2002.

[7]   J. George, Preparation of Thin Films, Marcel Dekker, INC., 1992.

[8]   http://en.wikipedia.org/wiki/Scanning_electron_microscope (accessed in August 2011)

Chapter 4
Experimentation

A number of experiments were performed to carry out the specific objectives mentioned in Chapter 2. However, the details of the following major experiments are given in this chapter:

1. Synthesis of samarium doped ceria (SDC).
2. Synthesis of SDC-carbonate composite with the addition of lithium and sodium carbonate i.e. $(LiNa)_2CO_3$-SDC (LN-SDC).
3. Synthesis of SDC at different pH to study the effects of pH of medium on the microstructure of SDC.
4. Synthesis of SDC-Carbonate composite by the addition of potassium carbonate to carry out the effects of calcination temperature on the microstructure of SDC-K_2CO_3.
5. Synthesis of Yttrium-SDC co-doped electrolyte to investigate study the effect of yttrium doping on the conductivity of SDC.
6. Chemical compatibility test of YSDC (electrolyte) with lithiated nickel oxide (cathode).

4.1 Experimentation and Characterization of samarium doped ceria (SDC)

4.1.1 Synthesis of SDC

The ceramic electrolyte $Ce_{1-x}Sm_xO_{2-\delta}$ (x = 0.2) was prepared by using co-precipitation method using cerium nitrate hexahydrate and samarium nitrate hexahydrate as the precursors. Stoichiometric amounts of $Ce(NO_3)_3.6H_2O$ and $Sm(NO_3)_3.6H_2O$ were dissolved in de-ionized water. The concentration of the precursor solution was 0.5 M. This solution was stirred to obtain a transparent homogenous solution. Then poured 25% Ammonia Solution in the precursor solution until the precipitation occurred with a curd type slurry look. Now again stirred the solution consisted of precipitates and dried it on a hot plate at 200 ºC for 2 hrs. Pale yellow matter was obtained after the complete drying. Then ground that matter to form a fine powder and afterwards calcined the dried sample in a furnace at 600 ºC for 2 hrs with the heating rate of 5ºC/min.

4.1.2 Characterization and conductivity measurement of SDC

Phase purity and crystal structure of the prepared electrolyte was determined by X-ray diffraction equipment (STOE Germany). X-ray powder diffraction (XRD) of the sample was recorded using CuKα radiation (λ = 1.5425 Å), with 2θ varying from 10° to 80°. The diffraction pattern was scanned in steps of 0.015°. The morphology and the particle size of the synthesized sample were examined by scanning electron microscopy (JEOL Analytical SEM). In order to the measure the conductivity of the electrolyte, a pellet was formed with the help of a hydraulic press. The pressure applied was 5 kg/cm^2 for about 10 minutes. The thickness of the pellet was 1.37 mm while the diameter was 10 mm. The pellet was sintered at 1100 °C for 3 hours. DC conductivity was measured by LCR meter (Wayne Kerr Electronics) up to the temperature of 650 °C.

4.2 Experimentation and characterization of (LiNa)₂CO₃-SDC (LN-SDC)

4.2.1 Synthesis of (LiNa)₂CO₃-SDC (LN-SDC)

Samarium doped ceria – carbonate (LN – SDC) ceramic electrolyte was prepared through one step co-precipitation method by the addition of lithium and sodium carbonate in SDC solution. Add 3.4702 g of Ce(NO₃)₃.6H₂O & 0.889 g of Sm(NO₃)₃.6H₂O in 20 mL of deionized water. Here Molarity = 0.5 M. Stir the above solution at room temperature for about 45 minutes, and then the solution was again stirred for about 45 minutes at 80 °C for homogenization. Then 0.7350 g of Li₂CO₃ & 1.06 g of Na₂CO₃ were added in 20 mL of deionized water and stirred at 100 °C for about one hour. Here Molarity = 0.5 M. Pour the carbonate solution in to the SDC solution (drop wise) and stirred the solution at room temperature for an hour. Then heat and stir the above solution on a hot plate at 160 °C for half an hour. Completely dry the above solution at 120 °C in a drying oven for about 10 hours. Finally, the dried powder was calcined at 800 °C for 5 h to obtain dense electrolyte, and then the calcined powder was ground in a mortar with a pestle to achieve homogeneity. Fig. 4.1 shows the flows chart for the preparation of (LiNa)₂CO₃–SDC composite electrolyte.

4.2.2 Characterization and conductivity measurement of (LiNa)₂CO₃-SDC

The phase purity, crystal structure and surface morphology were characterized by XRD and SEM as described in section 4.1.2. Furthermore, EDS was employed to determine

elemental composition of the composite electrolyte in order to confirm the presence of sodium and carbon. Conductivity was measured by using LCR meter. Pellet of the composite electrolyte was prepared by using a hydraulic press and a die in order to find its DC conductivity. The pressure of 5 kg/cm^2 was applied for 10 minutes to obtain a pellet of thickness 1.7 mm and a diameter of 13 mm. The pellet was sintered at 1000 °C for 1 h and the conductivity data was measured from room temperature to 700 °C.

```
┌──────────────┐ ┌──────────────┐ ┌──────────────┐ ┌────────┐ ┌────────┐
│ Ce(NO₃)₃.6H₂O│ │ Sm(NO₃)₃.6H₂O│ │ De-ionized H₂O│ │ Li₂CO₃ │ │ Na₂CO₃ │
└──────┬───────┘ └──────┬───────┘ └──────┬───────┘ └───┬────┘ └───┬────┘
       │                │                │             │          │
┌──────────────────────────────────────┐ ┌──────────────────────────────┐
│ Stirring & Heating (80°C, 45 min, 0.5 M)│ │ Stirring & Heating (100°C, 1 h, 0.5 M)│
└──────────────────┬─────────────────────┘ └────────────────┬─────────────┘
                   ▼                                          ▼
            ┌──────────────┐                          ┌──────────────┐
            │ SDC Solution │                          │ LN Solution  │
            └──────┬───────┘                          └──────┬───────┘
                   └───────────────┐    ┌────────────────────┘
                                ┌──▼────▼──┐
                                │ LN-SDC Solution │
                                └──────┬──────────┘
                                       ▼
                           ┌──────────────────────────┐
                           │ Stirring & Heating (160°C, 30 min)│
                           └──────────┬───────────────┘
                                      ▼
                              ┌──────────────┐
                              │ Precipitation│
                              └──────┬───────┘
                                     ▼
                           ┌──────────────────────┐
                           │ Drying (120°C, 10 hrs)│
                           └──────────┬───────────┘
                                      ▼
                    ┌──────────────────────────────────────┐
                    │ Sintering (800°C, 5h, 5°C/min. heating rate)│
                    └──────────────────────────────────────┘
```
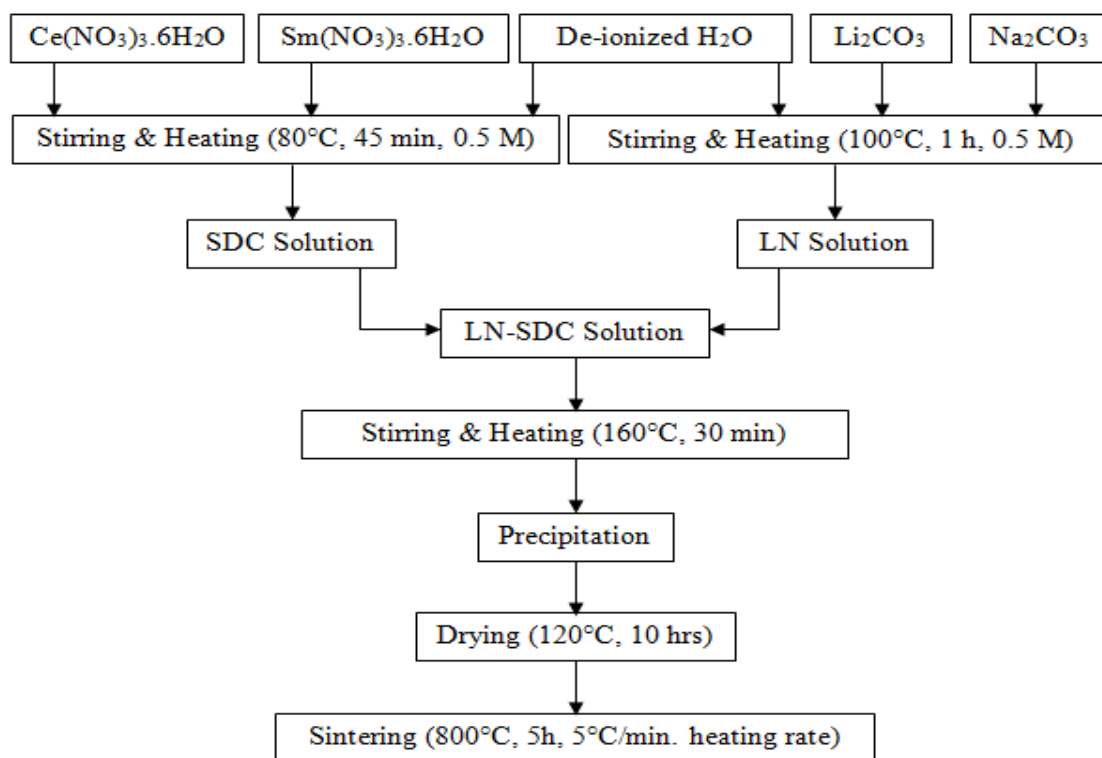
Fig. 4.1 Flow chart for the preparation of $(LiNa)_2CO_3$-SDC

4.3 Experimentation and Characterization of samarium doped ceria (SDC) at different pH values

4.3.1 Synthesis of samarium doped ceria (SDC) at different pH values

The flow chart given in Fig. 4.2 describes the procedure for the preparation of samarium doped ceria (SDC) electrolyte using co-precipitation method at different pH values. Calculated quantities of cerium nitrate hexahydrate and samarium nitrate hexahydrate were taken in a beaker and mixed in de-ionized water. The molarity of the solution was kept at 0.5 M. The heating of the solution was done at 80 °C. Then ammonia solution was added drop-wise into the first solution and the pH value was adjusted at 8, 10 and 11. The precipitation was occurred with a curd type slurry look. Afterwards, the

precipitates were dried at 120 °C in a drying oven. After the complete drying of the sample, the calcination of the sample was done at 800 °C for 3 h with the heating rate of 10 °C/min. Then grinding of the heat treated sample was done with the help of pestle and mortar to obtain fine particles of the electrolyte.

4.3.2 Characterization of SDC at different pH values

The microstructure and elemental composition of the synthesized samples were characterized by XRD, SEM/EDS as described in sections 4.1.2 and 4.2.2., respectively.
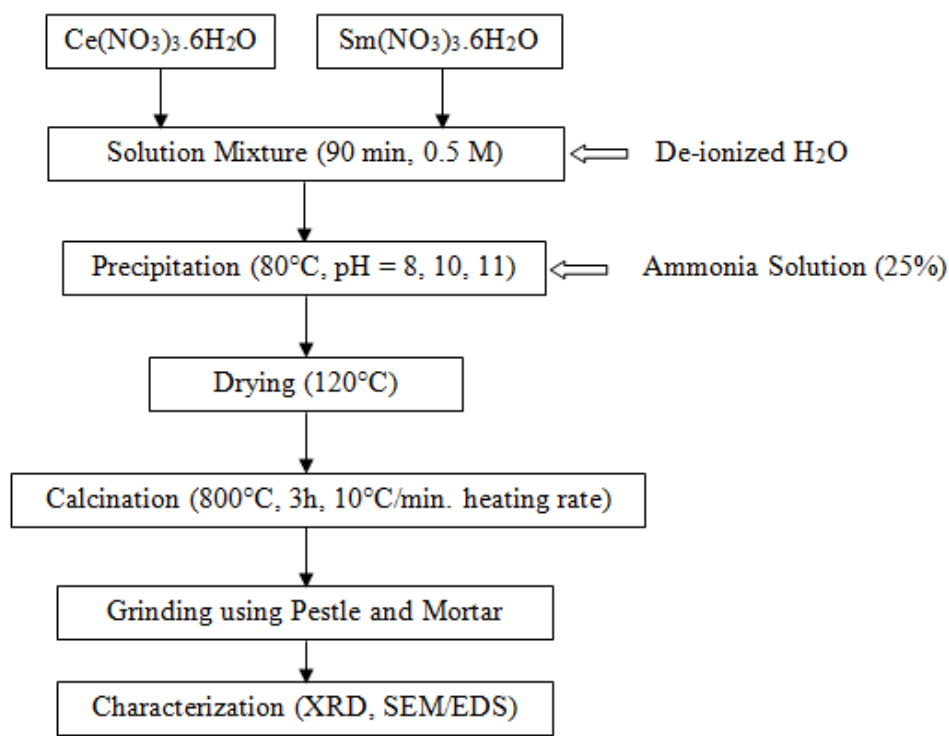
Fig. 4.2 Flow chart for the synthesis of SDC at different pH values

4.4 Experimentation and Characterization of SDC-K$_2$CO$_3$

4.4.1 Synthesis of SDC-K$_2$CO$_3$

In literature, lot of studies is present which describe the different aspects SDC-carbonate composite electrolytes by the addition of lithium and sodium carbonate. Therefore, in this experiment SDC-K$_2$CO$_3$ electrolyte was synthesized using the wet-chemistry route by employing one-step co-precipitation method in order to study the effect of calcination temperature on the microstructure of SDC-K$_2$CO$_3$. Stoichiometric amounts of Ce(NO$_3$)$_3$.6H$_2$O and Sm(NO$_3$)$_3$.6H$_2$O were added in 20 mL of deionized water. Here Molarity of the solution was kept at 0.5 M. Stir the above solution at room temperature

for about 15 minutes, and then the solution was again stirred for about 15 minutes at 80 °C for homogenization initiation of the reaction between cerium and the samarium salts. Then dissolve stoichiometric amount K_2CO_3 in 20 mL of deionized water and stirred at room temperature for about 15 minutes. Here Molarity = 0.5 M. Pour the carbonate solution in to the SDC solution (drop wise) and stirred the solution at 100 °C for an hour. Then completely dry the above solution at 120 °C in a drying oven. Finally, the dried powder was divided into three equal parts and calcined at 600 °C, 700 °C and 800 °C, respectively for 4 h to get the desired electrolyte, and then calcined samples were ground in a mortar with a pestle to obtain homogeneity and fine particles.

4.4.2 Characterization and conductivity measurement of SDC-K_2CO_3

XRD was employed to examine the crystal structure and phase purity of the composite electrolytes as described in section 4.1.2. The pellet of composite electrolyte calcined at 600 °C was formed by using hydraulic press and die. The thickness of the pellet was approximately 3.4 mm and the diameter was 13 mm, while the pellet was sintered at 1000 °C for 1 h. The DC conductivity of the pellet was determined from room temperature to 700 °C with the help of LCR meter.

4.5 Experimentation and characterization of co-doped SDC by the addition of yttrium (YSDC)

4.5.1 Synthesis of YSDC

Studies showed that co-doping is done in order to enhance the ionic conductivity of doped ceria based electrolyte materials [1,2]. In order to increase the ionic conductivity of SDC, co-doping of yttrium is done in this experiment. Co-precipitation method was employed for the preparation of co-doped SDC by the addition of yttrium. The composition of the electrolyte is $Ce_{0.8}Sm_{0.1}Y_{0.1}O_{1.9}$. First of all, stoichiometric quantities of precursors $Ce(NO_3)_3.6H_2O$, $Sm(NO_3)_3.6H_2O$ and $Y(NO_3)_3.6H_2O$ were dissolved in 20 mL of de-ionized water by stirring and heating at 60 °C for one hour. Then ammonia solution (25%) was added drop-wise into the precursor solution till the precipitation occurred and pH of the solution reached at 10. Afterwards, precipitates were heated at 80 °C for about two hours and then complete drying of the specimen was done in a drying oven at 120 °C. After drying, calcination of the dried sample was done at 800 °C for 3 h with the heating rate of 10 °C/min. At the end, the heat treated sample was ground with

the help of pestle and mortar to obtain homogenize and fine particles of the electrolyte. Flow chart for the synthesis of YSDC is shown in Fig. 4.3.

4.5.2 Characterization of YSDC

The crystal structure and phase purity was determined by employed X-ray diffraction (XRD) technique as described in section 4.1.2. The DC conductivity of the co-doped electrolyte was measured with the help of LCR meter. In order to measure the DC conductivity, pellet of the prepared sample was formed. The thickness of the pellet was 14 mm while its diameter was 13 mm. Sintering of the pellet was done at 1100 °C and the conductivity data was measured from room temperature to 700 °C.

```
┌──────────────┐   ┌──────────────┐   ┌──────────────┐
│ Ce(NO₃)₃.6H₂O│   │ Sm(NO₃)₃.6H₂O│   │ Y(NO₃)₃.6H₂O │
└──────┬───────┘   └──────┬───────┘   └──────┬───────┘
       ↓                  ↓                  ↓
┌──────────────────────────────────────────────────┐
│      Solution Mixture (60 min, 0.5 M, 60 °C)      │ ⇐ De-ionized H₂O
└──────────────────────┬───────────────────────────┘
                       ↓
        ┌──────────────────────────────┐
        │ Precipitation (80°C, pH = 10, 2 h) │ ⇐ Ammonia Solution
        └──────────────┬───────────────┘
                       ↓
             ┌──────────────────┐
             │  Drying (120°C)  │
             └────────┬─────────┘
                      ↓
      ┌────────────────────────────────────────┐
      │ Calcination (800°C, 3h, 10°C/min. heating rate) │
      └────────────────────┬───────────────────┘
                           ↓
          ┌───────────────────────────────┐
          │  Grinding using Pestle and Mortar  │
          └───────────────┬───────────────┘
                          ↓
             ┌───────────────────────┐
             │  Characterization (XRD) │
             └───────────────────────┘
```
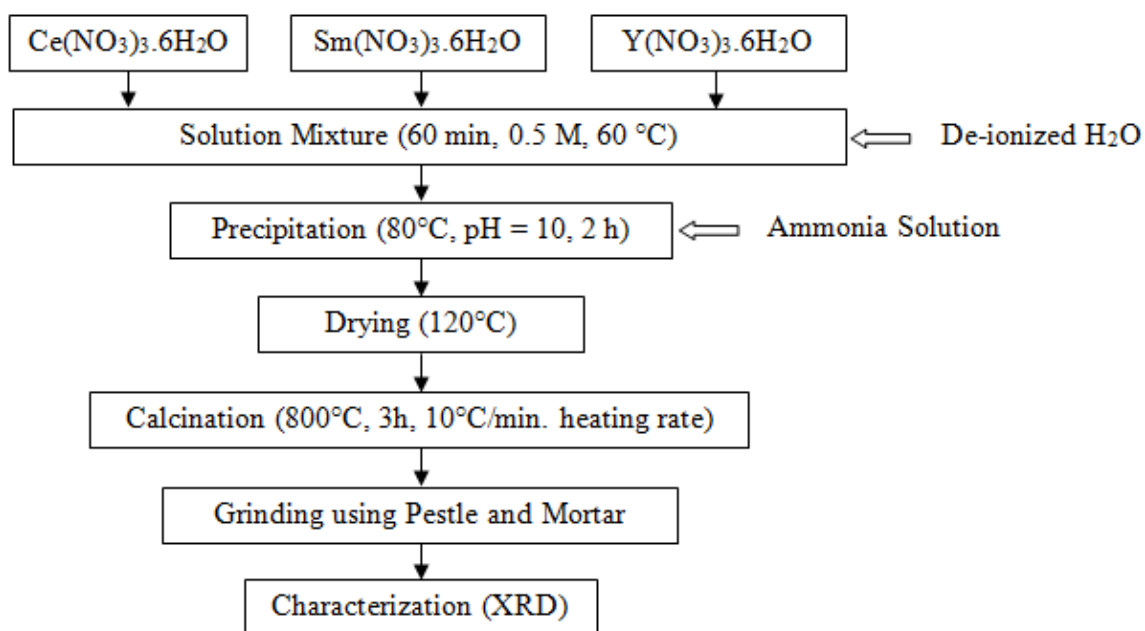
Fig. 4.3 Flow chart for the preparation of co-doped SDC (YSDC)

4.6 Chemical compatibility test of YSDC with lithiated nickel oxide

Chemical compatibility test was performed by employed solid state reaction method. Lithiated nickel oxide is employed as a cathode material in high temperature fuel cells (SOFC and MCFC). The starting materials for this solid state reaction method are lithiated nickel oxide and YSDC. Both lithiated nickel oxide and YSDC were already synthesized in the lab by sol-gel and co-precipitation methods, respectively. Stoichiometric amounts of both the precursors were taken in the weight ratio of 1:1. Then thorough mixing of these precursors was done with the help of pestle and mortar for about 60 minutes. After this, heat treatment of the sample was done at 800 °C for 3 h

at the heating rate of 10 °C/min. After calcination, XRD of the calcined sample was done in order to check the formation of any new phases or new products by the reaction of the precursors.

Summary

Initially, samarium doped ceria (SDC), and samarium doped ceria – based composite electrolyte with addition of lithium & sodium carbonates, $(LiNa)_2CO_3$-SDC were prepared by co-precipitation route. Then effects of pH of medium on the microstructure of SDC have been studied and SDC – based composite with addition of potassium carbonate ($SDC-K_2CO_3$) has also developed to investigate the effect of calcination temperature on the microstructure of SDC- K_2CO_3. Furthermore, co-doped SDC with the addition of yttrium has been developed in order to find the effect of yttrium co-doping on the conductivity of SDC. Chemical compatibility test of YSDC with lithiated nickel oxide cathode was performed at 800 °C for 3 h in order to check the compatibility of these two materials. XRD along with SEM/EDS were employed to determine the microstructure of all the electrolytes and two-probe DC conductivity method was employed to calculate the conductivity of the electrolytes.

References

[1] S. Xiwen, Z. Yongwang, W. Zhefeng, P. Jun, Z. Wenguang, Synthesis and characterization of $Sm_xGd_yCe_{1-x-y}O_{2-\delta}$ nanopowders, J. Mater. Sci. Technol, 21 (1), 2005

[2] L. Zhang, R. Lan, P.I. Cowin, S. Tao, Fabrication of solid oxide fuel cell based on doped ceria electrolyte by one-step sintering at 800°C, Solid State Ionics. 203 (2011) 47–51.

Chapter 5
Results and Discussion

The details of all the experiments have been given in Chapter 4. Now in this chapter results of these experiments along with the discussion will be given, in order to give some conclusive remarks and recommendations at the end of this dissertation.

5.1 Analysis of Samarium doped ceria and (LiNa)$_2$CO$_3$-SDC (LN-SDC)

Fig. 5.1 shows the XRD diffractograms of samarium doped ceria (SDC) i.e. $Ce_{0.8}Sm_{0.2}O_{1.9}$ calcined at 600 °C for 2 h and SDC with lithium and sodium carbonate inclusion (SDC-(LiNa)$_2$CO$_3$) calcined at 800°C for 5 hours. All peaks are associated to cubic fluorite crystal structure with the space group Fm-3m (225) (PDF Card#75-0158). There was no evidence of any other phases.
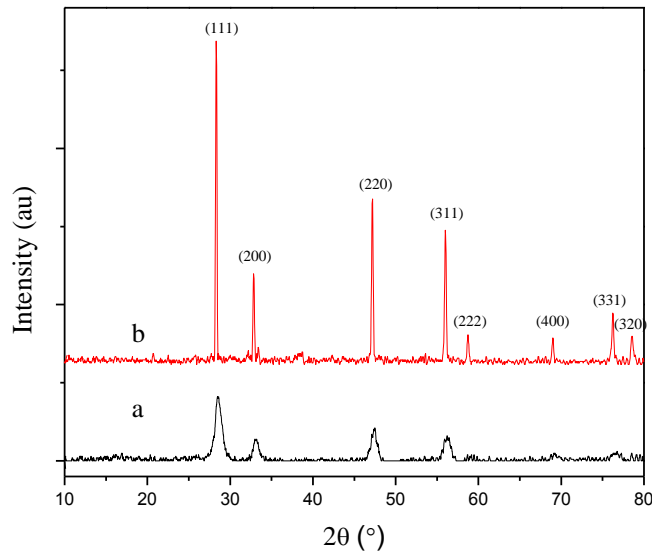
Fig. 5.1 XRD Patterns of (a) SDC and (b) (LiNa)$_2$CO$_3$-SDC

The crystallite sizes (D$_{XRD}$) of SDC and (LiNa)$_2$CO$_3$-SDC were calculated to be 14.1 nm and 55 nm, respectively calculated by Scherrer equation (Eq. 5.1) using FWHM on the (1 1 1) diffraction peak.

$$D_{XRD} = \frac{0.9\,\lambda}{\beta \cos\theta} \dots\dots\dots\dots\dots (5.1)$$

λ is the wavelength of the X-rays (nm), θ is the diffraction angle, and β is the corrected full width at half maximum (FWHM) intensity. The lattice parameter (a) of both the electrolyte materials is calculated by the help of the relations given below:

$$d = \lambda / 2 \sin \theta; \ a = d \sqrt{h^2 + k^2 + l^2} \ldots \ldots (5.2)$$

The theoretical density of the SDC crystal structure was found by the information obtained by XRD and is calculated according to equation (5.3) given below:

$$\rho_{XRD} = \frac{4 \left[(1-x).M_{Ce} + x.M_{Sm} + \left(2 - \left(\frac{x}{2} \right) \right).M_O \right]}{a^3.N_{Av}} \ldots \ldots (5.3)$$

M is atomic weight (g mol^{-1}), 'x' is the dopant mole fraction, 'a' is the lattice parameter of a unit cell (Å) and N_{Av} is Avogadro's constant. Table 5.1 show the different results based on XRD studies of both the electrolytes.

Table 5.1 Results based on XRD

Sample	d (nm)	a (nm)	V (nm^3)	D$_{XRD}$ (nm)	ρ$_{XRD}$ (g/cm^3)
SDC	0.3135	0.5430	0.1601	14.1	7.16
LN-SDC	0.3145	0.5447	0.1616	55.0	7.09

The XRD indexing of both the patterns shows that the dopant atoms were completely doped into the lattice of the CeO$_2$ crystals. The lattice constant of pure ceria is 5.411 Å, while the calculated lattice constants for SDC and LN-SDC were 5.430 Å and 5.447 Å, respectively, these lattice constants are larger than the lattice constant of pure ceria, which shows a good agreement with the Vegard's rule [1]. This shows that the samarium atoms have been doped into the crystal lattice of ceria.

In case of (LiNa)$_2$CO$_3$-SDC no peaks were identified for carbonates in XRD patterns and XRD diffractogram did not reveal the categorical present of carbonates as described in other similar studies [2–4]. Thus, we may say that (LiNa)$_2$CO$_3$-SDC nanocomposite electrolyte is present in the two separate phases; here, SDC and carbonates are present in a crystalline phase and an amorphous phase, respectiviely. It is concluded from the XRD indexing that no chemical reaction is occurred and no new compound is formed between the SDC and the carbonate phases.

The difference in the crystallite sizes of both the electrolytes is due to the difference in the calcination temperatures and the time for calcination. It is noticed that the peaks

become narrow as the calcination temperature increases from 600 to 800°C due to the growth of crystals and construction of larger clusters.

Scanning electron microscopy was used to study the morphology and the grain size of the SDC and LN-SDC nanoparticles. Fig. 5.2 shows the SEM image of samarium doped ceria electrolyte. The surface view of the micrograph of SDC, synthesized by co-precipitation method, shows that grains are well-developed and non-agglomerated. The synthesized $Ce_{0.8}Sm_{0.2}O_{1.9}$ nanopowder appeared to be spherical particles with a single crystalline structure and a uniform particle size ranges from $11 - 31$ nm, which shows a good agreement with the XRD studies of SDC electrolyte.
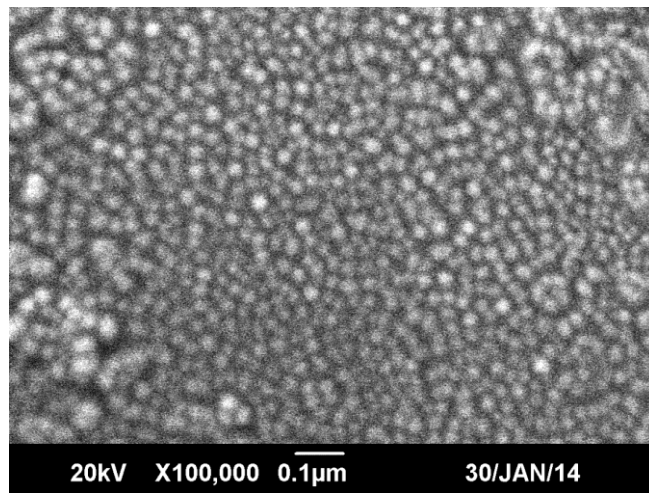
Fig. 5.2 SEM Micrograph of Samarium Doped Ceria Calcined at 600 °C
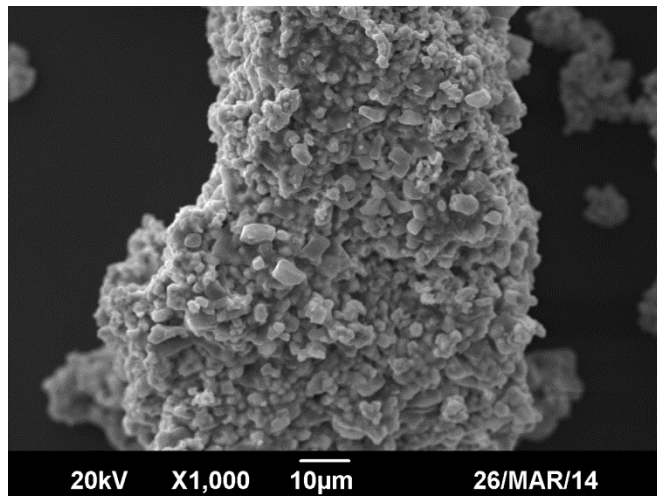
Fig. 5.3 SEM Image of $(LiNa)_2CO_3$-SDC calcined at 800 °C

Fig. 5.3 shows the SEM micrographs of SDC – $(Li_2Na_2)CO_3$. The image reveals that prepared LN – SDC composite nanoparticles are irregular in shape and consisted of

agglomerated nanocrystallites. The particle size is in the range of 50 nm to 80 nm which shows a good correspondence with the XRD studies of the composite electrolyte.
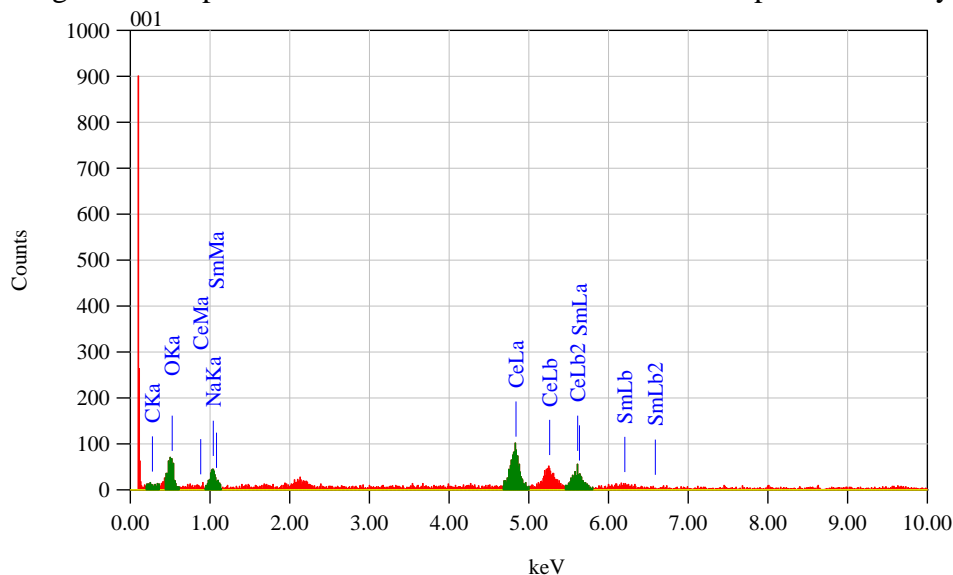
Fig. 5.4 EDS Spectrum of $(LiNa)_2CO_3$-SDC

The EDS analysis was done to determine the elemental composition of $(LiNa)_2CO_3$-SDC. Fig. 5.4 shows the EDS spectrum of the different elements found in the tested specimen. The elemental analysis was performed in a "global mode" in which a beam is rastering scanned over a complete range as shown in Fig. 5.5. Relative amounts of elements can be estimated from the peak heights. EDS analysis shows that sodium and carbon are present in the composite electrolyte this confirms the present of carbonates in the sample. Sodium and lithium carbonates are present in the amorphous phase. This secondary phase helps to improve the ionic conductivity of the ceramic electrolyte and also suppress the electronic conductivity of the electrolyte.
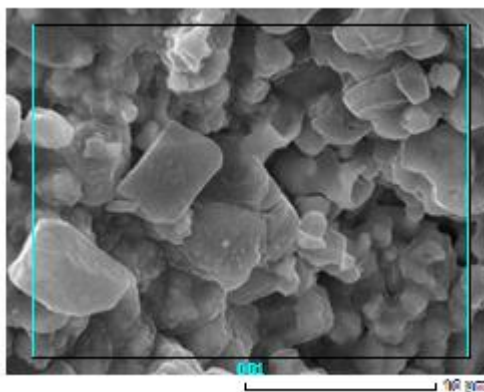
Fig. 5.5 SEM micrograph for EDS spectrum

DC conductivities of samarium doped ceria (SDC) and samarium doped ceria based composite with the addition of both lithium and sodium carbonates $(LiNa)_2CO_3$-SDC pellets were calculated by using following formula:

Conductivity (σ) = 1 / Resistivity (ρ) .... (5.4)

and,

Resistivity (ρ) = (R_{pellet} * A_{pellet}) / T_{pellet} .... (5.5)

where,

R_{pellet} = *Resistance of the pellet;*

A_{pellet} = *Area of the pellet;*

T_{pellet} = *Thickness of the pellet.*

The conductivity of the both these electrolytes mainly depend upon temperature and Arrhenius' law is used to express the relationship between conductivity and temperature. The mathematical form of the Arrhenius' law is following:

$$\sigma(T) = \sigma_o e^{(\frac{-E}{kT})} \dots\dots\dots\dots\dots (5.6)$$

where,

σ_o = *pre-exponential factor (constant);*

E = energy of activation,

k = Boltzmann's Constant; and

T = absolute temperature

The Arrhenius' plots of the two electrolytes are shown in Fig. 5.6. It is evident from Fig. 5.6 that conductivity of both the electrolytes increases with the increase in temperature and conductivity of composite electrolyte is higher than the traditional single-phase (SDC) electrolyte. The calculated value of conductivity of samarium doped ceria at 650 °C by using Eq. 5.4 and Eq. 5.5 is 5.502×10^{-5} S /cm and the calculated value of $(LiNa)_2CO_3$-SDC at 650 °C by using similar equations is 1.90×10^{-3} S/cm. Furthermore, the conductivity of $(LiNa)_2CO_3$-SDC is also calculated at 700 °C and found to be 2.94×10^{-3} S/cm.

The higher conductivity of the composite electrolyte is due to the multiple ion conduction in these electrolytes. Primarily these multiple ions are carbonate ions, oxide ions and proton (in case of hydrogen is supplied at the anode). In ceria based composite electrolyte carbonates are present in the amorphous phase as mentioned in the XRD

results. Studies concluded that carbonate phase formed a layer or coating over a doped ceria oxide and this interface layer enhances the ionic conduction mechanism. They called this interface layer as "superionic pathways" and these pathways facilitate the conduction of negative ions e.g. O^-, O^{2-} and O_2^- [5]. It was also concluded that the interface of two phases of composite electrolyte is in highly disordered arrangement, and the movement of large number of ions is possible which enhances the interfacial conductivity of such dual phase electrolytes [6].
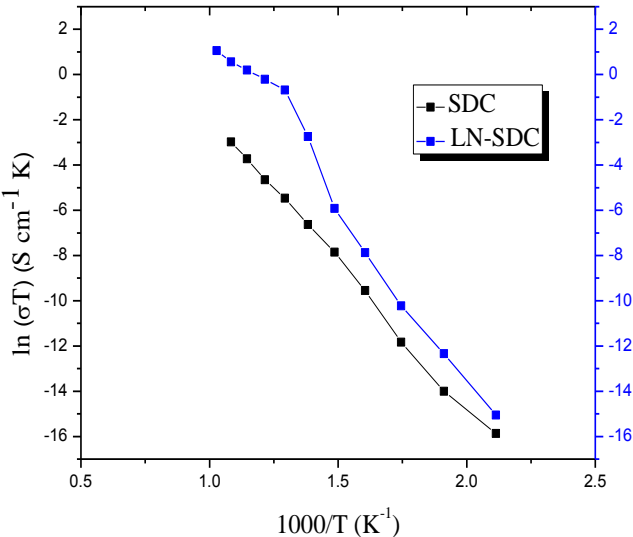
Fig. 5.6 Conductivities of SDC & LN-SDC versus Temperature

5.2 Effects of pH of medium on the microstructure of SDC electrolyte
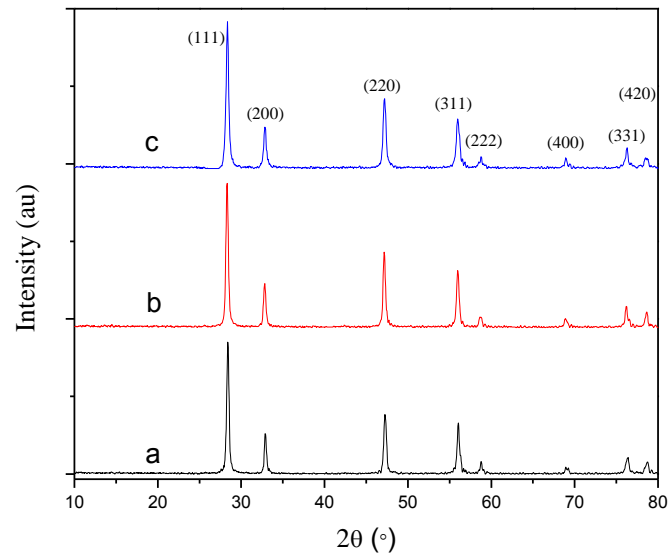
Fig. 5.7 XRD Patterns of SDC Electrolyte at (a) pH = 8, (b) pH = 10 and (c) pH = 11

Fig. 5.7 shows the XRD indexing of the SDC nanoparticles prepared at the pH value of 8, 10 and 11. All peaks were identified to be the cubic fluorite crystal structure with the space group Fm-3m (225) (PDF Card#75-0158). There was no evidence of any other phases. The crystallite sizes (D_{XRD}) of SDC at different pH values of 8, 10 and 11 were calculated using Scherrer equation and found to be 26.7 nm, 35.9 nm and 43.4 nm respectively. Table 2 shows the different parameters calculated from XRD results. Lattice strain is calculated by using X'pert HighScore software.
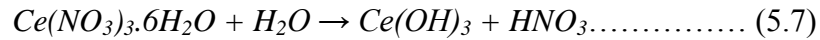
Table 5.2 Parameters calculated from XRD

Sample (SDC)	d (nm)	a (nm)	V (nm^3)	D $_{XRD}$ (nm)	ρ_{XRD} (g/cm^3)	Lattice Strain
pH = 8	0.3139	0.5437	0.1607	26.7	7.13	0.542 %
pH = 10	0.3151	0.5458	0.1626	35.9	7.05	0.408 %
pH = 11	0.3145	0.5447	0.1616	43.4	7.09	0.340 %

The precipitation mechanism of metal cations happens through the formation of solvated cation complexes, hydrolysis and condensation. The hydrolysis and condensation behaviour of the solution is affected by the pH during co-precipitation and therefore,

affects the crystallite size. With the increase in pH value the rate of hydrolysis decreases due to the gradual decrease in the concentration of the metal cations. The intensity and broadening of the peaks in the diffractogram is starting to increase by increasing the pH value. This shows that increase in pH facilitates in nucleation and growth of crystals. Therefore, crystallite size increases with the increase in pH value [7].

The mechanism of the formation of SDC is given below:
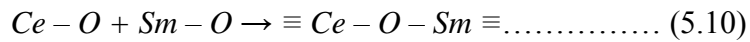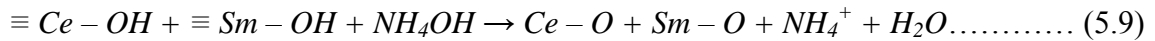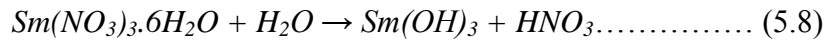
$$Ce(NO_3)_3.6H_2O + H_2O \rightarrow Ce(OH)_3 + HNO_3 \ldots\ldots\ldots\ldots (5.7)$$

$$Sm(NO_3)_3.6H_2O + H_2O \rightarrow Sm(OH)_3 + HNO_3 \ldots\ldots\ldots\ldots (5.8)$$

$$\equiv Ce - OH + \equiv Sm - OH + NH_4OH \rightarrow Ce - O + Sm - O + NH_4^+ + H_2O \ldots\ldots\ldots (5.9)$$

$$Ce - O + Sm - O \rightarrow \equiv Ce - O - Sm \equiv \ldots\ldots\ldots\ldots (5.10)$$

$Ce(OH)_3$ and $Sm(OH)_3$ are the basic precipitates, so by increasing OH^- ions the solubility of both these hydroxides decreases.

According to the XRD results, the lattice strain decreases with the increase in pH value this shows that the more precisely doped sample is obtained at pH 11 because the mismatch between the host ion and the doped ion is minimum at pH 11. Studies concluded that the ionic conductivity will be high when the lattice strain is less. So we may say that with the increase in pH value the precipitation will goes towards completion and we obtained a perfectly doped sample at higher pH value.

Fig. 5.8 shows the SEM micrographs of the SDC electrolyte synthesized at various pH values of 8, 10 and 11. SEM micrographs shows that the particles synthesized at various pH values have irregular shapes and more or less have same morphology. SEM images show that the particles are dispersed. The particle size ranges from $24 - 28$ nm for pH 8, 28.28 nm to 36.88 nm for pH 10, and 36 nm to 40 nm for pH 11. We may say that Ostwald's ripening is enhanced with the increase in pH of the solution due to the increase in the number density of nuclei [8,9].

The EDS analysis was done to determine the elemental composition of SDC. Analysis shows that no impurities were present in the synthesized sample and the particles of Ce and Sm are completely dispersed in the synthesized sample. The mass percentages of 74%, 26% and 10% were obtained for Ce, Sm and O, respectively.
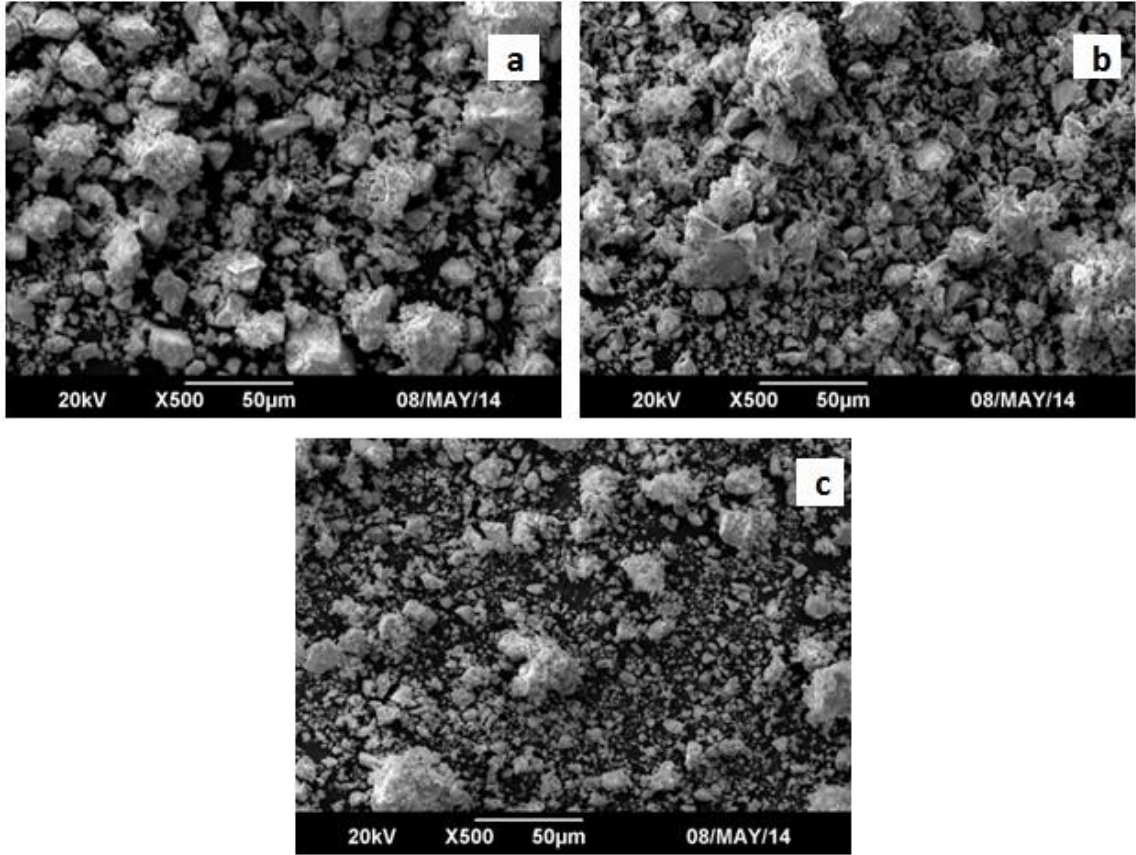
Fig. 5.8 SEM Micrographs of SDC synthesized at (a) pH = 8, (b) pH = 10, (c) pH = 11
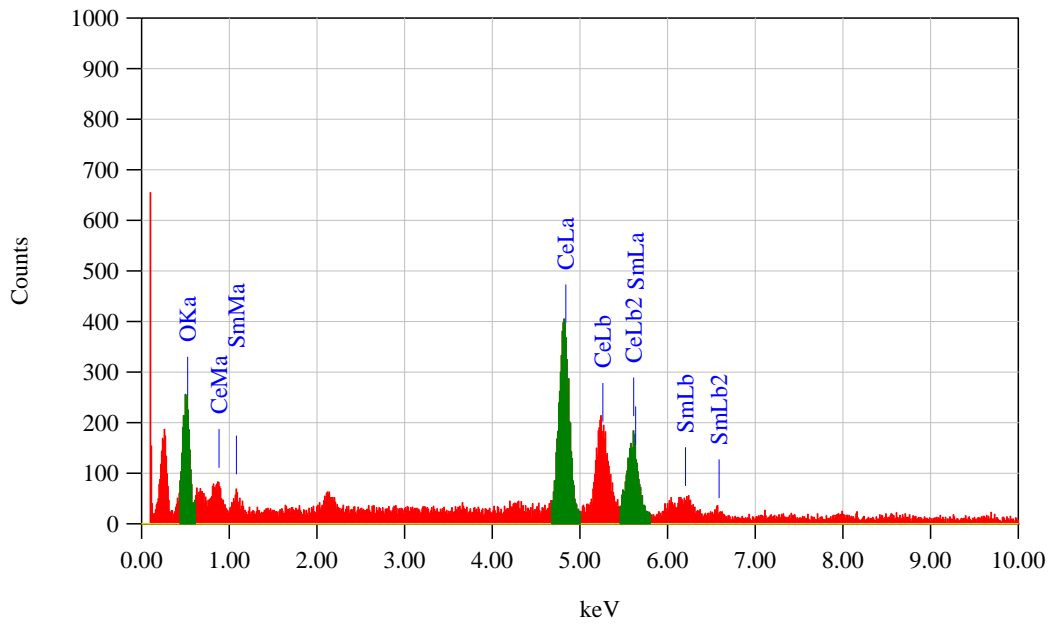

Fig. 5.9 EDS Spectrum of Samarium Doped Ceria

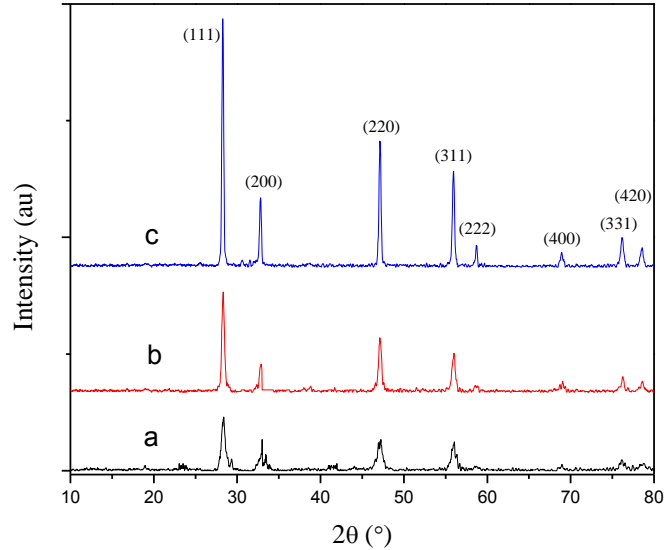## 5.3 Effects of calcination temperature on the microstructure of SDC-K₂CO₃

Fig. 5.10 XRD patterns of SDC-K₂CO₃ calcined at (a) 600 °C, (b) 700 °C and (c) 800 °C

The XRD diffractograms of composite electrolyte based on SDC with the addition of K₂CO₃ is shown in Fig. 5.10. All peaks were designated to be the cubic fluorite crystal structure of samarium doped ceria with the space group Fm-3m (225) (PDF Card#75-0158). There was no evidence of any other phases and no peak is present which detects the carbonate phase (K₂CO₃) thus; we may say that in SDC-K₂CO₃, potassium carbonate is present in the amorphous phase like in (LiNa)₂CO₃-SDC (LN-SDC).

The results obtained from XRD data are tabulated in Table 5.3. These results are calculated from equations 5.2 and 5.3.

Table 5.3 Parameters calculated from XRD Data

| Sample (SDC-K₂CO₃)	d (nm)	a (nm)	V (nm³)	D_{XRD} (nm)	ρ_{XRD} (g/cm³)	Lattice Strain
Calcined at 600 °C	0.3147	0.5451	0.1620	21.2	7.08	0.680 %
Calcined at 700 °C	0.3149	0.5454	0.1622	30.6	7.07	0.477 %
Calcined at 800 °C	0.3154	0.5463	0.1630	35.9	7.03	0.408 %

XRD results show that a sharpening in the peaks is noticed and the intensity of the peaks increases when the calcination temperature increases. The increase in the intensity of the peaks indicates an increase in the degree of crystallization. Furthermore, the crystallite size also increases with the increase in calcination temperature due to the crystallite growth during the calcination process results from an increase in the average crystallite sizes because of a tendency for minimization of the interfacial surface energy.

Fig. 5.11 shows the DC conductivity graph of SDC – K_2CO_3 calcined at 600 °C and then pellet was sintered at 1000 °C for 1 h. The DC conductivity of the composite electrolyte increases with the increase in temperature and the value of conductivity obtained at 700 °C are 3.2×10^{-3} S / cm.

Defect chemistry theory helps us to understand the conduction mechanism in dual phase SDC-carbonate electrolyte materials [5,10]. It is well known that oxygen ion conduction in doped ceria occurs because of the migration of oxygen ions via point defects i.e., oxygen vacancies. Oxygen vacancies are generated due to the addition (doping) of combination of Sm_2O_3 into CeO_2 as described by the following equation:

$$^{1}/_{2} \, Sm_2O_3 \leftrightarrow Sm'_{Ce} + ^{1}/_{2} \, V_o^{\bullet\bullet} + ^{3}/_{2} \, O_o^{\times} \ldots\ldots\ldots\ldots (5.11)$$
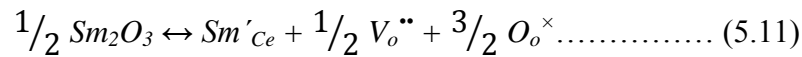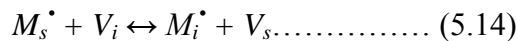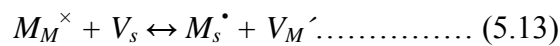
The accumulation of the oxygen ions occur at the surface of the SDC particle in the occurrence of second phase, i.e. carbonates, which subsequently increases the oxygen vacancy concentration in the bulk of SDC phase because of the interactions at the interface.

$$O_o^{\times} + V_s \leftrightarrow V_o^{\bullet\bullet} + O_s'' \ldots\ldots\ldots\ldots (5.12)$$
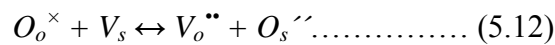
The high oxygen ion conductivity in SDC occurs because of the formation of successive conducting paths in the bulk phase of SDC and high mobility of oxygen vacancy at higher operating temperatures.

A surface reaction occurs at the bulk phase of alkaline metal carbonates i.e., Na_2CO_3, Li_2CO_3 and K_2CO_3 which increases the concentration of interstitial M^+ sites adjacent to the surface of one grain and equivalent M^+ vacancy concentration adjacent to the surface of another grain in contact. The equation for such surface reaction is given below:
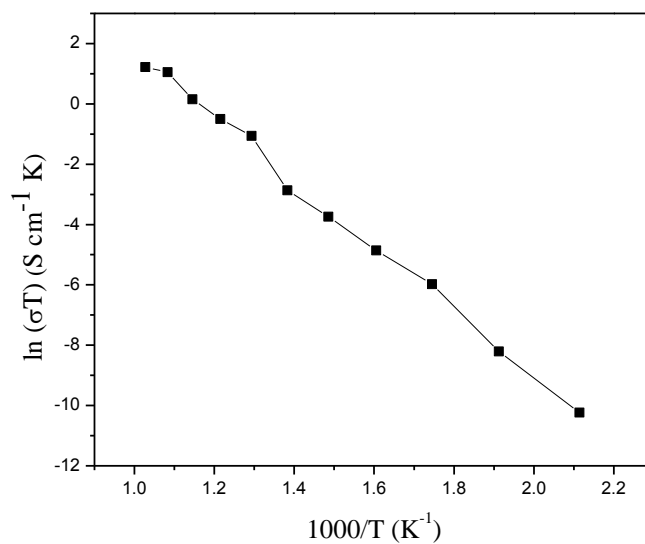
$$M_M^{\times} + V_s \leftrightarrow M_s^{\bullet} + V_M' \ldots\ldots\ldots\ldots (5.13)$$

$$M_s^{\bullet} + V_i \leftrightarrow M_i^{\bullet} + V_s \ldots\ldots\ldots\ldots (5.14)$$

Fig. 5.11 DC Conductivity of SDC - K_2CO_3

In all of the above equations, the subscript M represents a regular M lattice sites, S shows the surface site, i is the interstitial site and A represents the interface.

Because of the interfacial interaction, the formation of a space charge layer occurs at the interface of SDC-carbonate composite electrolyte. The rate of cation disorder reaction increases as a result of the formation of a space charge layer, which eventually leading to the enhancement of cations at the interface. Therefore, the amount of cation vacancies is increased in the bulk phase of the carbonates which gives rise to the improved ionic conductivity in SDC-carbonate composite electrolyte materials in an air atmosphere at definite temperatures less than the melting points of the carbonates [6].

5.4 Analysis of co-doped SDC by using Yttrium as co-dopant (YSDC)

XRD analysis of co-doped SDC with the addition of yttrium as a co-dopant is shown in Fig. 5.12. All the peaks are exactly matching with the cubic fluorite structure of cerium oxide having PDF Card#81-0792 as reported in the similar studies of other co-doped ceria based systems [11]. There is a no evidence of any new phases. The crystallite size obtained from the Scherrer's equation is found to be 43.4 nm while the value of lattice strain is 0.339 %.

The diffractogram shows that the dopants atoms were totally doped into the lattice of the CeO_2 crystals. Furthermore, the calculated value of lattice constant (5.442 Å) is greater

than the lattice constant of pure ceria (5.411 Å). Thus, we may say that the dopant atoms have been doped into the crystal lattice of CeO_2 because increase in the lattice constant shows the distortion in the lattice of ceria.
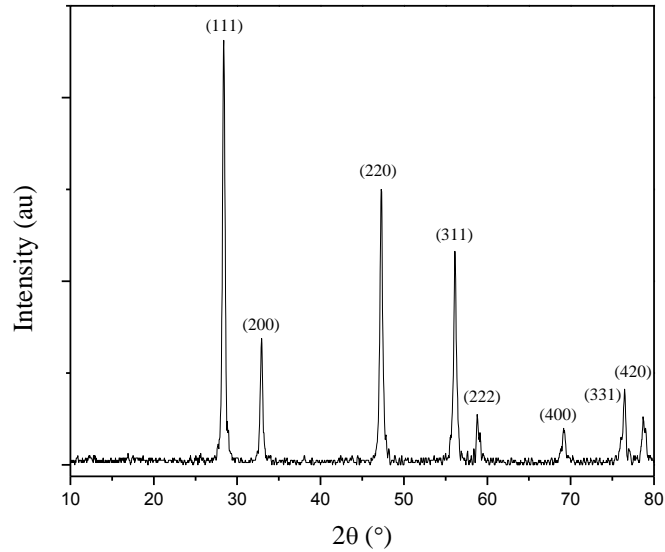

Fig. 5.12 XRD Analysis of Co-doped SDC (YSDC)

Fig. 5.13 shows the Arrhenius plot of SDC and YSDC. It is evident from the graph that the conductivity of both the electrolytes increases with the increase in temperature. However, the conductivity of SDC is less than that of YSDC. The calculated value of conductivity for SDC at 650 °C is 5.502×10^{-5} S / cm while the value of conductivity for YSDC at 650 °C is found to be 1.3×10^{-4} S / cm. These values are calculated by using equations (5.5) and (5.6). It is found that the ionic conductivity of doped ceria electrolytes reaches at a maximum value at an optimum dopant concentration. This is due to the electrostatic and elastic interactions between the dopant cation and point defect i.e., oxygen vacancy [12]. As a result of these interactions complex defect associates are formed. Most of the oxygen vacancies are bound in different traps at intermediate temperatures. Thus, in intermediate temperature range, ΔH of oxygen diffusion can be seen as a sum of migration enthalpy ($\Delta H_{migration}$) for oxygen ions and the association enthalpy ($\Delta H_{association}$) of the complex defect associates. In order to enhance ionic conductivity, the binding energy associated with complex defect associates should be minimized. This will subsequently maximize mobile oxygen vacancies. Various

61

studies [11,13] have been performed focusing on understanding the interactions between the dopant cations and oxygen vacancies and minimizing the activation energy for oxygen diffusion. Studies reported that, association energy is minimal when there is no elastic strain present in the host lattice. Using regression analysis, scientist proposed the critical dopant ionic radius (r_c), which is defined as the ionic radius of an ideal dopant that causes neither expansion nor contraction in the host ceria lattice [11]. The value of average dopant radius by using samarium and yttrium is 1.049 Å because the molar concentrations of both of the dopant ions are same i.e. $Ce_{0.8}Sm_{0.1}Y_{0.1}O_{1.9}$. This value is closely related to the value of critical radius (1.04 Å). Furthermore, the value of lattice strain for SDC electrolyte is obtained to be 0.408 % while the value of lattice strain for YSDC is found to be 0.339 %. The decrease in the lattice strain in YSDC as compared to SDC is another reason for the high ionic conductivity of co-doped YSDC electrolyte. The conductivity of co-doped electrolyte at 700 °C is found to be 2×10^{-4} S / cm.
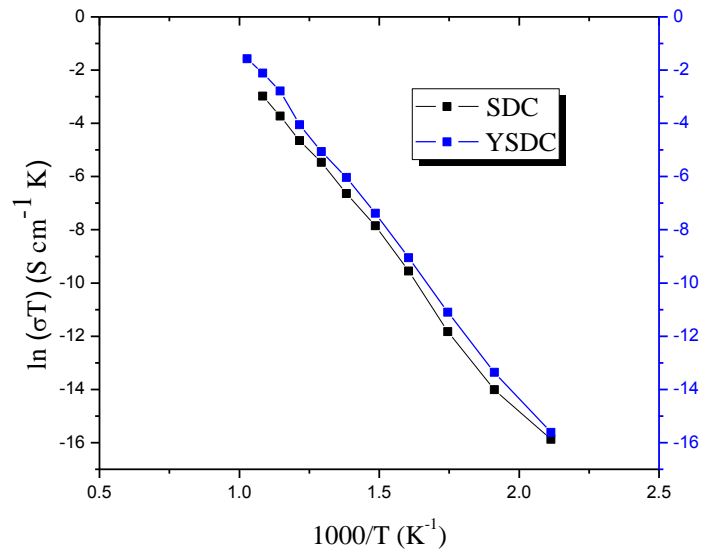

Fig. 5.13 DC Conductivity of SDC and YSDC

5.5 Analysis of Chemical Compatibility of YSDC electrolyte with lithiated nickel oxide cathode

Primarily, SOFC consists of three components i.e. cathode, anode and an electrolyte. With reference to the design considerations, chemical compatibility test is performed to check the chemical stability of YSDC electrolyte with lithiated nickel oxide cathode.

After the heat treatment of 800 °C for 3 h, the XRD data is obtained to verify the chemical stability. Fig. 5.14 shows the XRD diffractogram after the heat treatment of the mixed sample (cathode and an electrolyte). XRD shows that two distinct phases are present in the sample. The peaks of the electrolyte phase are clearly matching with the cubic fluorite crystal structure of cerium oxide having PDF card#81-0792 while the peaks of the cathode phase are matching with the cubic structure of lithiated nickel oxide ($Li_{0.4}Ni_{1.6}O_2$) having PDF card#81-0095. No evident is present of the mixed phase or a reaction between the electrolyte and a cathode as reported in the other similar studies [14,15]. However, before heat treatment the composition of lithiated nickel oxide was $Li_{0.68}Ni_{1.32}O_2$ having hexagonal crystal structure and after the heat treatment at 800 °C for 3 h the composition changes into $Li_{0.4}Ni_{1.6}O_2$ having a cubic crystal structure. The change in the composition and crystal structure occurs because of the crystallization mechanism of $LiNiO_2$. At 400 °C, the formation of the basic reactants i.e. Li_2O and NiO occurs and when the temperature is increased to approximately 600 °C, the formation of solid solution of $Li_xNi_{2-x}O_2$ occurs. When the temperature is further increased and reaches at about 700 °C, the lithiation of NiO continued. This addition of Li ion in to NiO results in the redistribution of Li and Ni ions and consequently the crystal structure changes from hexagonal to the cubic arrangement [16].
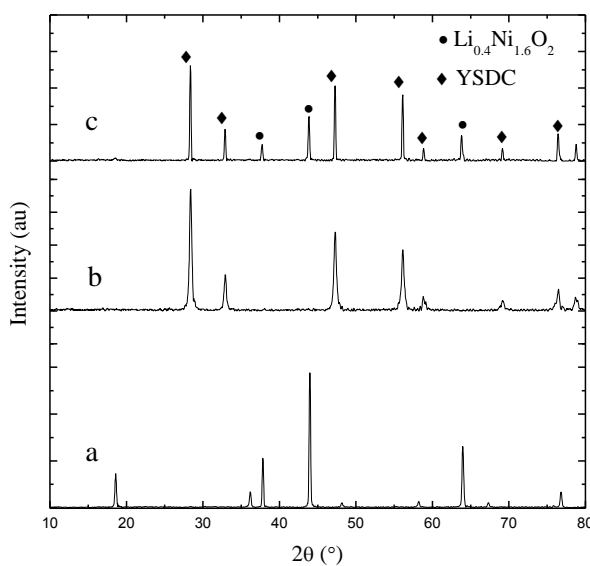

Fig. 5.14 XRD diffractograms of (a) $Li_{0.68}Ni_{1.32}O_2$ (b) YSDC and (c) Heat treated YSDC electrolyte and $Li_{0.4}Ni_{1.6}O_2$

References

[1] Y. P. Fu, S. B. Wen, C. H. Lu, Preparation and characterization of samaria-doped ceria electrolyte materials for solid oxide fuel cells, J. Am. Ceram. Soc. 91 (2007) 127–131.

[2] R. Raza, X. Wang, Y. Ma, X. Liu, B. Zhu, Improved ceria–carbonate composite electrolytes, Int. J. Hydrogen Energy. 35 (2010) 2684–2688.

[3] X. Wang, Y. Ma, R. Raza, M. Muhammed, B. Zhu, Novel core–shell SDC/amorphous Na_2CO_3 nanocomposite electrolyte for low-temperature SOFCs, Electrochem. Commun. 10 (2008) 1617–1620.

[4] X. Wang, Y. Ma, S. Li, B. Zhu, M. Muhammed, SDC/Na_2CO_3 nanocomposite: New freeze drying based synthesis and application as electrolyte in low-temperature solid oxide fuel cells, Int. J. Hydrogen Energy. 37 (2012) 19380–19387.

[5] L. Fan, C. Wang, M. Chen, J. Di, J. Zheng, B. Zhu, Potential low-temperature application and hybrid-ionic conducting property of ceria-carbonate composite electrolytes for solid oxide fuel cells, Int. J. Hydrogen Energy. 36 (2011) 9987–9993.

[6] L. Fan, C. Wang, J. Di, M. Chen, J. Zheng, B. Zhu, Study of ceria-carbonate nanocomposite electrolytes for low-temperature solid oxide fuel cells, J. Nanosci. Nanotechnol. 12 (2012) 4941–4945.

[7] V. Esposito, E. Traversa, Design of Electroceramics for Solid Oxides Fuel Cell Applications: Playing with Ceria, J. Am. Ceram. Soc. 91 (2008) 1037–1051.

[8] K. Sato, G. Okamoto, M. Naito, H. Abe, NiO/YSZ nanocomposite particles synthesized via co-precipitation method for electrochemically active Ni/YSZ anode, J. Power Sources. 193 (2009) 185–188.

[9] K. Sivakumar, V. S. Kumar, N. Muthukumarasamy, M. Thambidurai, T.S. Senthil, Influence of pH on ZnO nanocrystalline thin films prepared by sol – gel, 35 (2012) 327–331.

[10] L. Fan, C. Wang, M. Chen, B. Zhu, Recent development of ceria-based (nano)composite materials for low temperature ceramic fuel cells and electrolyte-free fuel cells, J. Power Sources. 234 (2013) 154–174.

[11] S. Omar, E. Wachsman, J. Nino, Higher conductivity Sm^{3+} and Nd^{3+} co-doped ceria-based electrolyte materials, Solid State Ionics. 178 (2008) 1890–1897.

[12] R.P. O'Hayre, Fuel Cell Fundamentals, second ed., John Wiley & Sons, INC., 2009.

[13] D. A. Andersson, S. I. Simak, N. V Skorodumova, I. A. Abrikosov, B. Johansson, Optimization of ionic conductivity in doped ceria., Proc. Natl. Acad. Sci. U. S. A. 103 (2006) 3518–21.

[14] W. Tan, L. Fan, R. Raza, M. Ajmal Khan, B. Zhu, Studies of modified lithiated NiO cathode for low temperature solid oxide fuel cell with ceria-carbonate composite electrolyte, Int. J. Hydrogen Energy. 38 (2013) 370–376.

[15] L. Zhang, S. Tao, An intermediate temperature solid oxide fuel cell fabricated by one step co-press-sintering, Int. J. Hydrogen Energy. 36 (2011) 14643–14647.

[16] P. Kalyani, N. Kalaiselvi, Various aspects of $LiNiO_2$ chemistry: A review, Sci. Technol. Adv. Mater. 6 (2005) 689–703.

Conclusions and Recommendations

Conclusions

In this work, samarium doped ceria (SDC) and SDC – based composite electrolytes with the addition of carbonates were successfully developed using co-precipitation method. Firstly, SDC and $(LiNa)_2CO_3$-SDC were synthesized and the XRD indexing of both the electrolyte materials exhibited cubic fluorite structure with the crystallite size of 14 nm and 55 nm, respectively. SEM images showed that SDC electrolyte appeared to be spherical particles with a uniform particle size of 11-31 nm, while $(LiNa)_2CO_3$-SDC composite nanoparticles were irregular in shape and consisted of agglomerated nanocrystallites with the particle size ranges from 50-80 nm. It is concluded from the microstructure analysis using XRD and SEM/EDS that in composite electrolyte carbonates were present as a secondary phase in an amorphous form and no chemical reaction or no new compound was formed between SDC and the carbonates. It is concluded that the conductivity of both the electrolyte materials increases with the increase in temperature and the DC conductivities of both the electrolyte materials at 650 °C were found to be 5.502×10^{-5} S / cm and 1.90×10^{-3} S / cm, respectively.

Secondly, it is concluded that pH of the medium during precipitation showed a significant effect on the microstructure of SDC electrolyte. Crystallite size and the particle size increases with increasing pH of the solution and the crystallite sizes obtained were 26.7 nm, 35.9 nm and 43.4 nm at the pH of 8, 10 and 11, respectively.

Thirdly, it is concluded that the crystallinity of SDC-K_2CO_3 composite electrolyte increases with the increase in calcination temperature ranges from 600-800 °C. The crystallite size increases while the lattice strain decreases by increasing the calcination temperature. The DC conductivity of SDC-K_2CO_3 composite electrolyte was found to be 3.2×10^{-3} S / cm and conductivity enhances with the increase in temperature.

At the end, co-doping of yttrium enhances the ionic conductivity of SDC electrolyte and from the chemical compatibility test of co-doped YSDC electrolyte with lithiated NiO cathode, it is concluded that no chemical reaction was occurred between these two materials at 800 °C for 3 h, however, the crystal structure of lithiated NiO changes from hexagonal to cubic arrangement after 700 °C so it may be concluded that lithiated NiO

can be used as a cathode material with YSDC electrolyte at temperature ranges up to 700 °C.

Recommendations

In the future, the ionic conductivity of SDC electrolytes synthesized at various pH values are required to be determined in order to optimize the pH during synthesis and to verify the results based on this study. It is also recommended to optimize the molar concentration of yttrium as a co-dopant in SDC electrolyte to achieve the best possible co-doped electrolyte (YSDC) with high ionic conductivity because in this study only one composition i.e., $Ce_{0.8}Sm_{0.1}Y_{0.1}O_{1.9}$ is studied. Chemical compatibility test of YSDC and lithiated NiO showed that no chemical reaction was occurred between these two compounds so it is recommended to manufacture a button cell and/or symmetrical cell by using these two materials and test the performance of these cells up to intermediate temperature range, which will definitely be the novel research in this area.

Acknowledgements

Annexure-A

Development of Samarium-Doped Ceria based electrolytes for use in Intermediate Temperature Solid Oxide Fuel Cells (IT-SOFCs)

Mustafa Anwar[a], M.N.Akbar[a], M.A.Rana[a], S.Shakir[a], Kamal Mustafa[a], Naveed K.Janjua[b], Z.S.Khan[a]

[a]Advanced Energy Materials & Fuel Cells Lab, Centre for Energy Systems, National University of Sciences & Technology, Sector H-12, Islamabad, Pakistan
[b]Department of Chemistry, Quaid-i-Azam University, Islamabad, Pakistan

Abstract

SOFCs have potential to be the most efficient and environmentally benign system for direct conversion of a wide variety of fuels to electricity. The electrolyte is the principal component of importance for SOFC. Ceria-based electrolyte materials have great potential in IT-SOFC applications. In the present study, Samarium doped ceria (SDC), and Samarium doped ceria – based composites with addition of lithium & sodium carbonates (LN-SDC) were prepared by a co-precipitation route. Meanwhile, the effect of pH on the microstructure and morphology of SDC was also investigated. XRD and SEM along with EDS were used to analyze the crystal structure, morphology and elemental composition of the electrolyte materials. Cubic fluorite structures have been observed and crystallite sizes were calculated by using Scherrer's formula. SEM images showed that SDC nanopowder appeared to be spherical particles while LN – SDC composite nanoparticles are irregular in shape and consisted of agglomerated nanocrystallites. Furthermore, XRD and SEM studies showed that the crystallite size and particle size of SDC increases with the increase in pH. The SEM images of all the samples of SDC synthesized at different pH values showed the irregular shaped and dispersed particles.

Keywords: SOFC, Electrolyte, SDC, Carbonates, pH

1. Introduction

Presently fuel cells are attracting enormous interest because of their great potential for power generation to meet the demands of diversified applications in a highly efficient and environmentally benign way. Among various types of fuel cells, generally classified by the electrolyte, solid oxide fuel cells (SOFCs) using an oxide ceramic electrolyte offer significant advantages for residential and auxiliary power units, as well as for larger industrial power applications: highest energy conversion efficiency with heat recovery or combined power generation, multi-fuel capability, and simplicity of system design by internal reforming and modular construction [1]. The electrolytic material, being the heart of an SOFC unit has been a topic of interest and continuous development. The main function of an electrolyte is to conduct a specific ion from cathode to anode in order to complete the oxidation – reduction reaction. Commonly, solid electrolyte materials which are used in SOFC are; yttria stabilized zirconia, doped ceria, stabilized Bi_2O_3, and strontium/magnesium doped lanthanum gallate [2]. Rare-earth doped ceria-electrolytes have been regarded among the most promising high-conducting and good-compatible with electrodes for SOFCs compared to other electrolytes in the intermediate-temperature range of around 500 – 800 °C [3]. Among them Sm^{+3} doped ceria (SDC) exhibits the highest oxygen ion conductivity at certain fixed doping levels, due to its smallest association enthalpy between the dopant cations and oxygen vacancies in the fluorite lattice [4,5]. The ionic conductivity increases with increasing Sm^{+3} doping and reaches the maximum for $Ce_{0.8}Sm_{0.2}O_{1.9}$ [6].

In the recent years, various techniques have been employed for the synthesis of SDC such as hydrothermal [7], sol-gel [8], solvothermal [9], co-precipitation [5], ultrasound assisted co-precipitation [4], glycine – nitrate [10] and carbon assisted spray pyrolysis [11]. The products obtained by wet – chemistry routes are of high purity, homogeneity, ultrafine and requires lower sintering temperature and time [12]. Among the various wet chemical routes, co-precipitation is a simple process with promising results for synthesizing very fine powders with high sinterability. Although samarium doped ceria have been widely investigated since past few decades, however up to best of our

knowledge there is no systematic study which describes the effects of pH of medium during co-precipitation using ammonium hydroxide on the microstructure of samarium doped ceria. Hence, in this work we present a systematic study in which effects of pH of the medium during co-precipitation on the crystallite size, particle size and the morphology of SDC is discussed. An experiment was also carried out to synthesize the samarium doped ceria based composite with the addition of lithium and sodium carbonate.

2. Experimentation and Characterization

2.1. Synthesis of Samarium-doped ceria

Initially the ceramic electrolyte of $Ce_{1-x}Sm_xO_{2-\delta}$ (x = 0.2) was synthesized by the co-precipitation method using cerium nitrate hexahydrate and samarium nitrate hexahydrate as starting materials. Stoichiometric amounts $Ce(NO_3)_3.6H_2O$ and $Sm(NO_3)_3.6H_2O$ were dissolved in de-ionized water and mixed. The solution was stirred until a transparent homogenous solution was obtained (normal average stirring time is 20 minutes). Then poured 25% Ammonia Solution in the precursor solution until the pH is greater than 10 and the precipitation occurred with a curd type slurry look. Now again stirred the solution consisted of precipitates and dried it on a hot plate at 200 ºC for 2 hrs and a pale yellow matter was obtained after complete drying. Then ground that matter to form fine particles. Now the fine powder was calcined in a furnace at 600 ºC for 2 hrs with the heating rate of 5ºC/min. The flow chart given in Fig. 1 describes the procedure for the synthesis of samarium doped ceria (SDC) electrolyte using co-precipitation method at different pH values. Phase purity and crystal structure were characterized by X-ray diffraction. X-ray powder diffraction (XRD) of the sample was recorded using CuKα radiation (λ = 1.5425 Å), with 2θ varying from 10° to 80°. The diffraction pattern was scanned in steps of 0.015°. Scanning electron microscope along with energy dispersive X-ray analysis (EDS) were used to determine the particle size, morphology and elemental composition of the synthesized material.

2.2. Synthesis of (LiNa)₂CO₃-SDC Composite (LN – SDC)

SDC:M_2CO_3 (M = Na, Li) electrolyte was prepared using the solution route with the one-step co-precipitation method. Add 3.4702 g of $Ce(NO_3)_3.6H_2O$ & 0.889 g of $Sm(NO_3)_3.6H_2O$ in 20 mL of deionized water. Here Molarity = 0.5 M. Stir the above

solution at room temperature for about 45 minutes, and then the solution was again stirred for about 45 minutes at 80 °C for homogenization. Then 0.7350 g of Li_2CO_3 & 1.06 g of Na_2CO_3 were added in 20 mL of deionized water and stirred at 100 °C for about one hour. Here Molarity = 0.5 M. Pour the carbonate solution in to the SDC solution (drop wise) and stirred the solution at room temperature for an hour. Then heat and stir the above solution on a hot plate at 160 °C for half an hour. Completely dry the above solution at 120 °C in an oven for about 10 hours. Finally, the dried powder was sintered at 800 °C for 5 h to obtain dense electrolyte, and the sintered powder was ground in a mortar with a pestle to obtain homogeneity. Phase purity and crystal structure were characterized by X-ray diffraction. SEM along with EDS was employed to study the morphology, particle size and elemental composition of the composite. Fig. 2 shows the flows chart for the preparation of LN - SDC
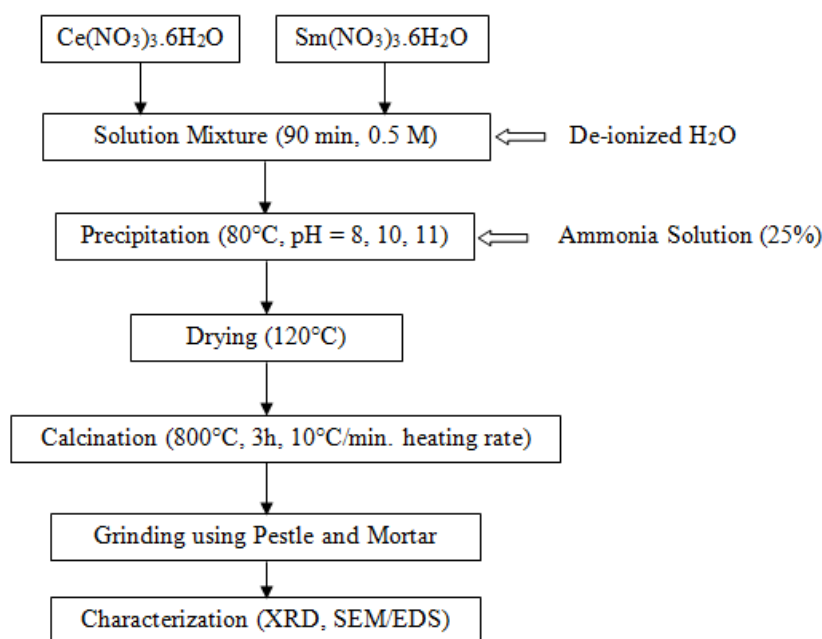

Fig. 1 Flow Chart for the Synthesis of Samarium Doped Ceria Electrolyte at different pH

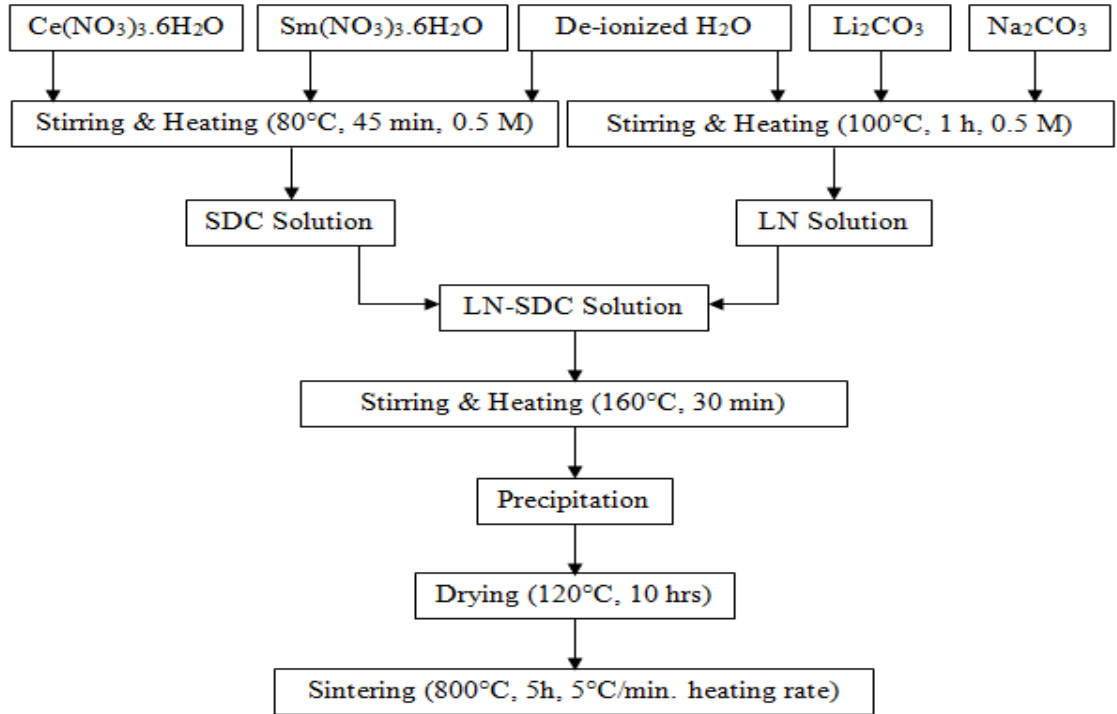Fig. 2 Synthesis of LN – SDC Composite

3. Results and Discussion
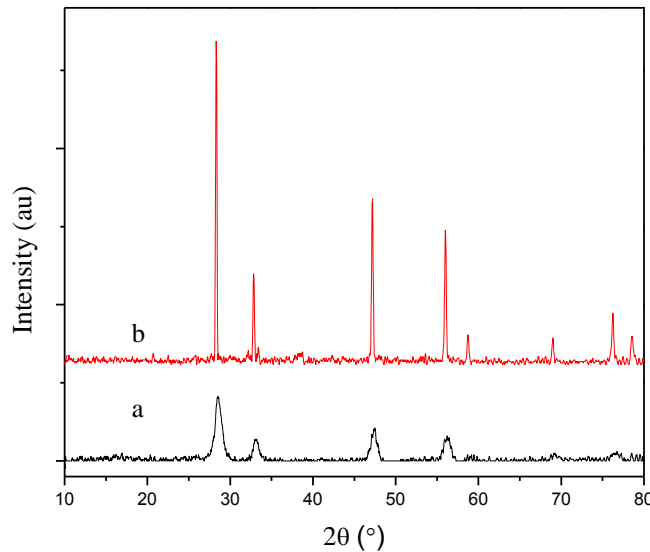

Fig. 3 XRD Patterns of (a) SDC and (b) $(LiNa)_2CO_3$-SDC

Fig. 3 presents the XRD patterns of SDC ($Ce_{0.8}Sm_{0.2}O_{1.9}$) calcined at 600°C for 2 h and SDC with lithium and sodium carbonate inclusion (SDC – $(Li_2Na_2)CO_3$) calcined at 800°C for 5 hours. All peaks were assigned to be the cubic fluorite crystal structure with

the space group Fm-3m (225) (PDF # 75-0158). There was no evidence of any other phases. The crystallite sizes (D_{XRD}) of SDC and LN-SDC were calculated to be 14.1 nm and 55 nm, respectively according to the Scherrer equation performed on the (1 1 1) diffraction. Scherrer equation;

$$D_{XRD} = 0.9\ \lambda\ /\ \beta.\ \cos\theta$$

λ is the wavelength of the X-rays (nm), θ is the diffraction angle, and β is the corrected full width at half maximum (FWHM) intensity. The lattice parameter (a) of both the electrolytes can be calculated by the following relations:

$$d = \lambda\ /\ 2\ \sin\theta;\ a = d\ \sqrt{h^2 + k^2 + l^2}$$

The theoretical density of the SDC crystal structure was calculated according to equation given below from the crystallographic information obtained by XRD.

$$\rho_{XRD} = \frac{4\left[(1-x).M_{Ce} + x.M_{Sm} + \left(2 - \left(\frac{x}{2}\right)\right).M_o\right]}{a^3.N_{Av}}$$

M is atomic weight (g mol⁻¹), 'x' is the dopant mole fraction, 'a' is the unit cell lattice parameter (Å) and N_{Av} is Avogadro's constant. Table 1 show the different results based on XRD studies of both the electrolytes.

Table 1 Results based on XRD Studies

Sample	d (nm)	a (nm)	V (nm³)	D_{XRD} (nm)	ρ_{XRD} (g/cm³)
SDC	0.3135	0.5430	0.1601	14.1	7.16
LN-SDC	0.3145	0.5447	0.1616	55.0	7.09

The indexing of both the patterns indicates that the samarium atoms were completely doped into the lattice of the CeO_2 crystals. Furthermore, the calculated lattice constants were 5.43 Å and 5.447 Å, larger than the lattice constant of pure CeO_2 (5.411 Å), which is in agreement with Vegard's rule. This confirms that the samarium atoms have been doped into the crystal lattice of CeO_2.

In the case of LN-SDC no reflections were detected for carbonates in XRD patterns. We may say that LN-SDC nanocomposite electrolyte may be present in the two distinct phases; here, SDC is in the crystalline phase, but the carbonates are in an amorphous

phase. Based on the XRD results, it may be concluded that there was no chemical reaction and no new compound formed between the SDC and the carbonate phases [13]. The difference in the crystallite sizes of both the electrolytes is due to the difference in the calcination temperatures and the time for calcination. It's noticed that the width of the peaks decreases as the calcination temperature increases from 600 to 800°C due to the growth of crystals and construction of larger clusters.

Electron microscopy was used to study the morphology and the grain size of the SDC and LN-SDC nanoparticles. Fig. 4 shows the SEM image of samarium doped ceria electrolyte. The surface view of the micrograph of SDC, synthesized by co-precipitation method, shows non-agglomerated well-developed grains. The synthesized $Ce_{0.8}Sm_{0.2}O_{1.9}$ nanopowders appeared to be spherical particles with a single crystalline structure and a uniform particle size of 11 – 31 nm, which shows a good agreement with the XRD studies of SDC electrolyte.

Fig. 5 shows the SEM micrographs of SDC – $(Li_2Na_2)CO_3$. The image reveals that prepared LN – SDC composite nanoparticles are irregular in shape and consisted of agglomerated nanocrystallites. The particle sizes are in the range of 50 nm to 80 nm which shows a good correspondence with the XRD studies of the composite electrolyte.
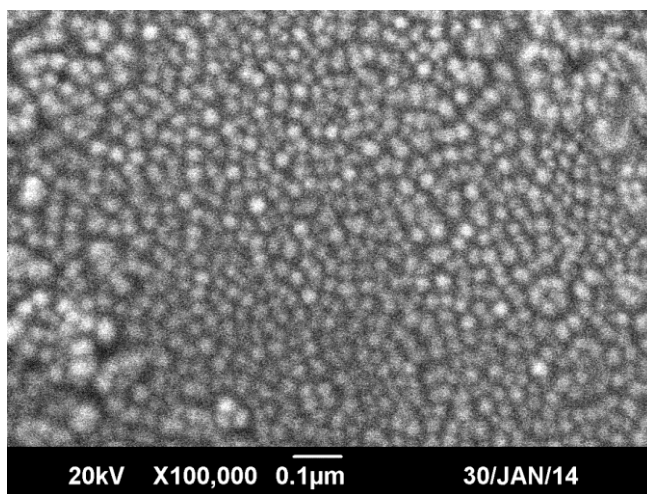

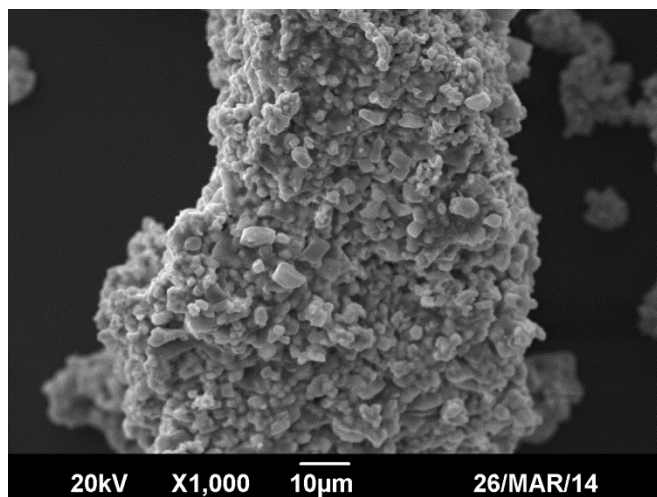Fig. 4 SEM Micrograph of Samarium Doped Ceria Calcined at 600 °C

Fig. 5 SEM Micrographs of LN - SDC Composite

The EDS analysis was done to determine the elemental composition of the LN – SDC. Fig.6 shows the EDS spectrum of the different elements found in the tested specimen. The elemental analysis was performed in a "global mode" in which a beam is localized on a complete image as shown in Fig. 5. The intensity of the peaks in the EDS is not a quantitative measure of elemental concentration, although relative amounts can be inferred from relative peak heights. EDS analysis shows that sodium is present in the composite electrolyte but no peaks were detected for sodium carbonate in the XRD pattern. Thus we may say that sodium and lithium carbonates are present in the amorphous phase. This secondary phase helps to improve the ionic conductivity of the ceramic electrolyte and also suppress the electronic conductivity of the electrolyte [14].
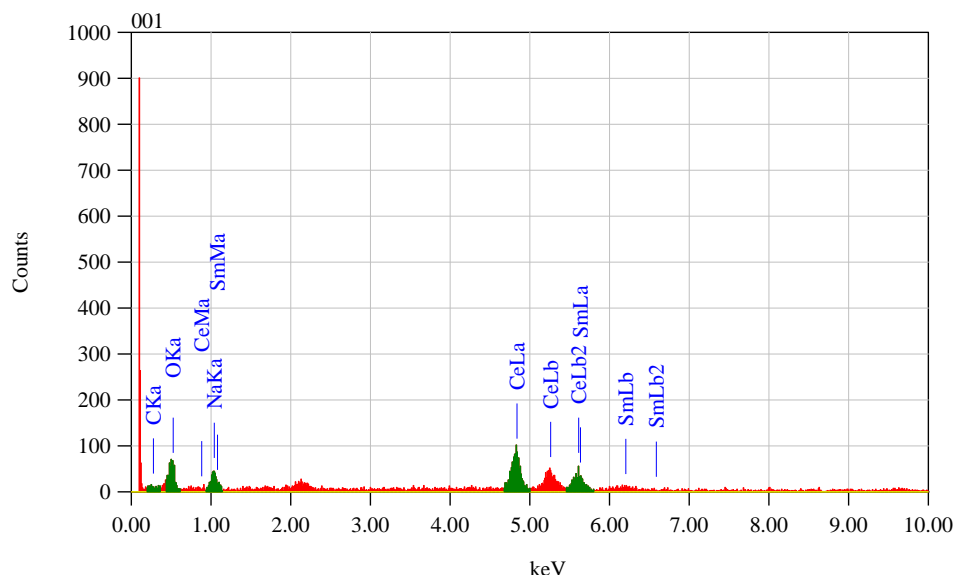

Fig. 6 EDS Spectrum of LN - SDC Composite

Fig. 7 shows the XRD patterns of the SDC nanoparticles synthesized at the pH value of 8, 10 and 11. All peaks were assigned to be the cubic fluorite crystal structure with the space group Fm-3m (225) (PDF # 75-0158). There was no evidence of any other phases. The crystallite sizes (D_{XRD}) of SDC at different pH values of 8, 10 and 11 were calculated using Scherrer equation and found to be 26.7 nm, 35.9 nm and 43.4 nm respectively. Table 2 shows the different parameters calculated from XRD results.
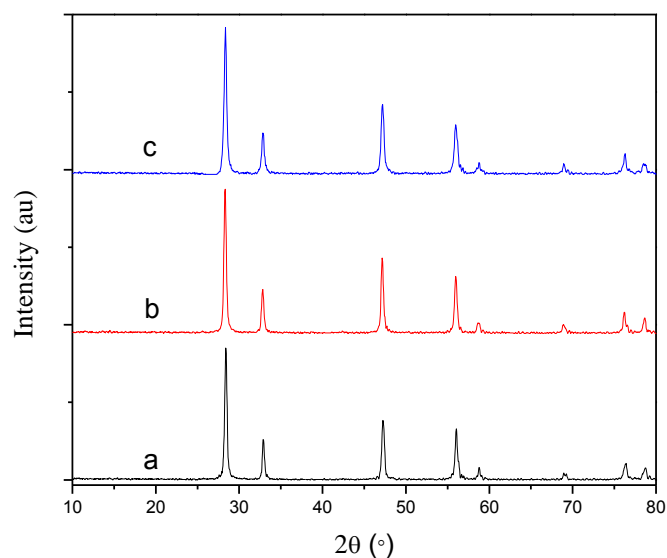
Fig. 7 XRD Patterns of SDC Electrolyte at (a) pH = 8, (b) pH = 10 and (c) pH = 11

Table 2 Results based on XRD of SDC synthesized at different pH Values

Sample (SDC)	d (nm)	a (nm)	V (nm^3)	D_{XRD} (nm)	ρ_{XRD} (g/cm^3)
pH = 8	0.3139	0.5437	0.1607	26.7	7.13
pH = 10	0.3151	0.5458	0.1626	35.9	7.05
pH = 11	0.3145	0.5447	0.1616	43.4	7.09

The precipitation mechanism of metal cations occurs through the formation of solvated cation complexes, hydrolysis and condensation. The pH affects the hydrolysis and condensation behaviour of the solution during co-precipitation and therefore, influences the crystallite size. The rate of hydrolysis decreases with increasing pH because the concentration of the metal cations decreases gradually. The intensity and broadening of

the peaks in the diffraction pattern is found to increase with increase in pH value. This suggests that increase in pH helps in nucleation and growth of crystals [15].

Fig. 8 shows the SEM micrographs of the SDC electrolyte synthesized at various pH values of 8, 10 and 11. SEM micrographs shows that the particles synthesized at various pH values have irregular shapes and more or less have same morphology. However, the particle size ranges from 24 – 28 nm from 24 – 28 nm for pH 8, 28.28 nm to 36.88 nm for pH 10, and 36 nm to 40 nm for pH 11. We may say that Ostwald's ripening is enhanced with the increase in pH of the solution since the number density of nuclei increases [15].

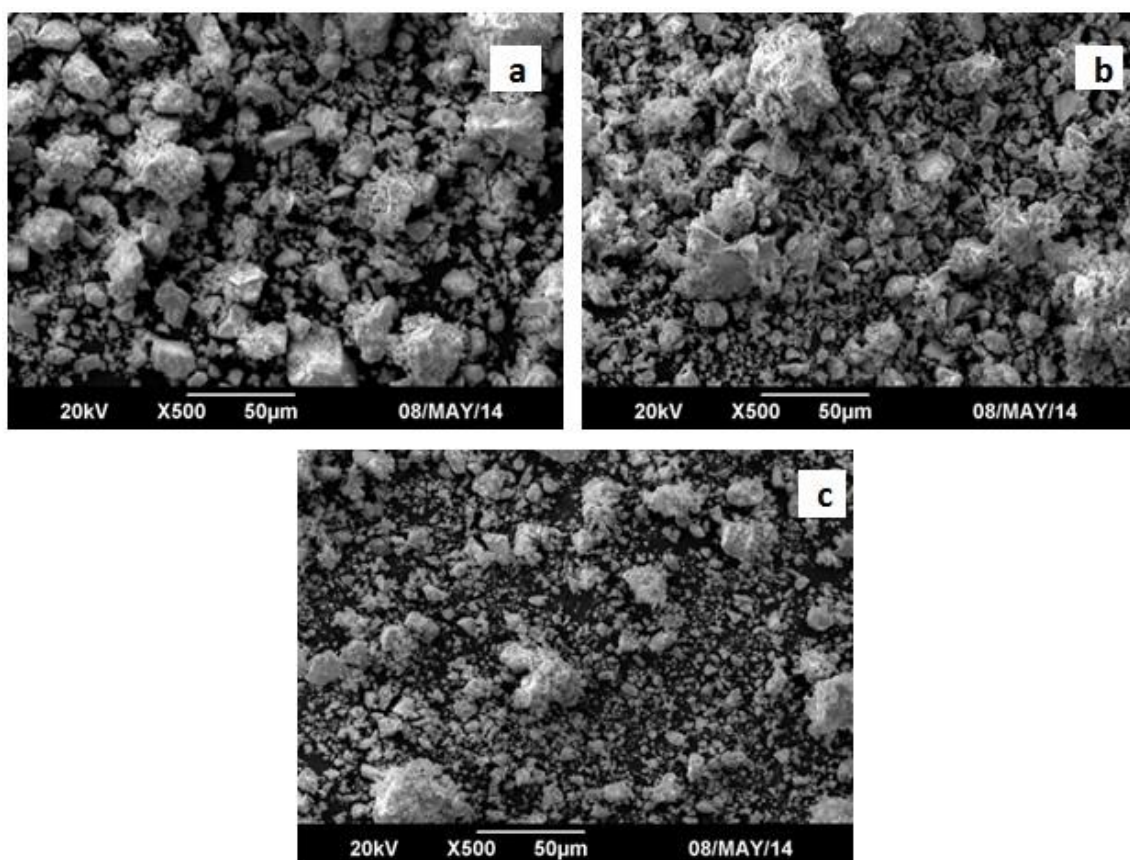Fig. 8 SEM Micrographs of SDC synthesized at (a) pH = 8, (b) pH = 10, (c) pH = 11

The EDS analysis was done to determine the elemental composition of SDC. Analysis shows that no impurities were present in the synthesized sample and the particles of Ce and Sm are completely dispersed in the synthesized sample. The mass percentages of 74%, 26% and 10% were obtained for Ce, Sm and O, respectively.
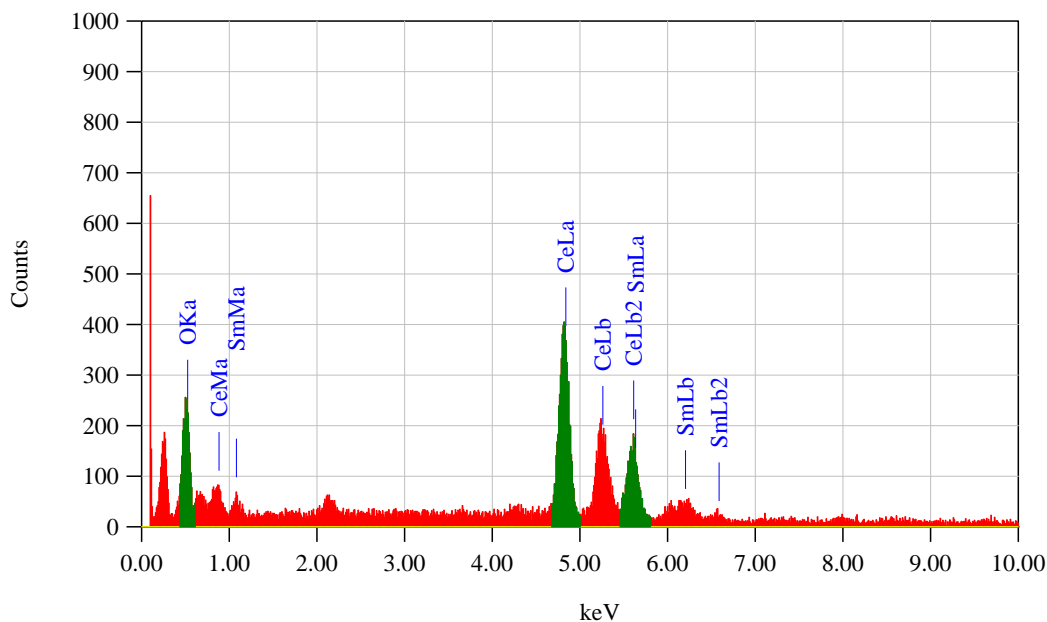
Fig. 9 EDS Spectrum of SDC

Conclusions

➢ The XRD indexing emphasizes that the electrolytes prepared by co-precipitation method exhibit cubic fluorite structure and the crystallite dimensions of 14.1 nm and 55 nm are obtained for SDC (calcined at 600 °C) and LN-SDC, respectively.

➢ It may be concluded from XRD results that in an LN-SDC electrolyte, incorporation of the (Li/Na) carbonate did not alter the phase structure of the ceramic and there was no chemical reaction or no new compound formed between the SDC and the carbonate phase.

➢ SEM images showed that SDC (calcined at 600 °C) appeared to be spherical particles and a uniform particle size of 11 – 31 nm, while LN-SDC composite nanoparticles are irregular in shape and consisted of agglomerated nanocrystallites with the particle size ranges from 50 – 80 nm.

➢ XRD and SEM reveal that the pH has a significant effect on the crystallite size and the particle size of the SDC, and with the increase in pH, both the crystallite size and particle size increases.

➢ The crystallite sizes obtained were 26.7 nm, 35.9 nm and 43.4 nm at pH values of 8, 10 and 11, respectively.

Acknowledgement

References

[1] J. Huang, F. Xie, C. Wang, Z. Mao, Development of solid oxide fuel cell materials for intermediate-to-low temperature operation, Int. J. Hydrogen Energy. 37 (2012) 877–883.

[2] A. J. Jacobson, Materials for solid oxide fuel cells †, Chem. Mater. 22 (2010) 660–674.

[3] V. Kharton, F. Marques, A Atkinson, Transport properties of solid oxide electrolyte ceramics: a brief review, Solid State Ionics. 174 (2004) 135–149.

[4] H. Okkay, M. Bayramoglu, M. Faruk Öksüzömer, $Ce_{0.8}Sm_{0.2}O_{1.9}$ synthesis for solid oxide fuel cell electrolyte by ultrasound assisted co-precipitation method., Ultrason. Sonochem. 20 (2013) 978–83.

[5] Y. P. Fu, S. B. Wen, C. H. Lu, Preparation and characterization of samaria-doped ceria electrolyte materials for solid oxide fuel cells, J. Am. Ceram. Soc. 91 (2007) 127–131.

[6] M. Dudek, Ceramic oxide electrolytes based on CeO_2—Preparation, properties and possibility of application to electrochemical devices, J. Eur. Ceram. Soc. 28 (2008) 965–971.

[7] S. Wang, C. Yeh, Y. Wang, Y. Wu, Characterization of samarium-doped ceria powders prepared by hydrothermal synthesis for use in solid state oxide fuel cells, 2 (2013) 141–148.

[8] M.R. Kosinski, R.T. Baker, Preparation and property–performance relationships in samarium-doped ceria nanopowders for solid oxide fuel cell electrolytes, J. Power Sources. 196 (2011) 2498–2512.

[9] T. Karaca, T.G. Altınçekiç, M. Faruk Öksüzömer, Synthesis of nanocrystalline samarium-doped CeO_2 (SDC) powders as a solid electrolyte by using a simple solvothermal route, Ceram. Int. 36 (2010) 1101–1107.

[10] R. Tian, F. Zhao, F. Chen, C. Xia, Sintering of samarium-doped ceria powders prepared by a glycine-nitrate process, Solid State Ionics. 192 (2011) 580–583.

[11] K. Myoujin, H. Ichiboshi, T. Kodera, T. Ogihara, Characterization of samarium doped ceria powders having high specific surface area synthesized by carbon-assisted spray pyrolysis, Key Eng. Mater. 485 (2011) 137–140.

[12]   Z. Shao, W. Zhou, Z. Zhu, Advanced synthesis of materials for intermediate-temperature solid oxide fuel cells, Prog. Mater. Sci. 57 (2012) 804–874.

[13]   M. A. Khan, R. Raza, R. B. Lima, M. A. Chaudhry, E. Ahmed, G. Abbas, Comparative study of the nano-composite electrolytes based on samaria-doped ceria for low temperature solid oxide fuel cells (LT-SOFCs), Int. J. Hydrogen Energy. (2013) 2–9.

[14]   X. Wang, Y. Ma, S. Li, B. Zhu, M. Muhammed, SDC/Na$_2$CO$_3$ nanocomposite: New freeze drying based synthesis and application as electrolyte in low-temperature solid oxide fuel cells, Int. J. Hydrogen Energy. 37 (2012) 19380–19387.

[15]   K. Sato, G. Okamoto, M. Naito, H. Abe, NiO/YSZ nanocomposite particles synthesized via co-precipitation method for electrochemically active Ni/YSZ anode, J. Power Sources. 193 (2009) 185–188.

Annexure-B

A Review on Synthesis Routes for Samarium Doped Ceria (SDC) and SDC - Carbonate Composite Electrolyte Materials for Intermediate Temperature Solid Oxide Fuel Cells (SOFCs)

Mustafa Anwar[a], Zuhair S. Khan[a*]

[a]Advanced Energy Materials & Fuel Cells Lab, Centre for Energy Systems, National University of Sciences & Technology, Islamabad-44000, Pakistan
*Corresponding Author;
Email: zskhan@ces.nust.edu.pk

Abstract

Solid oxide fuel cells (SOFCs) are the most efficient devices for clean energy that directly convert the chemical energy of fuels into electrical power. The overall performance of a SOFC strongly depends upon the electrical characteristics of the electrolyte. Traditional SOFCs employ yttria-stabilized zirconia (YSZ) as an electrolyte but YSZ exhibited sufficient ionic conductivities at high temperatures (800-1000 °C). Due to this high temperature, the commercial utilization of the conventional SOFCs is limited because of the resistive causes, e.g. expensive materials, thermal stress and long start-up and shut-down time etc. In the last decade, the research of SOFCs had concentrated on decreasing the operating temperature through the evolution of novel materials, notably the electrolyte materials having sufficient ionic conductivity. Doped ceria based electrolytes has higher oxygen ion conductivity than YSZ, especially at lower temperatures. Samarium doped ceria (SDC) is the most extensively studied electrolyte for SOFCs operating at 500-600 °C because of its high ionic conductivity. This article aims at providing a concise review and outlook of various synthesis routes for the development of SDC based electrolytes from single-phase SDC to two-phase nanocomposites of SDC with alkali carbonates (Na_2CO_3, K_2CO_3, Li_2CO_3). The ionic conductivities and electrical properties of the electrolytes at low temperature obtained through different synthesis methods are discussed.

Keywords: SOFC, Electrolyte, SDC, Synthesis routes, Ionic conductivity

1. Introduction

Energy drives the global economy. it is a keystone in the communications between nature and humanity and is considered a basic input for the climate and sustainable advancement [1]. Eventually the development has always been correlated with the growth of demand for energy [2]. Sustainable development craves a sustainable supply of environmentally benign and low cost energy resources that do not cause adverse social impacts. Now-a-days fossil fuels are the mostly used energy resources but they are depleting very quickly and in future there supplies will be limited [1]. It is already known that the use of standard technologies to harvest electricity based on fossil fuels cannot fulfill the ever-growing demand for energy [3]. In addition to this, fossil fuels are not environmental friendly; the combustion of fossil fuels is one of the major contributing factor in the air pollution because of the increase in the emission of greenhouse gases, especially CO_2, particularly in urban areas [2]. The sustainable future of the world energetic systems lies in the implementation of efficient and environmentally benign technologies to produce electricity [3]. In this context, advanced energy conversion technologies have attracted viable attention during the past few decades [4]. There is a great interest in electrochemical energy storage such as advanced batteries, fuel cells, etc. Among them, fuel cell is notably attractive as fuel cell is considered to be the most efficient and less polluting electricity generating device [5].

Fuel cell is an electrochemical device that directly converts the chemical energy of fuels such as natural gas, ethanol, hydrogen, methanol and hydrocarbons to electrical energy. Until now, six major types of fuel cells, namely, proton exchange membrane or polymer electrolyte membrane fuel cell (PEMFC), the phosphoric acid fuel cell (PAFC), the molten carbonate fuel cell (MCFC), the alkaline fuel cell (AFC), the direct methanol fuel cell (DMFC) and the solid oxide fuel cell (SOFC) have been primarily developed. The distinguishing factor among these fuel cells are the electrolyte used, which in turns determines the operating temperature [2,6]. Among different types of fuel cells, SOFCs have extraordinary potential for use as electricity production systems due to their high energy conversion efficiency ($\sim 60 - 65\%$). In addition, SOFCs have many advantages such as multi-fuel capability, simplicity of system design and the exhaust heat can be

used as a heat source for a variety of processes [6]. SOFC technology also offers systems for "zero" or "near zero" emissions [7].

The construction of SOFC based on three basic layers or components and is composed by a cathode, a solid electrolyte and an anode, respectively, unless an interlayer is essentially required for the improvement of the interface between the main layers [8]. The operating principle of SOFC with an oxide ion conductor is schematically shown in Fig. 1. After applying an external load to the cell, reduction of oxygen is occurred at the porous cathode and oxide ions are produced. These ions pass through the solid ceramic electrolyte to the anode which is a fuel electrode, and they react with the fuel (H_2 or CO), to produce H_2O or CO_2. Alternatively, a proton conducting solid electrolyte can be used, where oxidation of H_2 occurs to produce protons that eventually react with oxygen to form H_2O. Sometimes, CH_4 can also be utilized which oxidized directly on the anode to form CO_2 and H_2O [6]. SOFCs consisting of oxygen-ion conducting yttria-stabilized zirconia solid ceramic electrolyte were first demonstrated and electrically tested by Baur and Pries in 1937 [6]. This SOFC was operated at 1000 °C and in this cell, $ZrO_2 - 15$ weight% Y_2O_3 was used as the electrolyte. In 1899, Nernst first discovered that ZrO_2 with 15 weight% Y_2O_3 was a solid oxide ion conductor [6]. In the most advanced SOFCs at present, yttria stabilized zirconia with 8 mol% Y_2O_3 (YSZ) is still used as the electrolyte. The oxide ion conductivity of YSZ is > 0.1 S/cm at 1000 °C [9].
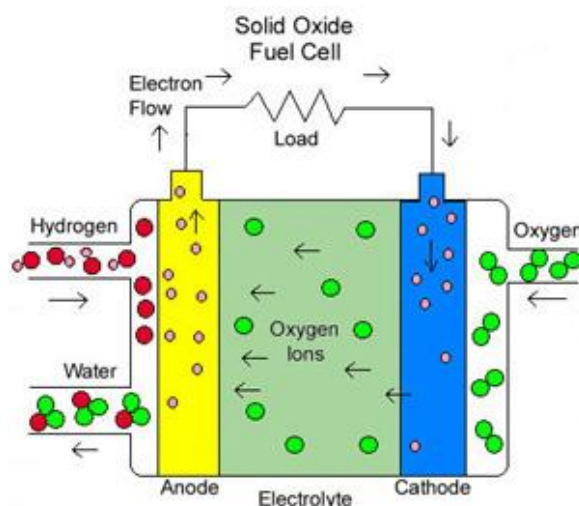

Fig. 1 Schematic Representation of SOFC Principle

The electrolytic material, being the heart of an SOFC unit has been a topic of interest and continuous development. The main function of an electrolyte is to conduct a specific

ion from cathode to anode in order to complete the oxidation – reduction reaction [10]. Some of the basic requirements for an electrolyte material are given in Table 1 [8].

Table 5 Requirement for the Electrolyte [8]

Electrochemical	High ionic conductivity and low electronic conductivity.
Chemical	Structure must be stable at high temperatures, no reactivity to the anode, cathode and other materials and lack of instability to oxygen and fuel gas at high temperature treatment and lack of phase immiscibility is also essential.
Thermal	Phase must be thermally stable and low thermal expansion coefficient close to those values of the remaining components of the cell.

SOFCs employed crystalline oxide ceramic electrolyte materials. The conduction occurs via defect hopping mechanisms. The conventional electrolytes of SOFCs exhibit acceptable ionic conductivities at high temperatures i.e. above 800°C [9]. This high operating temperature leads towards prohibitive causes, e.g. costly material, thermal stress, long start-up and shut-down time and high running cost, and those have inhibited the commercial utilization of SOFCs [9]. Therefore, to lower the operating temperature of the SOFCs has attracted an increasing interest in recent years.

To lower the operating temperature of SOFC, we must require a high ionic conductive electrolyte and increased reaction activity of the electrode. The major difficulty in decreasing the operating temperature is the ohmic loss of the electrolyte [11]. Taking in to the account that the overall performance of the SOFC highly depends on each component in the cell, a significant amount of efforts has been carried out on the development of electrolyte materials that exhibits sufficient ionic conductivities at low and intermediate temperatures

Cerium oxide (ceria or CeO_2) shows a cubic fluorite type crystal structure [10] and oxygen vacancies as main ionic defects. Fig. 2 shows the crystal structure of ceria. Pure CeO_2 ceramic is a mixed ionic electronic conductive material and is a poor oxide ion conductor [12]. Magdalena Dudek [13] reported that the bulk electrical conductivity of CeO_2 at 600°C is 6.16×10^{-5} S/cm. However, the ionic conductivity of ceria based

electrolytes can be significantly enhanced by introduction of some trivalent dopant ions, because the number of oxygen vacancies will be considerably increased by charge compensation [12]. The primary advantage of doped ceria based electrolytes such as gadolinium-doped ceria (GDC) and samarium-doped ceria (SDC) is that they generally show higher ionic conductivity than YSZ particularly at low temperatures [11]. So, considerable attention has been focused on these materials because they are promising electrolyte materials in low temperature solid oxide fuel cells applications.

Ionic conductivity in doped ceria is highly dependent on many factors e.g. type and concentration of the dopant ion, concentration of oxygen vacancy and the defect association enthalpy [12]. The relationships among the above mentioned four factors are closely and complicatedly related to the conductivity in doped ceria. Among the ceria solid electrolytes, samarium-doped ceria was found to have the highest ionic conductivity because ionic radius (1.08 Å) of the dopant ion (Sm^{3+}) is similar to the ionic radius of the host ion, resulting in the minimum association enthalpy between the dopant ion and oxygen vacancy [12]. The optimal dopant concentration for SDC is 20 mole% i.e. $Ce_{0.8}Sm_{0.2}O_{1.9}$ after which conductivity starts to decrease with the increase in dopant concentration [13] because of the increase interaction between the dopant ions and the oxygen vacancies and as a result mobility decreases.

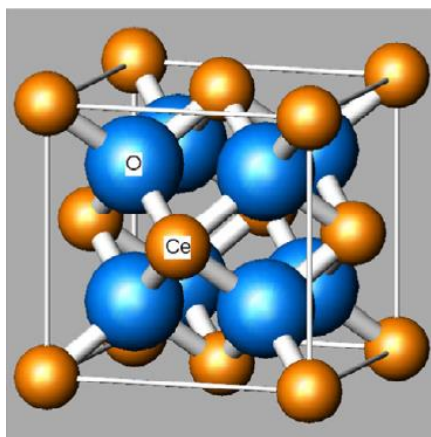Fig. 2 Cubic fluorite crystal structure of ceria-based electrolytes [10]

The ionic conductivity of SDC can be influenced and significantly enhanced by the different factors like grain boundary, microstructure, grain size and processing conditions [11]. These parameters are closely related to each other and they are predominantly depending upon the synthesis route. The ionic conductivity of SDC

electrolyte can also be increased by the addition of carbonates as the secondary phase. In addition to this, the inclusion of carbonates also improved the thermal stability of SDC. Furthermore, electronic conduction of SDC is also decreased by the carbonate addition [14]. In this work, different synthesis methods are discussed for the preparation of SDC and SDC-carbonate composite electrolytes to study the effect of synthesis routes on the ionic conductivity or activation energy of the electrolyte and the electrical properties of SOFCs.

2. Synthesis Methods for Samarium doped ceria

Synthesis method has a great influence on the properties of doped ceria based electrolyte materials. These properties include the particle size, surface area, etc. Thus, SDC electrolyte have been synthesized by different methods which include solid-state reaction and wet chemistry based routes e.g. sol-gel, co-precipitation, hydrothermal synthesis etc.

2.1. Overview of the Synthesis Routes

The solid-state reaction method is mostly employed to synthesize the ceramic compounds due to its simplicity, high yields and absence of solvents. The major disadvantages of solid-state reaction method are high calcination temperature, poor compositional homogeneity, uncontrollable particle size distribution, low surface area, poor sintering of products [15] and repeated milling to achieve high ionic conductivity powders. This process causes contamination by the crucibles, reagents or other impurities and results in the blocking of the oxygen ion migration and decrease in conductivity [15]. To overcome the disadvantages of solid-state reaction method, a number of wet chemistry based routes have been developed for the synthesis of samarium doped ceria electrolyte. The advantages of these methods include the homogeneous mixing of raw materials on atomic scale. Furthermore, the particle size, particulate morphology and surface area can be made controllable [15]. Among the numerous wet chemistry routes, sol-gel, co-precipitation and hydrothermal methods have found great interest due to their simplicity, versatility, and easy scale-up capability.

2.2. Experimental Description

2.2.1. Citrate complexation route

Marcin R. Kosinski and Richard T. Baker [16] prepared the SDC by citrate complexation route. The dopant concentration varies from 10 – 30 mole % and the nanopowders were sintered at 1300 °C, 1400 °C and 1450 °C using two sintering times, 4 h and 6 h. It was found that $Sm_{0.2}Ce_{0.8}O_{1.9}$ sintered at 1450 °C for 6 h showed the highest value of total ionic conductivity i.e. 0.0181 S/cm at 600°C.

2.2.2. Co-precipitation Method

Yen-Pei Fu et al. [12] used the co-precipitation technique to synthesize a solid samarium doped ceria electrolyte ($Ce_{0.8}Sm_{0.2}O_{1.9}$) and investigated the microstructure, thermal expansion, mechanical property and ionic conductivity of SDC. The starting materials were cerium nitrate hexahydrate ($Ce(NO_3)_3.6H_2O$) and samarium nitrate hexahydrate ($Sm(NO_3)_3.6H_2O$). NH_4OH solution was used as a precipitating agent. SDC pellets were sintered at 1500 °C for 5 h. The results showed that the average particle size varied from 10.9±0.4 to 13.5±0.5 nm. The relative density was 95% and the maximum ionic conductivity was 0.0223±0.00114 S/cm at 800°C.

2.2.3. Carbonate Co-precipitation Method

Changrong Xia et al. [17] employed the carbonate co-precipitation technique at low processing temperature for the synthesis of samarium doped ceria powder. The nitrates of cerium and samarium were used as the starting reagents. Ammonium carbonate was used as a precipitating agent. The powder was sintered at 1100 °C for 5 h and 98% of theoretical density was obtained. The value of conductivity was 0.022 S/cm at 600 °C and the activation energy was only 0.66 eV.

J. Manjanna et al. [18] recently developed the SDC electrolyte using carbonate co-precipitation method with different dopant concentrations ranged from 10 to 30%. On the basis of their results of AC-impedance, $Ce_{0.8}Sm_{0.2}O_{1.9}$ shows the highest value of the total oxygen ionic conductivity in the temperature range of 200 – 350 °C. In this range the total value of activation energy is 0.84 eV. They believed that SDC20 can be employed as potential electrolyte for low to intermediate temperature SOFCs as the oxygen-ion conductivity might increase with increase in temperature.

2.2.4. Ultrasound assisted Co-precipitation method

Hikmet Okkay et al. [19] synthesized $Ce_{0.8}Sm_{0.2}O_{1.9}$ electrolyte by ultrasound assisted (US) co-precipitation method. They were explored the effects of ultrasound power, ultrasound pulse ratio and probe type upon the ionic conductivity of SDC as well as the lattice parameter, the microstructure and the density. In their research work, they also compared the results of conventional (non-US) co-precipitation method and Ultrasound assisted (US) co-precipitation method. The sintering was done at 1200 °C for 6 h and relative density obtained was 95% in US assisted co-precipitation method. In US assisted co-precipitation method, the highest value of ionic conductivity was achieved at 800 °C and found to be 0.0307 S/cm with activation energy = 0.871 kJ mol^{-1}. This value was obtained with pulsed ultrasound for an acoustic intensity of 14.94 W/cm^2, employing 199 mm probe and 8:2 pulse ratio, while in the case of non-US co-precipitation method the value of ionic conductivity at 800 °C was 0.0167 S/cm with the activation energy of 0.888 kJ / mol. Thus ultrasound assisted (US) co-precipitation method was found to be a more promising and facile route for the synthesis of SDC as compared to conventional (non-US) co-precipitation method.

2.2.5. Hydrothermal Synthesis

Sea-Fue Wang et al. [20] prepared the samarium-doped ceria powders using co-precipitation method followed by hydrothermal synthesis. The electrical conductivity of sintered $Ce_{0.8}Sm_{0.2}O_{1.9}$ ceramics was 0.048 S/cm at 700 °C and activation energy of 0.73 eV was registered.

2.2.6. Glycine-Nitrate Process

GNP is relatively inexpensive technique to prepare fine and homogeneous particles. This process is mainly based on the exothermicity of the reaction between glycine (the fuel) and nitrate (the oxidizer). Ruifen Tian et al. [21] were prepared the SDC ($Ce_{0.8}Sm_{0.2}O_{1.9}$) ceramic electrolytes by the glycine-nitrate process and studied the sintering characteristics and electrical properties of SDC. $Ce(NH_4)_2(NO_3)_6$ and $Sm(NO_3)_3$ were used as the precursors to form solution in a distilled water and then glycine was added. The heating was done on a hot plate and as water evaporated, viscous gel was formed and eventually heated to flame. The resulted yellow fine powders were heat treated at 600 °C for 2 h. After calcination, pellets of the resulted powders were formed by

uniaxial pressing and then sintered from 1000 to 1500 °C for 5 h. The highest ionic conductivity of 0.0154 S/cm was exhibited at 600 °C, when the SDC pellet was sintered at 1300 °C.

Recently, Zhangbo Liu et al. [22] synthesized the SDC ($Ce_{0.8}Sm_{0.2}O_{1.9}$) from mixed cerium sources ($Ce(NO_3)_3.6H_2O$ and $Ce(NH_4)_2(NO_3)_6$) using glycine-nitrate process. $Sm(NO_3)_3.6H_2O$, $Ce(NO_3)_3.6H_2O$ and $Ce(NH_4)_2(NO_3)_6$ were used as the starting materials. Glycine as added as both the complexing agent and the fuel. Stirring was done for about half an hour to allow full complexation and then solution was heated to ignite self-sustaining combustion. After combustion, the resulted ashes were calcined at 600 °C for 2 h to obtain crystalline SDC. NiO – SDC and SSC ($Sm_{0.5}Sr_{0.5}CoO_3$) were used as anode and cathode, respectively. Single cell was fabricated by co-pressing and co-sintering techniques. For the testation of the single cell, hydrogen was used as fuel while ambient air was used as the oxidant. When the molar ratio of the two cerium precursors is around 1:1, the obtained SDC exhibited the highest conductivities of 0.020 S/cm, with activation energy of approximately 0.70 eV and the power density of 0.725 W/cm^2 at 600 °C.

3. Synthesis Methods for SDC – Carbonate Composite Electrolytes

SDC – carbonate composite electrolytes can be prepared by two processes i.e. multi – step process and single – step process. In the initial step of multi – step process, SDC was prepared in the form of a solid electrolyte usually through wet-chemistry routes and then carbonates are added in the SDC powder generally by solid-state reaction method, while in the single – step process addition of carbonates and preparation of a SDC both are taking place in a single step.

3.1. Multi – Step Process

C. M. Lapa et al. [23] synthesized Samaria-doped ceria-based composites using a multi-step process. In the first step SDC ($Ce_{0.8}Sm_{0.2}O_{1.9}$) was prepared through co-precipitation route. Cerium and samarium nitrates were used as the starting materials while sodium carbonate and ammonia were used as the precipitating agents. The precipitate was dried at 120 °C and heat treatment was done at 700 °C for 2 h. The SDC-carbonate composites were synthesized using solid-state method combining the already prepared SDC powder with Na_2CO_3 (30 wt. %) and $(Li,Na)_2CO_3$ (30 wt. %) while Li/Na molar ratio was 1:2.

Then heat treatment of the composite electrolytes was done at 680 °C for 1 h. and subsequently pellets were formed and sintered at 680 °C for 0.5 h for densification. The electrical conductivity of the SDC-carbonate composites were measured using impedance spectroscopy carried out in air and it was found that composite based on $(Li,Na)_2CO_3$ had the highest value of electrical conductivity at 500 °C i.e., 0.2 S/cm.

Jianbing Huang et al. [24] synthesized SDC-carbonate composite using two-step process. Initially, SDC ($Ce_{0.8}Sm_{0.2}O_{1.9}$) was synthesized by oxalate co-precipitation method. Then SDC powder was mixed with binary carbonates (53 mol. % Li_2CO_3:47 mol. % Na_2CO_3) in various contents (10-35 wt. %). Before the heat treatment at 680 °C for 40 min, the mixtures of the composite electrolytes were ground intensively for homogenization. After the heat treatment the cylindrical pellets of the composite electrolytes were formed and then pellets were sintered at 600 °C for 1 h. For the fabrication of the single cells based on the composite electrolytes, NiO was used as anode and lithiated NiO was used as cathode. The performance of the single cells was tested between 400 and 600 °C using hydrogen as fuel and air as the oxidant. The maximum power density of 1085 mW/cm^2 and an open circuit voltage of 0.95 V was obtained at 600 °C for 25 wt. % SDC- carbonates.

Muhammed Ali S.A. et al. [25] prepared the SDC-carbonate composite electrolytes using solid state reaction method and studied the effects of sintering temperature on the power density of composite electrolytes. Firstly SDC was prepared employing sol-gel technique. $Ce(NO_3)_3.6H_2O$, $Sm(NO_3)_3.6H_2O$ and citric acid were used as the starting materials and the resulting gel was completely dried in a pre-heated oven. Afterwards, calcination of the dried powder was done at 850 °C for 5 h to obtain the SDC. Secondly Li/Na carbonate was prepared in a high-speed ball mill by mixing Li_2CO_3 and Na_2CO_3 (Li/Na molar ratio 2:1) for 16 h. Then Li/Na carbonate and SDC were mixed in a weight ratio of 2:8 by wet ball milling using ethanol for 16 h. After thorough mixing, the sample was dried in an oven for the evaporation the ethanol. The resultant dried sample was heat treated in a furnace at 680 °C for 1 h to get the desired SDC-carbonate composite electrolyte. The pellets of the composite electrolyte were formed by applying a die-press and pellets were sintered at four different temperatures i.e., 500 °C, 550 °C, 600 °C and 650 °C for 5 h. These pellets were tested using hydrogen as fuel and air as an oxidant in

the temperature range of 500 – 650 °C. Results showed that the pellets sintered at 550 °C exhibited a maximum power density i.e., 63.5 mW/cm^2 and an open circuit voltage of 1.14 V at an operating temperature of 650 °C.

Ning Zuo et al. [26] synthesized the samarium doped ceria - carbonate composite electrolyte based on $Ce_{0.8}Sm_{0.2}O_{1.9}$ – 25 wt. % K_2CO_3 by two step process. In the first step, SDC powder was prepared through carbonate co-precipitation process. Cerium nitrate hexahydrate ($Ce(NO_3)_3.6H_2O$) and samarium oxide (Sm_2O_3) were used as the precursors. Dilute nitric acid was used as the solvent for the dissolution of the precursors. Ammonium carbonate solution was used as a precipitating agent. The precipitates were dried at 80 °C for 12 h and then calcination was done at 750 °C for 3 h to get the SDC. In the next step, SDC was mixed with 25 wt. % K_2CO_3 and heat treated at 680 °C for 30 min to obtain the SDC – carbonate composite electrolyte. A mixture of 45 wt. % electrolyte, 45 wt. % NiO and 10 wt. % starch was used as an anode while the mixture of 40 wt. % electrolyte and 60 wt. % SSC ($Sm_{0.5}Sr_{0.5}CoO_2$) was used as a cathode. For the fabrication of the anode-supported single cell, a composite electrolyte, an anode and a cathode were uni-axially pressed and the resulted pellets were sintered at 600 °C for 30 min. The single cell was tested in a temperature ranged from 550 °C to 700 °C using hydrogen as a fuel and air as an oxidant. The maximum power density and open circuit voltage achieved were 602 mW/cm^2 and 1.05 V at 700 °C, respectively.

3.2. Single - Step Process

Rizwan Raza et al. [27] successfully developed the ceria-carbonate composite electrolyte with one-step chemical co-precipitation process i.e. prepared the SDC and mixed the carbonates in the same process. Hexahydrates of cerium and samarium were used as the starting reagents. A suitable amount of Na_2CO_3 solution was gradually added to complete the ceria – carbonate composites within a wet-chemical co-precipitation process. In this way a mixture of carbonate and SDC was obtained in the same process. The resulted precipitates were dried in an oven at 50 °C. The dried powder was ground thoroughly in a mortar with pestle. Finally, the sample was sintered at 800 °C for 2 h to get the SDC-Na_2CO_3 composite electrolyte. The composite electrodes were synthesized by solid state reaction method using lithium, copper and nickel carbonates. The sintering of the electrodes was done at 800 °C for 4 h. The fabrication of the fuel cell was done by

hot pressing technique. Anode, electrolyte and cathode were pressed in one step to form a fuel cell assembly. The resulted pellets were sintered at 600 °C for 0.5 h. I-V and I-P characteristics of the single fuel cell were determined and it was found that the maximum power density of 1150 mW/cm^2 and an open circuit voltage of 1.018 V were obtained at 500 °C.

Some researchers [14,28] developed the SDC – carbonate composite electrolytes by a freeze drying technique and improved freeze drying technique based on the formation of lanthanide citrate complex solution/gel. This improved freeze drying method has several advantages over the single-step co-precipitation method. In the one-step co-precipitation process, it is difficult to control the carbonate content accurate because most of the carbonate salt is lost from the solution after filtration. The freeze drying method assisted by the formation of lanthanide citrate complex solution/gel enables the mixing of the SDC phase with the carbonate phase in molecular scale and also keep the carbonate content accurate. By applying this method, the interface area between the SDC crystal phase and the carbonate phase can be increased to improve the ionic conductivity. In this method normal mixing is taking place instead of precipitation and the solvent will be removed in the freeze dryer. Thus the mixture will keep the same morphology which was existed in the liquid state. By applying this improved method, Yifu Jing et al. [28] developed the composite electrolyte based on SDC and $(Li,Na,K)_2CO_3$ having the $Li_2CO_3:Na_2CO_3:K_2CO_3 = 15:7.5:7.5$ and $(Li,Na,K)_2CO_3:SDC = 30:70$ was prepared. This electrolyte exhibited the ionic conductivity of 0.4 S/cm at 600 °C.

4. Conclusions

Lowering the working temperature (500 – 600 °C) of the SOFC will definitely enhance the possibilities for their commercialization. SDC ($Ce_{0.8}Sm_{0.2}O_{1.9}$) prepared through different wet chemistry based routes especially with co-precipitation is a promising electrolyte for intermediate temperature SOFCs. However, the performance of the SDC electrolyte can be significantly enhanced by adding carbonates as the secondary phase. In SDC – carbonate composite electrolytes SDC is present in the crystalline phase while carbonates are present in an amorphous phase. SDC – carbonate composites are multi ions (O^{2-}, H^+, CO_3^{2-}) conductive electrolytes and these materials also decreases the electronic conduction of SDC. SDC – carbonate composites prepared through a single

step process either from co-precipitation or freeze drying method exhibited an excellent performance at intermediate temperatures (500 – 600 °C). Single – step process offers a precise control on the microstructure and morphology of the composite electrolytes. Furthermore, composite electrolytes prepared through single – step process were more homogeneous and this method is also cost effective. Therefore, it may be concluded that SDC – carbonate composites prepared through the single – step process are the promising electrolytes for intermediate temperature SOFCs but their mechanical and thermal properties at intermediate temperatures are still needed to be investigated in detail.

Acknowledgement

References

[1]   I. Dincer, Environmental and sustainability aspects of hydrogen and fuel cell systems, Int. J. Energy Res. 31 (2007) 29–55.

[2]   U. Lucia, Overview on fuel cells, Renew. Sustain. Energy Rev. 30 (2014) 164–169.

[3]   D. Medvedev, A. Murashkina, E. Pikalova, A. Demin, A. Podias, P. Tsiakaras, $BaCeO_3$: Materials development, properties and application, Prog. Mater. Sci. 60 (2014) 72–129.

[4]   L. Fan, C. Wang, M. Chen, B. Zhu, Recent development of ceria-based (nano)composite materials for low temperature ceramic fuel cells and electrolyte-free fuel cells, J. Power Sources. 234 (2013) 154–174.

[5]   S. Jiang, Advances and challenges of intermediate temperature solid oxide fuel cells: A concise review, J. Electrochemistry, 18 (2012) 479-495.

[6]   O. Yamamoto, Solid oxide fuel cells: fundamental aspects and prospects, Electrochim. Acta. 45 (2000) 2423–2435.

[7]   P. Singh, N. Q. Minh, Solid Oxide Fuel Cells: Technology Status, Int. J. Appl. Ceram. Technol. 1 (2005) 5–15.

[8]   S. Simeonov, S. Kozhukharov, M. Machkova, N. Saliyski, V. Kozhukharov, Innovative methods and technologies for elaboration of sofc ceramic materials (Review), Journal of University of Chemical Technology and Metallurgy, 47 (2012) 485–492.

[9]   Y. Zhao, C. Xia, L. Jia, Z. Wang, H. Li, J. Yu, et al., Recent progress on solid oxide fuel cell: Lowering temperature and utilizing non-hydrogen fuels, Int. J. Hydrogen Energy. 38 (2013) 16498–16517.

[10]   M. Lo Faro, D. La Rosa, V. Antonucci, A. Salvatore, Intermediate temperature solid oxide fuel cell electrolytes, Journal of the Indian Institute of Science, 89 (2009) 363-380.

[11]   S. (Rob) Hui, J. Roller, S. Yick, X. Zhang, C. Decès-Petit, Y. Xie, et al., A brief review of the ionic conductivity enhancement for selected oxide electrolytes, J. Power Sources. 172 (2007) 493–502.

[12] Y. P. Fu, S. B. Wen, C. H. Lu, Preparation and Characterization of Samaria-Doped Ceria Electrolyte Materials for Solid Oxide Fuel Cells, J. Am. Ceram. Soc. 91 (2007) 127–131.

[13] M. Dudek, Ceramic oxide electrolytes based on CeO_2—Preparation, properties and possibility of application to electrochemical devices, J. Eur. Ceram. Soc. 28 (2008) 965–971.

[14] X. Wang, Y. Ma, S. Li, B. Zhu, M. Muhammed, SDC/Na_2CO_3 Nanocomposite: New freeze drying based synthesis and application as electrolyte in low-temperature solid oxide fuel cells, Int. J. Hydrogen Energy. 37 (2012) 19380–19387.

[15] Z. Shao, W. Zhou, Z. Zhu, Advanced synthesis of materials for intermediate-temperature solid oxide fuel cells, Prog. Mater. Sci. 57 (2012) 804–874.

[16] M. R. Kosinski, R. T. Baker, Preparation and property–performance relationships in samarium-doped ceria nanopowders for solid oxide fuel cell electrolytes, J. Power Sources. 196 (2011) 2498–2512.

[17] D. Ding, B. Liu, Z. Zhu, S. Zhou, C. Xia, High reactive $Ce_{0.8}Sm_{0.2}O_{1.9}$ powders via a carbonate co-precipitation method as electrolytes for low-temperature solid oxide fuel cells, Solid State Ionics. 179 (2008) 896–899.

[18] K. C. Anjaneya, G. P. Nayaka, J. Manjanna, G. Govindaraj, K. N. Ganesha, Preparation and characterization of $Ce_{1-x}Sm_xO_{2-\delta}$ (x = 0.1–0.3) as electrolyte material for intermediate temperature SOFC, Solid State Sci. 26 (2013) 89–96.

[19] H. Okkay, M. Bayramoglu, M. Faruk Öksüzömer, $Ce_{0.8}Sm_{0.2}O_{1.9}$ synthesis for solid oxide fuel cell electrolyte by ultrasound assisted co-precipitation method., Ultrason. Sonochem. 20 (2013) 978–83.

[20] S. Wang, C. Yeh, Y. Wang, Y. Wu, Characterization of samarium-doped ceria powders prepared by hydrothermal synthesis for use in solid state oxide fuel cells, J Mater Res Technol 2 (2013) 141–148.

[21] R. Tian, F. Zhao, F. Chen, C. Xia, Sintering of Samarium-doped ceria powders prepared by a glycine-nitrate process, Solid State Ionics. 192 (2011) 580–583.

[22]   Z. Liu, D. Ding, M. Liu, X. Li, W. Sun, C. Xia, et al., Highly active $Sm_{0.2}Ce_{0.8}O_{1.9}$ powders of very low apparent density derived from mixed cerium sources, J. Power Sources. 229 (2013) 277–284.

[23]   C. M. Lapa, F. M. L. Figueiredo, D. P. F. De Souza, L. Song, B. Zhu, F. M. B. Marques, Synthesis and characterization of composite electrolytes based on samaria-doped ceria and Na/Li carbonates, Int. J. Hydrogen Energy. 35 (2010) 2953–2957.

[24]   J. Huang, Z. Mao, Z. Liu, C. Wang, Development of novel low-temperature SOFCs with co-ionic conducting SDC-carbonate composite electrolytes, Electrochem. Commun. 9 (2007) 2601–2605.

[25]   S. A. Muhammed Ali, A. Muchtar, A. Bakar Sulong, N. Muhamad, E. Herianto Majlan, Influence of sintering temperature on the power density of samarium-doped-ceria carbonate electrolyte composites for low-temperature solid oxide fuel cells, Ceram. Int. 39 (2013) 5813–5820.

[26]   N. Zuo, M. Zhang, Z. Mao, Z. Gao, F. Xie, Fabrication and characterization of composite electrolyte for intermediate-temperature SOFC, J. Eur. Ceram. Soc. 31 (2011) 3103–3107.

[27]   R. Raza, X. Wang, Y. Ma, X. Liu, B. Zhu, Improved ceria–carbonate composite electrolytes, Int. J. Hydrogen Energy. 35 (2010) 2684–2688.

[28]   Y. Jing, J. Patakangas, P. D. Lund, B. Zhu, An improved synthesis method of ceria-carbonate based composite electrolytes for low-temperature SOFC fuel cells, Int. J. Hydrogen Energy. (2013) 1–7.

Annexure-C

Development of Samarium-Doped Ceria (SDC) and SDC-based composite electrolytes for use in Intermediate Temperature Solid Oxide Fuel Cells (IT-SOFCs)

Mustafa Anwar[a], M. N. Akbar[a], M. A. Rana[a], K. Mustafa[a], S. Shakir[a], Zuhair. S. Khan[a*]
[a]Advanced Energy Materials & Fuel Cells Lab, Centre for Energy Systems, National University of Sciences & Technology, Sector H-12, Islamabad, Pakistan
*Corresponding Author; Email: zskhan@ces.nust.edu.pk

Abstract

SOFCs have potential to be the most efficient and environmentally benign system for direct conversion of a wide variety of fuels to electricity. The electrolyte is the principal component of importance for SOFC. Ceria-based electrolyte materials have great potential in IT-SOFC applications. In the present study, samarium doped ceria (SDC), and samarium doped ceria–based composite with addition of potassium carbonate were prepared by co-precipitation route. Meanwhile, the effect of pH of solution during synthesis on the microstructure and morphology of SDC and the effects of calcination temperature on the crystallite size and lattice strain of SDC-K_2CO_3 were also investigated. An experiment is also performed in order to enhance the ionic conductivity of pure SDC by the co-doping of yttrium. At the end, chemical compatibility test was performed between the co-doped electrolyte (YSDC) and lithiated NiO cathode. XRD and SEM studies showed that the crystallite size and particle size of SDC increases with the increase in pH. The SEM images of all the samples of SDC synthesized at different pH values showed the irregular shaped and dispersed particles. SDC-K_2CO_3 was calcined at 600 °C, 700 °C and 800 °C for 4 h and XRD results showed that crystallite size increases while lattice strain decreases with the increase in calcination temperature and no peaks were detected for K_2CO_3 because it is present in the electrolyte as amorphous phase. The ionic conductivity of the electrolytes increases with the increase in temperature and SDC-K_2CO_3 shows the highest value of ionic conductivity as compared to SDC and YSDC. Chemical compatibility test shows that lithidated NiO cathode and YSDC electrolyte can be used together up to the temperature of 700 °C.

Keywords: SOFC, Electrolyte, SDC, Carbonates, Co-doping

1. Introduction

Now-a-days there is a great concern of human society in sustainable, environmental friendly and efficient energy conversion technologies because of the ever growing energy demand and the fast depletion of fossil fuels. Presently fuel cells are attracting enormous interest because of their great potential for power generation to meet the demands of diversified applications in a highly efficient and environmentally benign way. Fuel cells are electrochemical devices that directly convert the chemical energy of a fuel into the electrical energy. Among various types of fuel cells, generally classified by the electrolyte, solid oxide fuel cells (SOFCs) using an oxide ceramic electrolyte offer significant advantages for residential and auxiliary power units, as well as for larger industrial power applications: highest energy conversion efficiency with heat recovery or combined power generation, fuel flexibility, and simplicity of system design by internal reforming and modular construction [1]. The electrolytic material, being the heart of an SOFC unit has been a topic of interest and continuous development. The main function of an electrolyte is to conduct a specific ion from cathode to anode in order to complete the oxidation – reduction reaction. Commonly, solid electrolyte materials which are used in SOFC are; yttria stabilized zirconia, doped ceria, stabilized Bi_2O_3, and strontium/magnesium doped lanthanum gallate [2]. Rare-earth doped ceria-electrolytes have been regarded among the most promising high-conducting and good-compatible with electrodes for SOFCs compared to other electrolytes in the intermediate-temperature range of around 500–800 °C [3]. Among them Sm^{+3} doped ceria (SDC) exhibits the highest oxygen ion conductivity at certain fixed doping levels, due to its smallest association enthalpy between the dopant cations and oxygen vacancies in the fluorite lattice [4,5]. The ionic conductivity increases with increasing Sm^{+3} doping and reaches the maximum for $Ce_{0.8}Sm_{0.2}O_{1.9}$ [6].

In the recent years, various techniques have been employed for the synthesis of SDC such as hydrothermal [7], sol-gel [8], solvothermal [9], co-precipitation [5], ultrasound assisted co-precipitation [4], glycine – nitrate [10] and carbon assisted spray pyrolysis [11]. The products obtained by wet – chemistry routes are of high purity, homogeneity, ultrafine and requires lower sintering temperature and time [12]. Among the various wet chemical routes, co-precipitation is a simple process with promising results for

synthesizing very fine powders with high sinterability. Although samarium doped ceria have been widely investigated since past few decades, however up to best of our knowledge there is no systematic study which describes the effects of pH of medium during co-precipitation using ammonium hydroxide on the microstructure of samarium doped ceria. Hence, in this work we present a systematic study in which effects of pH of the medium during co-precipitation on the crystallite size, lattice strain, particle size and the morphology of SDC is discussed. However, SDC has low ionic conductivity as compared to the value which is sufficiently require for high performance SOFCs, and in reducing conditions Ce^{4+} is partially reduced to Ce^{+3} which causes electronic conduction and thus significantly decreases the efficiency of the fuel cell [13].

In the recent years, researchers are working to enhance the ionic conductivity and suppress the electronic conductivity of doped ceria systems by adding alkali carbonates (Na_2CO_3, Li_2CO_3) in the doped ceria systems. These electrolytes are commonly known as composite electrolytes because these are two-phase systems where carbonates are present as secondary phase in an amorphous form [13,14]. Lot of research is being carried out on SDC systems by adding lithium, potassium and sodium carbonates as a secondary phase [13–19] but until now there is not enough literature which shows the effect of calcination temperature on the crystallite size and the lattice strain of SDC-K_2CO_3. Thus this study also presents the effects of calcination temperature on the microstructure of SDC-K_2CO_3 composite electrolyte.

Co-doping with some other element is another useful approach to enhance the ionic conductivity of doped ceria systems. Results showed that co-doping of yttrium and neodymium in gadolinium doped ceria and samarium doped ceria electrolytes respectively, increases the ionic conductivity of these electrolytes [20,21]. Thus in this study an experiment is also done to report the effect of co-doping with Yttrium on the ionic conductivity of SDC electrolyte (YSDC).

In order to obtain a durable and high performance intermediate temperature SOFCs, the development of new cathode materials that are compatible with doped ceria based systems is also very important. Studies [20,22] showed that lithiated NiO is a promising cathode material for doped ceria based systems. But up to best of our knowledge no systematic study is present that shows the chemical compatibility of lithiated NiO

cathode with YSDC co-doped electrolyte. Hence in this study we also performed a chemical compatibility test of both these materials.

2. Experimentation and Characterization

2.1. Experimentation

2.1.1. Synthesis of samarium-doped ceria (SDC) at different pH values

Cerium nitrate hexahydrate ($Ce(NO_3)_3.6H_2O$) and samarium nitrate hexahydrate ($Sm(NO_3)_3.6H_2O$) were used as precursors. Stoichiometric amounts of $Ce(NO_3)_3.6H_2O$ and $Sm(NO_3)_3.6H_2O$ were taken in a beaker and mixed in de-ionized water. The molarity of the solution was kept at 0.5 M. The heating of the solution was done at 80 °C. Then ammonia solution was added drop-wise into the precursor's solution and the pH value was adjusted at three different values i.e., 8, 10 and 11. After the addition of ammonia solution the precipitation was occurred with a curd type slurry look. Then the precipitates were dried at 120 °C in a drying oven. After the complete drying, the calcination of the samples was done at 800 °C for 3 h with the heating rate of 10 °C/min. Then grinding of the heat treated sample was done with the help of pestle and mortar to obtain fine and homogeneous particles of the electrolyte. In order to the measure the conductivity of the electrolyte, a pellet was formed with the help of a hydraulic press. The pressure applied was 5 kg/cm^2 for about 10 minutes. The thickness of the pellet was 1.37 mm while the diameter was 10 mm. The pellet was sintered at 1100 °C for 3 hours.

2.1.2. Synthesis of samarium doped ceria by the addition of potassium carbonate (SDC-K_2CO_3) at different calcination temperatures

In this experiment, SDC-K_2CO_3 composite electrolyte was synthesized using the wet-chemistry route by employing one-step co-precipitation method. Stoichiometric amounts of $Ce(NO_3)_3.6H_2O$ and $Sm(NO_3)_3.6H_2O$ were added in 20 mL of deionized water. Here molarity of the solution was kept at 0.5 M. Then the solution was stirred for about 15 minutes at 80 °C for homogenization and initiation of the reaction between cerium and samarium salts. Then dissolve the stoichiometric amount of K_2CO_3 in 20 mL of deionized water and stirred at room temperature for about 15 minutes. Here Molarity = 0.5 M. Pour the carbonate solution in to the SDC solution (drop wise) and stirred the resulting solution at 100 °C for an hour. After sometime the precipitates were formed. Then completely dry the precipitates at 120 °C in a drying oven. Finally, the dried

powder was divided into three equal parts and calcined at 600 °C, 700 °C and 800 °C, respectively for 4 h to obtain the desired electrolyte, and then calcined samples were ground in a mortar with a pestle to obtain homogeneity and fine particles. In order to find the ionic conductivity, the pellet of the composite electrolyte calcined at 600 °C was formed by using hydraulic press and die. The thickness of the pellet was approximately 3.4 mm and the diameter was 13 mm, while the pellet was sintered at 1000 °C for 1 h.

2.1.3. Synthesis of co-doped SDC by the addition of yttrium as a co-dopant (YSDC)

Co-precipitation method was employed for the preparation of co-doped SDC by the addition of yttrium. The composition of the electrolyte is $Ce_{0.8}Sm_{0.1}Y_{0.1}O_{1.9}$. First of all, stoichiometric quantities of precursors i.e., $Ce(NO_3)_3.6H_2O$, $Sm(NO_3)_3.6H_2O$ and $Y(NO_3)_3.6H_2O$ were dissolved in 20 mL of de-ionized water by stirring and heating at 60 °C for one hour. Then ammonia solution was added drop-wise into the precursor's solution till the precipitation occurred at the pH of 10. Afterwards, precipitates were heated at 80 °C for about two hours and then complete drying of the precipitates was done in a drying oven at 120 °C. After drying, calcination of the dried sample was done at 800 °C for 3 h with the heating rate of 10 °C/min. At the end, the heat treated sample was ground with the help of pestle and mortar to obtain homogenize and fine particles of the electrolyte. In order to measure the conductivity, pellet of the prepared sample was formed. The thickness of the pellet was 14 mm while its diameter was 13 mm. Sintering of the pellet was done at 1100 °C for about 3 h.

2.1.4. Chemical compatibility test of co-doped electrolyte (YSDC) with lithiated NiO cathode

Chemical compatibility test was performed by employed solid state reaction method. Lithiated nickel oxide is employed as a cathode material in high temperature fuel cells i.e., SOFC and MCFC. The starting materials for this solid state reaction method are lithiated nickel oxide ($Li_{0.68}Ni_{1.32}O_2$) and YSDC. Both lithiated nickel oxide and YSDC were synthesized by employing sol-gel and co-precipitation methods, respectively. Stoichiometric amounts of both the precursors were taken in the weight ratio of 1:1. Then thorough mixing of these precursors was done with the help of pestle and mortar for about 60 minutes. After this, heat treatment of the sample was done at 800 °C for 3 h at the heating rate of 10 °C/min. After calcination, XRD of the calcined sample was done

in order to check the formation of any new phases or new products by the reaction of the precursors.

2.2. Characterization

Phase purity and crystal structure of the prepared electrolyte was determined by X-ray diffraction equipment (STOE Germany). X-ray powder diffraction (XRD) of the sample was recorded using CuKα radiation (λ = 1.5425 Å), with 2θ varying from 10° to 80°. The diffraction pattern was scanned in steps of 0.015°. The morphology, particle size and elemental composition of the synthesized samples were examined by scanning electron microscope along with energy dispersive spectroscopy (JEOL Analytical SEM). Conductivity was measured by LCR meter (Wayne Kerr Electronics) up to the temperature of 700 °C.

3. Results and Discussion

3.1. Effects of pH of medium on the microstructure of SDC electrolyte
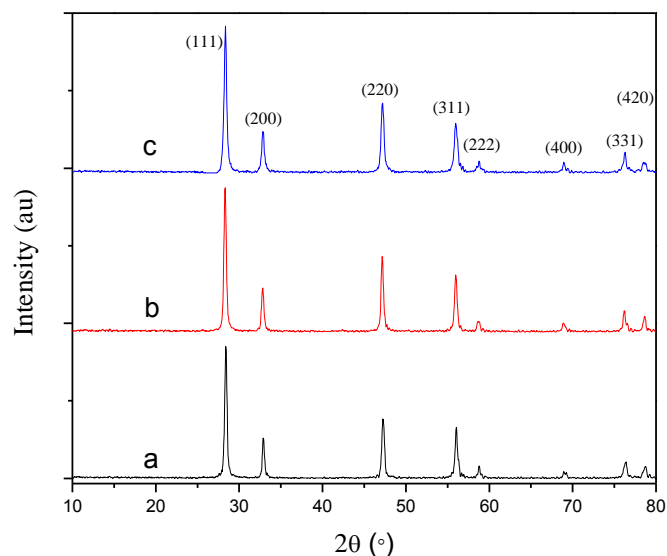

Fig. 3 XRD Patterns of SDC Electrolyte at (a) pH = 8, (b) pH = 10 and (c) pH = 11

Fig. 1 shows the XRD indexing of the SDC nanoparticles prepared at the pH value of 8, 10 and 11. All peaks were identified to be the cubic fluorite crystal structure with the space group Fm-3m (225) (PDF Card#75-0158). There was no evidence of any other phases. The crystallite sizes (D_{XRD}) of SDC at different pH values of 8, 10 and 11 were calculated using Scherrer's equation and found to be 26.7 nm, 35.9 nm and 43.4 nm

respectively. Table 1 shows the different parameters calculated from XRD results. Lattice strain is calculated by using X'pert HighScore software. The mathematical form of the Scherrer's equation is given below:

$$D_{XRD} = 0.9\,\lambda / \beta.\cos\theta$$

λ is the wavelength of the X-rays (nm), θ is the diffraction angle, and β is the corrected full width at half maximum (FWHM) intensity. The lattice parameter (a) of both the electrolytes can be calculated by the following relations:

$$d = \lambda / 2\sin\theta;\ a = d\,\sqrt{h^2 + k^2 + l^2}$$

The theoretical density of the SDC crystal structure was calculated according to equation given below from the crystallographic information obtained by XRD.

$$\rho_{XRD} = \frac{4\left[(1 - x).M_{Ce} + x.M_{Sm} + \left(2 - \left(\frac{x}{2}\right)\right).M_o\right]}{a^3.N_{Av}}$$

M is atomic weight (g mol^{-1}), 'x' is the dopant mole fraction, 'a' is the unit cell lattice parameter (Å) and N_{Av} is Avogadro's constant.

Table 6 Results based on XRD Studies

Sample (SDC)	d (nm)	a (nm)	V (nm^3)	D $_{XRD}$ (nm)	ρ_{XRD} (g/cm^3)	Lattice Strain
pH = 8	0.3139	0.5437	0.1607	26.7	7.13	0.542 %
pH = 10	0.3151	0.5458	0.1626	35.9	7.05	0.408 %
pH = 11	0.3145	0.5447	0.1616	43.4	7.09	0.340 %

The precipitation mechanism of metal cations happens through the formation of solvated cation complexes, hydrolysis and condensation. The hydrolysis and condensation behaviour of the solution is affected by the pH during co-precipitation and therefore, affects the crystallite size. With the increase in pH value the rate of hydrolysis decreases due to the gradual decrease in the concentration of the metal cations. The intensity and broadening of the peaks in the diffractogram is starting to increase by increasing the pH value. This shows that increase in pH facilitates in nucleation and growth of crystals. Therefore, crystallite size increases with the increase in pH value [23]. Ce(OH)$_3$ and Sm(OH)$_3$ are the basic precipitates, so by increasing OH− ions the solubility of both these hydroxides decreases.

According to the XRD results, the lattice strain decreases with the increase in pH value this shows that the more precisely doped sample is obtained at pH 11 because the mismatch between the host ion and the doped ion is minimum at pH 11. Studies concluded that the ionic conductivity will be high when the lattice strain is less. So we may say that with the increase in pH value the precipitation will goes towards completion and we obtained a perfectly doped sample at higher pH value.

Fig. 2 shows the SEM micrographs of the SDC electrolyte synthesized at various pH values of 8, 10 and 11. SEM micrographs shows that the particles synthesized at various pH values have irregular shapes and more or less have same morphology. SEM images show that the particles are dispersed. The particle size ranges from 24 – 28 nm for pH 8, 28.28 nm to 36.88 nm for pH 10, and 36 nm to 40 nm for pH 11. We may say that Ostwald's ripening is enhanced with the increase in pH of the solution due to the increase in the number density of nuclei [24,25].
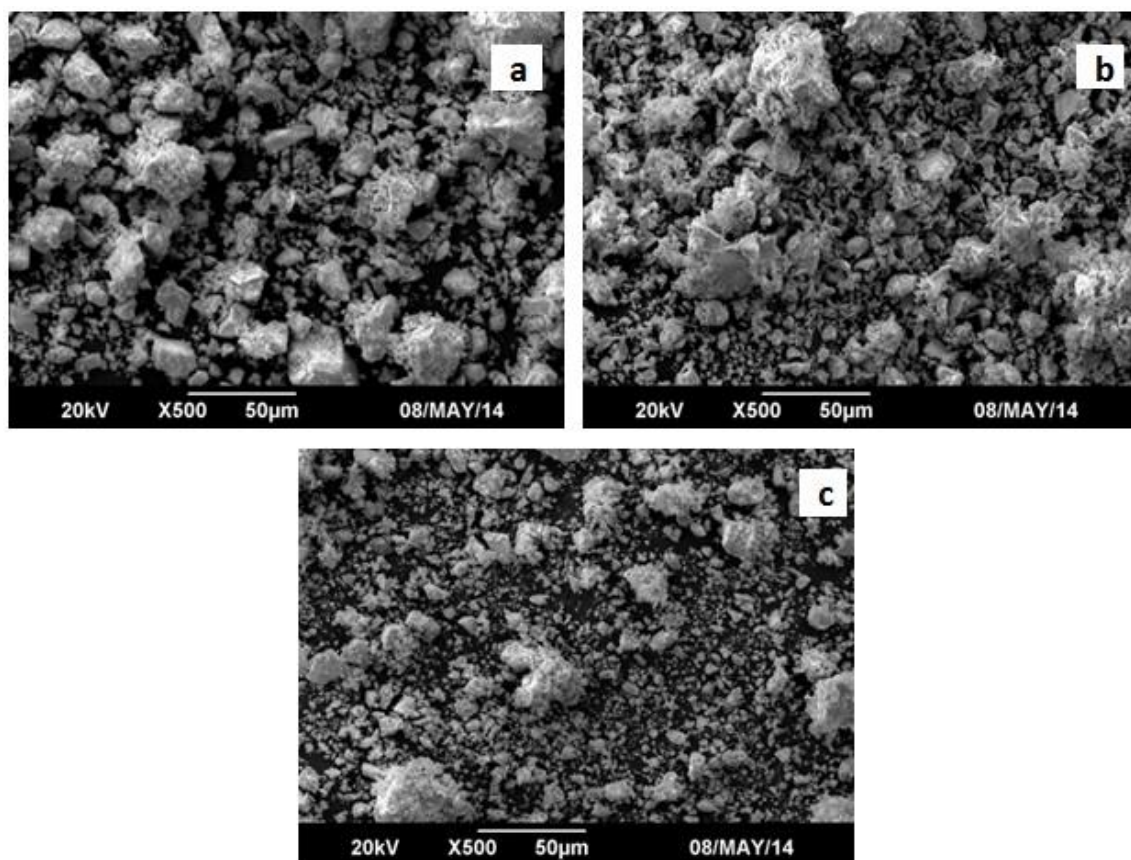

Fig. 4 SEM Micrographs of SDC synthesized at (a) pH = 8, (b) pH = 10, (c) pH = 11

The EDS analysis was done to determine the elemental composition of SDC. Analysis shows that no impurities were present in the synthesized sample and the particles of Ce and Sm are completely dispersed in the synthesized sample. The mass percentages of 74%, 26% and 10% were obtained for Ce, Sm and O, respectively.
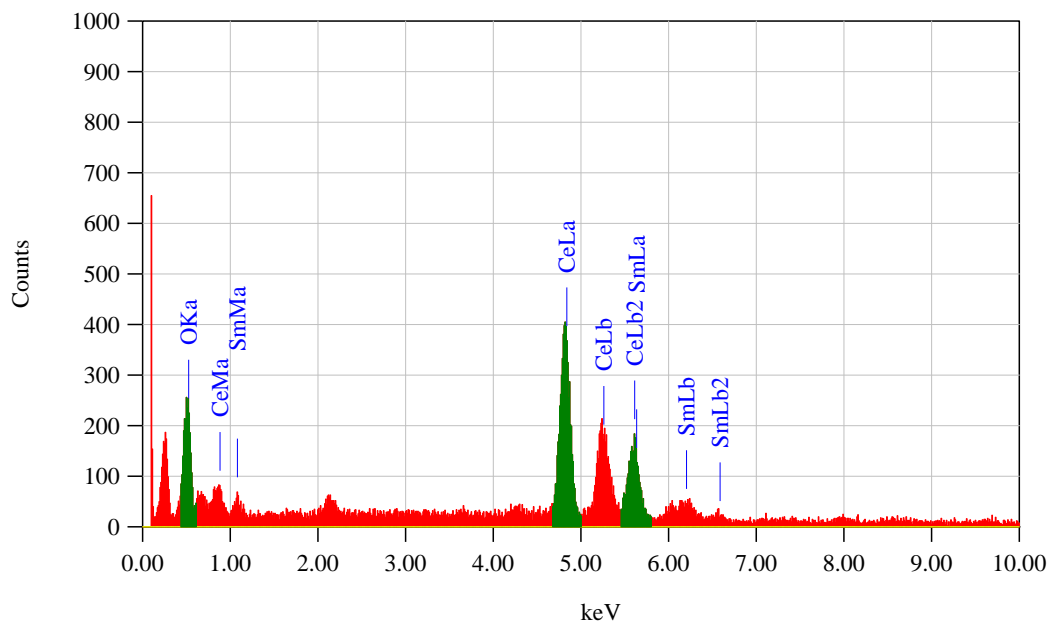

Fig. 9 EDS spectrum of samarium-doped ceria

3.2. Effects of calcination temperature on the microstructure of SDC-K$_2$CO$_3$

The XRD diffractograms of composite electrolyte based on SDC with the addition of K$_2$CO$_3$ is shown in Fig. 4. All peaks were designated to be the cubic fluorite crystal structure of samarium doped ceria with the space group Fm-3m (225) (PDF Card#75-0158). There was no evidence of any other phases and no peak is present which detects the carbonate phase (K$_2$CO$_3$) thus; we may say that in SDC-K$_2$CO$_3$, potassium carbonate is present in the amorphous phase. The results obtained from XRD data are tabulated in Table 2.

XRD results show that a sharpening in the peaks is noticed and the intensity of the peaks increases when the calcination temperature increases. The increase in the intensity of the peaks indicates an increase in the degree of crystallization. Furthermore, the crystallite size also increases with the increase in calcination temperature due to the crystallite growth during the calcination process results from an increase in the average crystallite sizes because of a tendency for minimization of the interfacial surface energy.
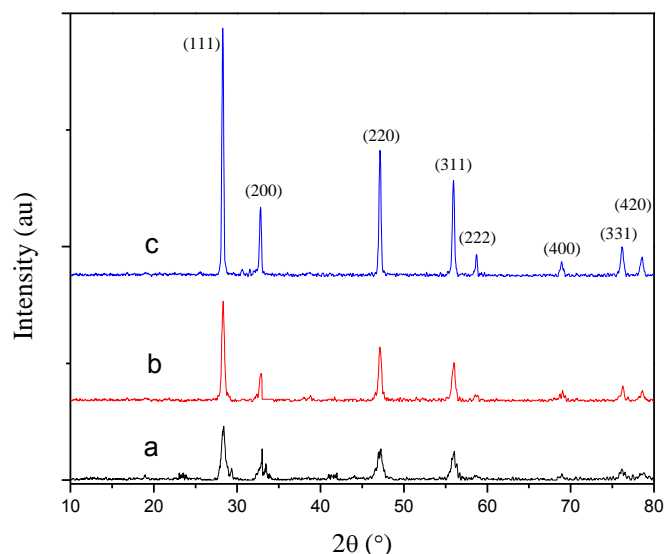
Fig. 6 XRD patterns of SDC-K_2CO_3 calcined at (a) 600 °C, (b) 700 °C and (c) 800 °C

Table 7 Parameters calculated from XRD Data

Sample (SDC-K_2CO_3)	d (nm)	a (nm)	V (nm^3)	D $_{XRD}$ (nm)	ρ_{XRD} (g/cm^3)	Lattice Strain
Calcined at 600 °C	0.3147	0.5451	0.1620	21.2	7.08	0.680 %
Calcined at 700 °C	0.3149	0.5454	0.1622	30.6	7.07	0.477 %
Calcined at 800 °C	0.3154	0.5463	0.1630	35.9	7.03	0.408

3.3. XRD analysis of co-doped SDC electrolyte by the addition of yttrium (YSDC)

XRD analysis of co-doped SDC with the addition of yttrium as a co-dopant is shown in Fig. 5. All the peaks are exactly matching with the cubic fluorite structure of cerium oxide having PDF Card#81-0792 as reported in the similar studies of other co-doped ceria based systems [21]. There is a no evidence of any new phases. The crystallite size obtained from the Scherrer's equation is found to be 43.4 nm while the value of lattice strain is 0.339 %.

The diffractogram shows that the dopants atoms were totally doped into the lattice of the CeO_2 crystals. Furthermore, the calculated value of lattice constant (5.442 Å) is greater than the lattice constant of pure ceria (5.411 Å). Thus, we may say that the dopant atoms

have been doped into the crystal lattice of CeO2 because increase in the lattice constant shows the distortion in the lattice of ceria.
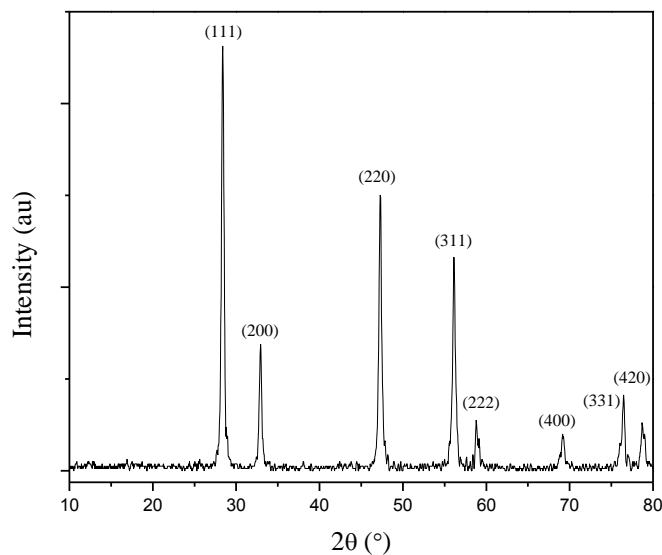

Fig. 7 XRD pattern of Co-doped SDC (YSDC)

3.4. Chemical compatibility of YSDC electrolyte with lithiated NiO cathode

Primarily, SOFC consists of three components i.e. cathode, anode and an electrolyte. With reference to the design considerations, chemical compatibility test is performed to check the chemical stability of YSDC electrolyte with lithiated nickel oxide cathode. After the heat treatment of 800 °C for 3 h, the XRD data is obtained to verify the chemical stability. Fig. 6 shows the XRD diffractogram after the heat treatment of the mixed sample (cathode and an electrolyte). XRD shows that two distinct phases are present in the sample. The peaks of the electrolyte phase are clearly matching with the cubic fluorite crystal structure of cerium oxide having PDF card#81-0792 while the peaks of the cathode phase are matching with the cubic structure of lithiated nickel oxide (Li0.4Ni1.6O2) having PDF card#81-0095. No evident is present of the mixed phase or a reaction between the electrolyte and a cathode as reported in the other similar studies [22,26]. However, before heat treatment the composition of lithiated nickel oxide was $Li_{0.68}Ni_{1.32}O_2$ having hexagonal crystal structure and after the heat treatment at 800 °C for 3 h the composition changes into $Li_{0.4}Ni_{1.6}O_2$ having a cubic crystal structure. The change in the composition and crystal structure occurs because of the crystallization

mechanism of $LiNiO_2$. At 400 °C, the formation of the basic reactants i.e. Li_2O and NiO occurs and when the temperature is increased to approximately 600 °C, the formation of solid solution of $Li_xNi_{2-x}O_2$ occurs. When the temperature is further increased and reaches at about 700 °C, the lithiation of NiO continued. This addition of Li ion in to NiO results in the redistribution of Li and Ni ions and consequently the crystal structure changes from hexagonal to the cubic arrangement [27].
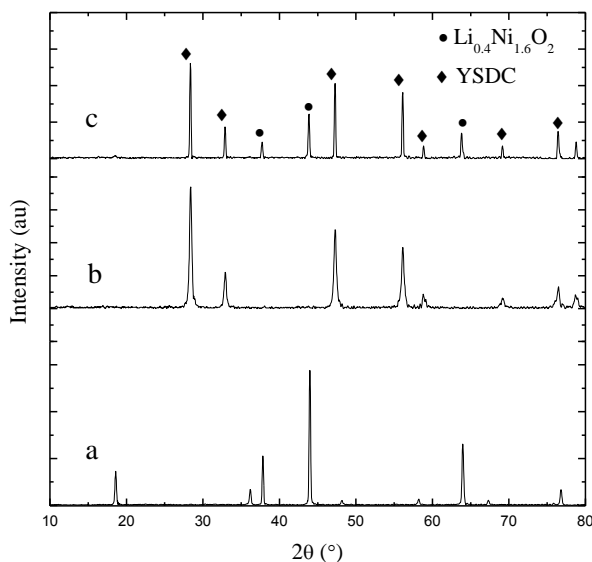

Fig. 8 XRD diffractograms of (a) $Li_{0.68}Ni_{1.32}O_2$ (b) YSDC and (c) Heat treated YSDC electrolyte and $Li_{0.4}Ni_{1.6}O_2$

3.5. Conductivity of the electrolytes

Ionic conductivities of samarium doped ceria (SDC), samarium doped ceria based composite with the addition of potassium carbonate K_2CO_3-SDC and co-doped SDC pellets were calculated by using following formula:

$$Conductivity\ (\sigma) = 1\ /\ Resistivity\ (\rho)$$

and,

$$Resistivity\ (\rho) = (R_{pellet} * A_{pellet})\ /\ T_{pellet}$$

where,

R_{pellet} = *Resistance of the pellet;*

A_{pellet} = *Area of the pellet;*

T_{pellet} = *Thickness of the pellet.*

The conductivity of the both these electrolytes mainly depend upon temperature and Arrhenius' law is used to express the relationship between conductivity and temperature.
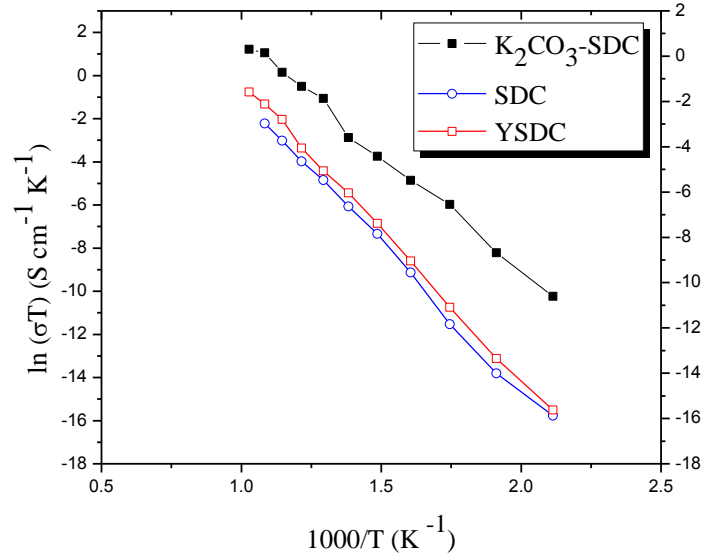

Fig. 9 Ionic conductivity of the electrolytes

The mathematical form of the Arrhenius' law is following:

$$\sigma(T) = \sigma_o e^{\left(\frac{-E}{kT}\right)}$$

where,

σ$_o$ = pre-exponential factor (constant);

E = energy of activation,

k = Boltzmann's Constant; and

T = absolute temperature

The Arrhenius' plots of the electrolytes are shown in Fig. 7. It is evident from Fig. 7 that conductivity of the electrolytes increases with the increase in temperature and conductivity of composite electrolyte is higher than the traditional single-phase (SDC) electrolyte and co-doped electrolyte. The calculated value of conductivity of samarium doped ceria at 650 °C by using above equations is 5.502×10^{-5} S /cm and the calculated value of ionic conductivity of K_2CO_3-SDC at 700 °C by using similar equations is 3.2×10^{-3} S/cm. The conductivity of co-doped electrolyte (YSDC) at 700 °C is found to be 2×10^{-4} S / cm.

The higher conductivity of the composite electrolyte is due to the multiple ion conduction in these electrolytes. Primarily these multiple ions are carbonate ions, oxide ions and proton (in case of hydrogen is supplied at the anode). In ceria based composite electrolyte carbonates are present in the amorphous phase as mentioned in the XRD results. Studies concluded that carbonate phase formed a layer or coating over a doped ceria oxide and this interface layer enhances the ionic conduction mechanism. They called this interface layer as "superionic pathways" and these pathways facilitate the conduction of negative ions e.g. O^-, O^{2-} and O_2^- [28]. It was also concluded that the interface of two phases of composite electrolyte is in highly disordered arrangement, and the movement of large number of ions is possible which enhances the interfacial conductivity of such dual phase electrolytes [29].

The conductivity of co-doped YSDC is higher than that of SDC because in order to enhance ionic conductivity, the binding energy associated with complex defect associates should be minimized. This will subsequently maximize mobile oxygen vacancies. Various studies [21,30] have been performed focusing on understanding the interactions between the dopant cations and oxygen vacancies and minimizing the activation energy for oxygen diffusion. Studies reported that, association energy is minimal when there is no elastic strain present in the host lattice. Using regression analysis, scientist proposed the critical dopant ionic radius (r_c), which is defined as the ionic radius of an ideal dopant that causes neither expansion nor contraction in the host ceria lattice [21]. The value of average dopant radius by using samarium and yttrium is 1.049 Å because the molar concentrations of both of the dopant ions are same i.e. $Ce_{0.8}Sm_{0.1}Y_{0.1}O_{1.9}$. This value is closely related to the value of critical radius (1.04 Å). Furthermore, the value of lattice strain for SDC electrolyte is obtained to be 0.408 % while the value of lattice strain for YSDC is found to be 0.339 %. The decrease in the lattice strain in YSDC as compared to SDC is another reason for the high ionic conductivity of co-doped YSDC electrolyte.

Conclusions

Samarium doped ceria (SDC) and SDC – based composite electrolytes with the addition of potassium carbonate were successfully developed using co-precipitation method. It is concluded from the microstructure analysis using XRD that in composite electrolyte

carbonate was present as a secondary phase in an amorphous form and no chemical reaction or no new compound was formed between SDC and the carbonate. pH of the solution during precipitation showed a significant effect on the microstructure of SDC electrolyte. Crystallite size and the particle size increases with increasing pH of the solution. The crystallinity of SDC-K_2CO_3 composite electrolyte increases with the increase in calcination temperature ranges from 600-800 °C. The crystallite size increases while the lattice strain decreases by increasing the calcination temperature.

The ionic conductivity of the electrolyte materials increases with the increase in temperature and the addition of carbonate enhance the conductivity of the single-phase SDC electrolyte. Co-doping of yttrium also enhances the ionic conductivity of SDC electrolyte but less than the addition of carbonate. From the chemical compatibility test of co-doped YSDC electrolyte with lithiated NiO cathode, it is concluded that no chemical reaction was occurred between these two materials at 800 °C for 3 h, however, the crystal structure of lithiated NiO changes from hexagonal to cubic arrangement after 700 °C so we may say that lithiated NiO can be used as a cathode material with YSDC electrolyte at temperature ranges up to 700 °C.

Acknowledgement

References

[1]   J. Huang, F. Xie, C. Wang, Z. Mao, Development of solid oxide fuel cell materials for intermediate-to-low temperature operation, Int. J. Hydrogen Energy. 37 (2012) 877–883.

[2]   A. J. Jacobson, Materials for solid oxide fuel cells †, Chem. Mater. 22 (2010) 660–674.

[3]   V. Kharton, F. Marques, A. Atkinson, Transport properties of solid oxide electrolyte ceramics: A brief review, Solid State Ionics. 174 (2004) 135–149.

[4]   H. Okkay, M. Bayramoglu, M. Faruk Öksüzömer, $Ce_{0.8}Sm_{0.2}O_{1.9}$ synthesis for solid oxide fuel cell electrolyte by ultrasound assisted co-precipitation method., Ultrason. Sonochem. 20 (2013) 978–83.

[5]   Y. P. Fu, S. B. Wen, C. H. Lu, Preparation and characterization of samaria-doped ceria electrolyte materials for solid oxide fuel cells, J. Am. Ceram. Soc. 91 (2007) 127–131.

[6]   M. Dudek, Ceramic oxide electrolytes based on CeO_2—Preparation, properties and possibility of application to electrochemical devices, J. Eur. Ceram. Soc. 28 (2008) 965–971.

[7]   S. Wang, C. Yeh, Y. Wang, Y. Wu, Characterization of samarium-doped ceria powders prepared by hydrothermal synthesis for use in solid state oxide fuel cells, J Mater Res Technol 2 (2013) 141–148.

[8]   M. R. Kosinski, R. T. Baker, Preparation and property–performance relationships in samarium-doped ceria nanopowders for solid oxide fuel cell electrolytes, J. Power Sources. 196 (2011) 2498–2512.

[9]   T. Karaca, T. G. Altınçekiç, M. Faruk Öksüzömer, Synthesis of nanocrystalline samarium-doped CeO_2 (SDC) powders as a solid electrolyte by using a simple solvothermal route, Ceram. Int. 36 (2010) 1101–1107.

[10]   R. Tian, F. Zhao, F. Chen, C. Xia, Sintering of samarium-doped ceria powders prepared by a glycine-nitrate process, Solid State Ionics. 192 (2011) 580–583.

[11]   K. Myoujin, H. Ichiboshi, T. Kodera, T. Ogihara, Characterization of samarium doped ceria powders having high specific surface area synthesized by carbon-sssisted spray pyrolysis, Key Eng. Mater. 485 (2011) 137–140.

[12] Z. Shao, W. Zhou, Z. Zhu, Advanced synthesis of materials for intermediate-temperature solid oxide fuel cells, Prog. Mater. Sci. 57 (2012) 804–874.

[13] R. Raza, X. Wang, Y. Ma, X. Liu, B. Zhu, Improved ceria–carbonate composite electrolytes, Int. J. Hydrogen Energy. 35 (2010) 2684–2688.

[14] X. Wang, Y. Ma, R. Raza, M. Muhammed, B. Zhu, Novel core–shell SDC/amorphous Na_2CO_3 nanocomposite electrolyte for low-temperature SOFCs, Electrochem. Commun. 10 (2008) 1617–1620.

[15] X. Wang, Y. Ma, S. Li, B. Zhu, M. Muhammed, SDC/Na_2CO_3 nanocomposite: New freeze drying based synthesis and application as electrolyte in low-temperature solid oxide fuel cells, Int. J. Hydrogen Energy. 37 (2012) 19380–19387.

[16] S. A. Muhammed Ali, A. Muchtar, A. Bakar Sulong, N. Muhamad, E. Herianto Majlan, Influence of sintering temperature on the power density of samarium-doped-ceria carbonate electrolyte composites for low-temperature solid oxide fuel cells, Ceram. Int. 39 (2013) 5813–5820.

[17] C. M. Lapa, F. M. L. Figueiredo, D. P. F. De Souza, L. Song, B. Zhu, F. M. B. Marques, Synthesis and characterization of composite electrolytes based on samaria-doped ceria and Na/Li carbonates, Int. J. Hydrogen Energy. 35 (2010) 2953–2957.

[18] C. Xia, Y. Li, Y. Tian, Q. Liu, Z. Wang, L. Jia, et al., Intermediate temperature fuel cell with a doped ceria–carbonate composite electrolyte, J. Power Sources. 195 (2010) 3149–3154.

[19] N. Zuo, M. Zhang, Z. Mao, Z. Gao, F. Xie, Fabrication and characterization of composite electrolyte for intermediate-temperature SOFC, J. Eur. Ceram. Soc. 31 (2011) 3103–3107.

[20] L. Zhang, R. Lan, P. I. Cowin, S. Tao, Fabrication of solid oxide fuel cell based on doped ceria electrolyte by one-step sintering at 800°C, Solid State Ionics. 203 (2011) 47–51.

[21] S. Omar, E. Wachsman, J. Nino, Higher conductivity Sm^{3+} and Nd^{3+} co-doped ceria-based electrolyte materials, Solid State Ionics. 178 (2008) 1890–1897.

[22] W. Tan, L. Fan, R. Raza, M. Ajmal Khan, B. Zhu, Studies of modified lithiated NiO cathode for low temperature solid oxide fuel cell with ceria-carbonate composite electrolyte, Int. J. Hydrogen Energy. 38 (2013) 370–376.

[23] M. A. Khan, R. Raza, R. B. Lima, M. A. Chaudhry, E. Ahmed, G. Abbas, Comparative study of the nano-composite electrolytes based on samaria-doped ceria for low temperature solid oxide fuel cells (LT-SOFCs), Int. J. Hydrogen Energy. (2013) 2–9.

[24] K. Sato, G. Okamoto, M. Naito, H. Abe, NiO/YSZ nanocomposite particles synthesized via co-precipitation method for electrochemically active Ni/YSZ anode, J. Power Sources. 193 (2009) 185–188.

[25] K. Sivakumar, V. S. Kumar, N. Muthukumarasamy, M. Thambidurai, T.S. Senthil, Influence of pH on ZnO nanocrystalline thin films prepared by sol − gel, 35 (2012) 327–331.

[26] L. Zhang, S. Tao, An intermediate temperature solid oxide fuel cell fabricated by one step co-press-sintering, Int. J. Hydrogen Energy. 36 (2011) 14643–14647.

[27] P. Kalyani, N. Kalaiselvi, Various aspects of $LiNiO_2$ chemistry: A review, Sci. Technol. Adv. Mater. 6 (2005) 689–703.

[28] L. Fan, C. Wang, M. Chen, J. Di, J. Zheng, B. Zhu, Potential low-temperature application and hybrid-ionic conducting property of ceria-carbonate composite electrolytes for solid oxide fuel cells, Int. J. Hydrogen Energy. 36 (2011) 9987–9993.

[29] L. Fan, C. Wang, J. Di, M. Chen, J. Zheng, B. Zhu, Study of ceria-carbonate nanocomposite electrolytes for low-temperature solid oxide fuel cells, J. Nanosci. Nanotechnol. 12 (2012) 4941–4945.

[30] D. A. Andersson, S. I. Simak, N. V Skorodumova, I. A. Abrikosov, B. Johansson, Optimization of ionic conductivity in doped ceria., Proc. Natl. Acad. Sci. U. S. A. 103 (2006) 3518–21.